Aus dem Institut für Biomedizinische Technik

Influence of polymer surface modification and specific growth factor stimulation on cellular adhesion at the implant/endothelium interface

Dissertation

zur

Erlangung des akademischen Grades

doctor rerum naturalium (Dr. rer. nat.)

an der Mathematisch-Naturwissenschaftlichen Fakultät der

Universität Rostock

vorgelegt von

Dipl.-Biol. M.Sc. (Hons.) Thilo Storm

aus Rostock

Rostock, im November 2014

urn:nbn:de:gbv:28-diss2016-0085-0

Gutachter:

1. Gutachter:

   Prof. Dr. Birgit Piechulla

   Institut für Biowissenschaften, Universität Rostock

2. Gutachter:

   PD Dr. Marina Hovakimyan

   Institut für Biomedizinische Technik, Universität Rostock

3. Gutachter:

   Prof. Dr. Mathias Wilhelmi

   Klinik für Herz-, Thorax-, Transplantations- und Gefäßchirurgie und

   Kompetenzzentrum für Kardiovaskuläre Implantate, Medizinische Hochschule

   Hannover

Datum der Einreichung: 20. November 2014

Datum der Verteidigung: 24. April 2015

List of abbreviations

A	adenine
A	alanine
AMS	absorbable magnesium stent
ANOVA	analysis of variance
APTES	aminopropyltriethoxysilane
bFGF	basic fibroblast growth factor
BMS	bare metal stent
bp	base pairs
BrdU	5-bromo-2'-deoxyuridine
C	cysteine
C	cytosine
CABG	coronary artery bypass grafting
CAD	coronary artery disease
calcein AM	acetomethoxy derivate of calcein
CAS	coronary artery stenting
cat.no.	catalog number
cDNA	complementary DNA
$CHCl_3$	chloroform
CLSM	confocal laser scanning microscopy
COOH	carboxyl group
CQB	CellQuanti-Blue™
DEB	drug eluting balloon
DES	drug eluting stent
DNA	deoxyribonucleic acid
dNTP	deoxyribonucleoside triphosphate
DSC	N,N-disuccinimidyl carbonate
DTT	dithiothreitol
EC	endothelial cell
ECGS	endothelial cell growth supplement
ECM	extracellular matrix
EDC	1-Ethyl-3-(3-dimethylaminopropyl)carbodiimide
e.g.	*exempli gratia*

EGF	epidermal growth factor
eNOS	endothelial nitric oxide synthase
ESEM	environmental scanning electron microscopy
FBGC	foreign body giant cell
FBR	foreign body reaction
FCS	fetal calf serum
FITC	fluorescein isothiocyanate
FKBP12	Fk506-binding protein 12
FN	fibronectin
fwd	forward
G	glycine
G	guanine
HCAEC	human coronary artery endothelial cell
HCl	hydrochloric acid
HEPES	4-(2-hydroxyethyl)-1-piperazineethanesulfonic acid
HMDA	hexane-1,6-diamine
HRP	horseradish peroxidase
HUVEC	human umbilical vein endothelial cell
ICAM-1	intercellular adhesion molecule 1
i.e.	*id est*
IL	interleukin
ISR	in-stent restenosis
KCl	potassium chloride
KDR	kinase-insert domain-containing receptor
kV	kilovolt
LDL	low density lipoprotein
LPS	lipopolysaccharide
M	molarity
MDI	4,4′-methylenebis(phenyl-isocyanate)
$MgCl_2$	magnesium chloride
MHz	megahertz
mRNA	messenger ribonucleic acid

NaCl	sodium chloride
NaOH	sodium hydroxide
NBD-Cl	4-chloro-7-nitrobenzo-2-oxa-1,3-diazol
NCBI	National Center for Biotechnology Information
NCO	isocyanate
NF-κB	nuclear factor-κB
NH_2	amino group
NH_3	ammonia
NHS	N-hydroxysuccinimide
NO	nitric oxide
O_2	oxygen
OH	hydroxyl group
qPCR	quantitative PCR
PBS	phosphate buffered saline
pH	negative log scale (base 10) of $[H^+]$ of a solution
PCL	poly(ε-caprolactone)
PCL/electrospinning	PCL manufactured by electrospinning
PCL/HMDA	PCL activated with HMDA
PCL/MDI/NH_3	PCL activated with MDI
PCL/NaOH	PCL modified with NaOH
PCL/NH_3 plasma/FN	PCL activated with NH_3 plasma and coated with fibronectin
PCL/O_2/APTES/FN	PCL activated with O_2 plasma, then activated with APTES, then coated with fibronectin
PCL/O_2 plasma/FN	PCL activated with O_2 plasma and coated with fibronectin
PCL/salt leaching	PCL modified by salt leaching
PCR	polymerase chain reaction
PECAM-1	platelet/ endothelial cell adhesion molecule 1
PEEK	polyetheretherketone
PlGF	placental growth factor
PMMA	polymethyl methacrylate
PTCA	percutaneous transluminal coronary angioplasty
PTFE	polytetrafluoroethylene
rev	reverse
RNA	ribonucleic acid

RNase	ribonuclease
rpm	revolutions per minute
rRNA	ribosomal RNA
SD	standard deviation
SEM	scanning electron microscopy
sPCL-A	4-star-shaped poly(ε-caprolactone) with terminal acrylate groups
SMC	smooth muscle cell
ST	stent thrombosis
T	thymine
TETD	tetraethylthiuram disulfide
TLR	target lesion revascularization
TNS	trypsin neutralising solution
TNF-α	tumor necrosis factor α
Tris-HCl	tris(hydroxymethyl)aminomethane
Tween 20	polyoxyethylen(20) sorbitan monolaurate
v/v	volume per volume
VCAM-1	vascular cell adhesion molecule 1
VEGF	vascular endothelial growth factor
w/v	weight per volume

List of figures

Chapter 1

Chapter 2

Chapter 3

Appendix

List of tables

Chapter 1

Chapter 2

Chapter 3

Appendix

Table of contents

CHAPTER 2

CHAPTER 3

1. Introduction

Coronary artery disease (CAD) causes the death of hundreds of thousands of people all over the world every month. A crucial and common strategy for treatment involves vascular implants, which is not without its shortcomings in certain respects. This thesis therefore is concerned with a fundamental issue that governs the final outcome of this interventional therapy – the behavior of endothelial cells on the implant surface and how particular changes in the composition of that surface can potentially enhance implant performance.

1.1. Anatomy of blood vessels

Arteries, veins and capillaries form the most important transport system of the human body, providing continuous circulation of blood, nutrients, metabolites, respiratory gases, hormones, water and electrolytes. The significance of the circulatory system is illustrated by the fact that dysfunction results from just a few seconds of circulatory arrest, and irreparable brain damage ensues after 3-5 minutes [1].

The vessel wall itself is tripartite: the intima (tunica intima) contains endothelial cells only, the media (tunica media) is made up of smooth muscle cells and the underlying fibroblasts constitute the outer adventitia (tunica adventitia). The three layers of different cell types are separated by thin elastic laminae (**figure 1.1**). Different types of blood vessels are distinguished by morphological differences in the three layers. The wall thickness of veins is much smaller than that of arteries of comparable diameter. Thickness and cell density of the media differ in arteries such that they are categorized as arteries of the elastic type (thick intima with many elastic fibers, e.g. aorta) and arteries of the muscular type (higher density of smooth muscle cells in an overall thinner tunica intima).

1.2. The endothelium

1.2.1. General characteristics

The endothelium is a monolayer of cells at the boundary of the bloodstream and the underlying tissue which makes it a crucial player in terms of nutrient supply as well as barrier function. Moreover, endothelial cells are instrumental in the formation and maintenance of blood vessels and the regulation of immune responses. They form the innermost layer of the wall of every blood vessel and thus fulfil the major task of keeping up the barrier between blood and vascularized tissue while regulating the molecular traffic

across that border. Other functions of the endothelium include the regulation of blood flow and vascular tone, contribution to vascular repair and homeostasis, modulation of haematopoietic cell proliferation, and the maintenance of an anti-coagulant surface [2]. An intact endothelium is inherently nonthrombogenic [3].

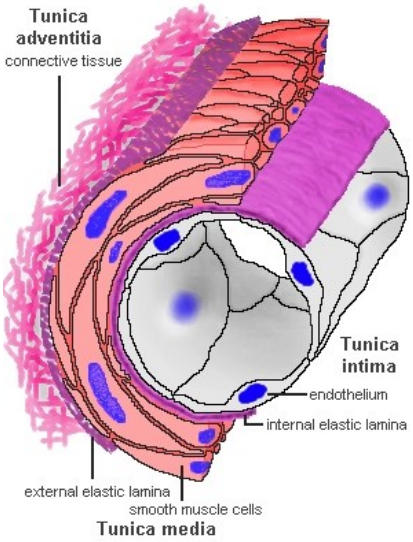

Figure 1.1. Schematic buildup of a blood vessel. Taken from lab.anbh.uwa.edu.au, University of Western Australia

1.2.2. Endothelial marker molecules

On their surface, endothelial cells express a vast array of molecules that conduct interactions with other endothelial cells as well as with white blood cells. Adhesion molecules are paramount for the regulation of the barrier function of endothelial cells. Some of these lend themselves to closer scrutiny because they are very important in inflammatory settings such as after the implantation of a vascular graft or stent, and will therefore be briefly introduced here.

PECAM-1

Platelet endothelial cell adhesion molecule-1 (PECAM-1; CD31) is a cell surface glycoprotein concentrated in cell-cell junctions. In endothelial cells, it is important for mediating contact inhibition [4]. Modest levels of PECAM-1 expression are also found in platelets, neutrophils, monocytes and some T lymphocytes [5]. It has been shown that homophilic PECAM-1/PECAM-1 interactions are necessary for leukocyte transmigration [6]. Changes in shear stress, the force of friction on the vessel wall created by blood flow, lead to the abrupt dissociation of PECAM-1/endothelial nitric oxide synthase (eNOS) complexes, which makes PECAM-1 a chemical signal converter, a regulator of eNOS activation and a key molecule for detection of mechanoreception and -transduction [5]. Through alternative splicing, eight isoforms of PECAM-1 are generated [7], and gene polymorphisms have been linked to increased risk for severe coronary heart disease and myocardial infarction [5]. PECAM-1$^{-/-}$ double knockout mice have significantly reduced eNOS expression and nitric

oxide (NO) bioavailability (i.e. less intracellular NO) as well as impaired transendothelial leukocyte migration. At the same time they show reduced levels of endothelial cell apoptosis and of atherosclerotic lesions [5, 7]. Therefore PECAM-1 is regarded as a critical mediator of atherosclerosis [5] and as such has become a target in vascular immunotargeting with antibodies [8].

ICAM-1

Intercellular adhesion molecule-1 (ICAM-1) is constitutively expressed on the apical and basolateral surfaces of endothelial cells, and, albeit in orders of magnitude less, on leukocytes and fibroblasts [9]. It binds to the integrins LFA-1 and MAC-1 on the surface of leukocytes [10] and thus regulates their adhesion to endothelial cells. Through the transcription factor NF-κB, ICAM-1 expression is upregulated by IL-1 and TNF-α [11]. Along with VCAM-1 and E-selectin, it is therefore seen as a marker of an inflammatory phenotype of endothelial cells [12]. In PECAM$^{-/-}$ mice, ICAM-1 is downregulated [5]. Its participation in outside-in signal transduction impacts on inflammatory cell trafficking and leukocyte effector functions [9].

VCAM-1

Vascular cell adhesion molecule-1 (VCAM-1) binds to the integrin VLA-4 on the surface of monocytes, basophils and eosinophils and thus facilitates their early attachment to endothelial cells [10, 11]. Together with ICAM-1, it is the most important adhesion molecule for the recruitment of white blood cells to sites of inflammation [9]. It is not constitutively expressed but induced by proinflammatory cytokines such as platelet-associated IL-1. In response to such a stimulus, the expression of VCAM-1 peaks earlier than that of ICAM-1 [11].

1.2.3. Endothelial homeostasis

The phenotype of endothelial cells depends on their location within the organism. Over twenty different kinds of endothelial cells have been morphologically characterized and are commercially available as primary cells. All of them grow as monolayers with a high density of adherens junctions and a more or less spindle-like cell shape.

The interplay between endothelial cells, blood cells and smooth muscle cells is very intricate and requires an enormous degree of balancing and counterbalancing of the production and mediation of signaling molecules such as NO, cytokines, interleukins, interferons and colony stimulating factors [11]. For example, the endothelial barrier serves to shield the smooth muscle cells (SMCs) from circulating growth factors, while endothelial

cells also secret inhibitory factors, e.g. NO, against SMC proliferation [13]. Any dysregulation of that balance has the potential to shift the homeostatic situation towards a malicious path leading to vascular pathologies and on to cardiovascular disease.

1.3. Clinical background

1.3.1. Coronary artery disease

Cardiovascular disease continues to claim the most lives in the industrialized world. Here the focus shall be put on CAD which affects tens of millions of people worldwide and is the most common cause of morbidity and mortality [14]. A very broad outline of disease progression could be sketched along the features of hypolipidemia, atherosclerosis and, as a consequence either of ischemia (localized lack of perfusion) or thrombosis (sudden obstruction of blood flow due to platelet aggregation), eventually acute myocardial infarction and heart failure. The latter is responsible for a third of all deaths [1]. Globally, 3.4 million women and 3.8 million men die of CAD every year [15]. Interventional procedures are usually required once the later stages of atherosclerosis have been identified and CAD is manifest. A key element for treatment is percutaneous transluminal coronary angioplasty (PTCA) which has become standard practice over the last two decades [14, 16].

Even in early asymptomatic atherosclerosis, endothelial dysfunction is present and can be detected via assessment of the vasomotor regulatory function of the endothelium, e.g. by intravascular ultrasound or quantitative angiography upon infusion of acetylcholine or other vasoactive stimuli, or through peripheral arterial tonometry [2].

1.3.2. Atherosclerosis plaque

1.3.2.1. Plaque formation

Plaques are made of cholesterol, lipid and calcium and accumulate on the inside of blood vessels, and, once large enough, will restrict perfusion of the affected vessel (**figure 1.2**). As one of the first steps in atherosclerosis, monocytes adhere to endothelial cells. Following their transendothelial migration, they accumulate lipid deposits and transform into foam cells, secreting proinflammatory cytokines [17]. Plaque formation starts with intracellular accumulation of lipid in macrophages and smooth muscle cells of the intima [18]. Along with fibers from the extracellular matrix (ECM) and smooth muscle cells themselves, over time a so-called fatty streak is formed beneath the endothelium. These asymptomatic fatty streaks are frequently found even in young individuals [19]. But atherosclerosis is a slowly progressing disease with a long asymptomatic initial phase [2]. With time, fatty streaks may just disappear or, accumulating collagen and elastin as well as more lipid, turn into the subendothelial preatheroma, progressing to atheroma and fibroatheroma, with concurrent growth of the atherosclerotic lesion and disorganization of

the intima layer of the blood vessel (figure 1.2). In effect, atheromata (or 'plaques') represent asymmetric focal intimal thickenings [19]. The different stages of the disease can be diagnosed by clinical assessment of endothelial function, i.e. the response of affected vessels to endothelial dependent stimuli [2].

The World Health Organization defines atherosclerosis as variable combination of changes in the intima of arteries, consisting of focal accumulations of lipids, complex carbohydrates, blood and blood components, connective tissue and calcium, associated with changes in the media [1]. The latter involve predominantly smooth muscle cell hyperplasia, characterized by migration of dedifferentiated and proliferating SMCs from the media to the intima, where they increasingly synthesize ECM.

On the intracellular level, these cells generate much more protein by virtue of an enlarged rough endoplasmic reticulum and Golgi apparatus and increased number of ribosomes [18]. They are in the synthetic state, as opposed to the contractile, or quiescent state, where the contractile apparatus with its thick actin-myosin filaments fills 80-90% of the cytoplasm [18].

On the molecular level, inhibitors of SMC growth (e.g. NO, heparin sulfate, transforming growth factor-β) regulate hyperplasia along with growth promoters (e.g. interleukin 1, platelet-derived growth factor, basic fibroblast growth factor).

On the macroscopic level, lipid cores containing foam cells form between fibrous regions, obstructing the lumen of the vessel and leading to an outward 'ulceration' of the vascular wall in response to the narrowing [18]. This outward remodeling of the vessel wall can initially compensate for plaque growth [20] but is ultimately detrimental. As a result, arteries lose their elasticity and become increasingly rigid, or sclerotic, as calcification takes place. Muscular as well as elastic arteries are prone to atherosclerosis, especially in regions of curvature and bifurcation [21].

The most affected blood vessels in terms of plaque prevalence are: 1. abdominal aorta and iliac arteries, 2. coronary arteries, 3. thoracic aorta and femoral arteries, 4. aorta carotis interna, 5. brain stem arteries [1].

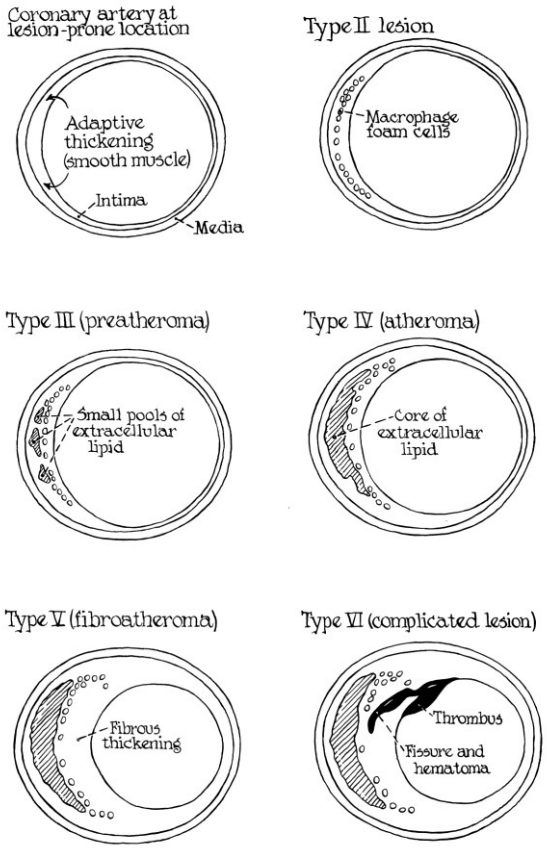

Figure 1.2.

Pathogenesis and progression of atherosclerotic lesions (plaque). From Stary H et al. *Circulation* 1995; 92:1355-1374 [22]

1.3.2.2. Plaque activation and pathological features

Extracellular matrix components, in particular collagen, and smooth muscle cells cap the intraluminal plaque. Infiltration of T cells, macrophages and mast cells ensues, and the production of inflammatory cytokines, matrix metalloproteinases (MMPs; they lyse matrix proteins and induce plaque rupture) and cysteine proteases leads to the activation of plaque and subsequent pathological events [19]. Atherosclerosis and CAD can be viewed as a state of unresolved inflammation [23]; neutrophils as 'first responders' of the innate immune system are responsible for the removal of cell debris, get directly in contact with plaque and thus promote its destabilization [24]. There is a direct correlation between this plaque destabilization, high amounts of MMP and a high neutrophil count [24]. The clinical symptoms of advanced atherosclerosis vary, as several mechanisms are at work: ischemia is caused by the slow narrowing of the vessel, hemorrhage into an atheroma or thrombosis is caused by the sudden occlusion of the blood vessel through a growing plaque, embolism may result from thrombosis, and the obstructed vessel may form aneurysms or even rupture because of its weakened wall [18]. A completely occluded coronary artery will cause a heart attack, i.e. acute ischemia of the surrounding cardiac tissue and death of the affected cardiomyocytes. In 60-70% of cases with coronary thrombosis, prothrombotic

material is exposed to the blood as a consequence of plaque rupture [19]. Because of the life-threatening consequences, clinical intervention is very common.

One important contributor to inflammation at the vessel wall is an imbalanced lipid metabolism. Excess low density lipoprotein (LDL) is retained in the intima and becomes modified by enzymes and oxidation [19]. Residing macrophages take up the resulting inflammatory lipids and turn into foam cells which are a major component of the plaque core. For this reason, hypercholesterolemia carries a high risk of atherosclerosis, which in turn is the direct cause of peripheral artery occlusive disease and CAD [19, 23].

1.3.3. Treatment options

Unless the arterial blockage is so severe that coronary artery bypass grafting (CABG) becomes necessary, the therapy of choice for obstructed blood vessels is their physical widening by means of balloon catheter and stent(s), i.e. coronary artery stenting (CAS). Mounted on a balloon catheter and aided by a guidewire and radiopaque dye, the stent is inserted into the obstructed segment and the balloon is inflated for 20 s to 3 min, embedding the stent in the arterial wall [15] and leaving behind a thin multilayered thrombus between the wall and the lumen. During stenting, the endothelial monolayer is inevitably compromised, as the vessel wall gets partially or completely denuded (**figure 1.3**). By means of scanning electron microscopy, it was demonstrated that the thrombus resolves around six to 12 weeks post-implantation, while the stented segment begins to be re-endothelialized [25]. Endothelial recovery, i.e. the formation of an intact lining of the blood vessel as well as of the inner surface of the stent, is crucial for the ultimate success of the implant. The advent of coronary stents has decreased the share of CABG to less than 20% of all coronary revascularization procedures performed [16]. However, a sizeable number of patients present with either re-stenosis or thrombosis after stenting, both of which are potentially life-threatening complications [26]. The main reason for these undesirable outcomes is a dysfunctional endothelium at the implant site.

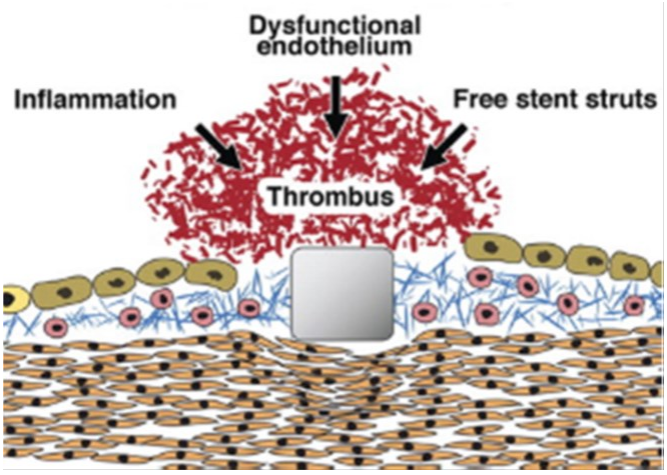

Figure 1.3.

Mechanical trauma caused by stenting denudes the endothelium (green) locally and leads to multi-layered thrombus formation. From Zimmer S and Nickenig G, *Eur Heart J* 2010; 31(21):2569-2571 [27]

1.3.3.1. Bare metal stents

The first angioplasty was performed in 1964, the first balloon coronary angioplasty in 1977 [28]. The first stents implanted into human patients were metal cylinders without any coating (bare metal stents, BMS). They have been in use since the mid-1980s. In the absence of complications, post-implantation vascular healing is linear [29] and re-endothelialization is near complete by 3-4 months [30].

However, endothelial injury due to stenting (**figure 1.3**) can initiate a complex inflammatory cascade that may ultimately lead to thrombosis or in-stent restenosis [13, 31, 32] (**figure 1.4**). The latter is the re-narrowing of the remodelled artery and is preceded by intimal hyperplasia, i.e. uncontrolled vascular smooth muscle cell proliferation and migration, as well as deposition of extracellular matrix and negative remodeling, eventually occluding the lumen of the stented vessel and requiring re-intervention in the form of so-called repeat revascularization procedures (also target lesion revascularization, TLR) [33]. In order to overcome widespread problems with a 30-40% TLR rate due to restenosis (from around 3 months post-stenting) associated with the use of bare metal (or 1st generation) stents [34], drug-eluting (or 2nd generation) stents (DES) containing reservoirs of usually anti-proliferative agents have been developed and found to reduce the restenosis rate sharply [35-37].

Stent implantation is routinely accompanied by dual antiplatelet therapy with aspirin and thienopyridine for at least one month [38]. In the absence of these drugs, around 20% of emergency procedures following BMS implantation were due to stent thrombosis [30]. Nowadays, that incidence is down to 0.5-2% [30]. Depending on the time point after stenting, there is acute (<24 h), subacute (1 to 30 days), late (30 days and later), and very

late stent thrombosis (1 year and later) [39]. The majority of these thrombotic events occurs within the first six months of stenting [30].

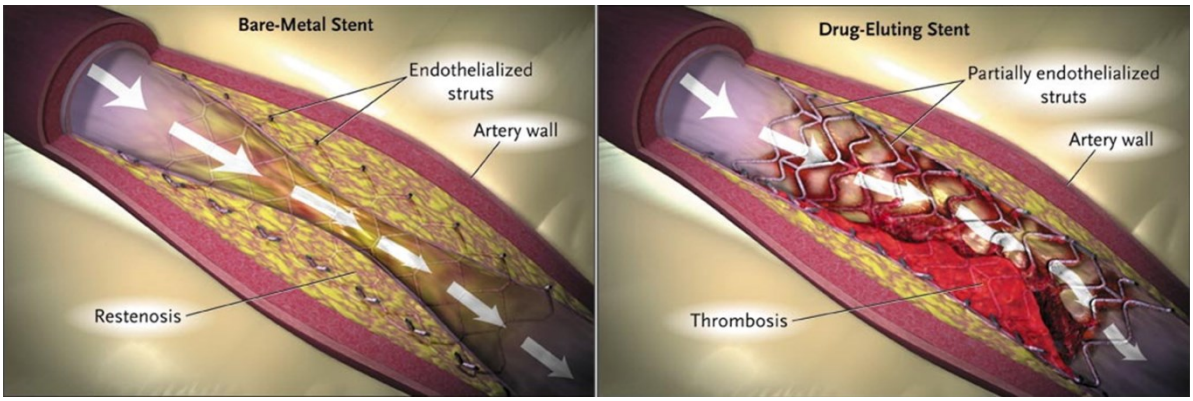

Figure 1.4. Post-operative complications commonly associated with DES and BMS. Modified from Curfman GD et al.: *N Engl J Med* 2007; 356:1059-1060 [40]

1.3.3.2. Drug eluting stents

Up to 40 per cent of the patients receiving first-generation BMS suffered from restenosis [34]. To reduce this rate of complications, coatings were developed to cover the metal struts of stents. In drug eluting stents (DES), the carrier polymer constitutes a reservoir for a drug that will be released either as the polymer degrades or through diffusion, and the kinetics of drug release can be tailored by polymer modification [15]. This modification can be achieved rather simplyby changing physical parameters such as surface area or coating thickness, or through complex chemical mechanisms generating covalent bonds between the drug and the polymer [37]. The number of cases where repeat revascularization was needed indeed dropped by 70% [33]. Depending on age and general health of the patients, the incidence of restenosis after DES implantation can drop as low as 3% [41]. So even though the first DES was approved in 2003, by 2006 DES had around 80% market share in the U.S. [30]. A detrimental side effect of DES is delayed endothelial healing coupled with an increased risk of in-stent thrombosis [31, 37] (**figure 1.4**). This is in part due to thicker struts necessary to make up for reduced radial strength [26]. The long-term efficacy of DES was callled into question when it became apparent that the rates of late and very late stent thrombosis (ST) were problematic. Dual antiplatelet therapy is consequently prolonged to at least 12 months after DES implantation [38]. A meta-analysis found the incidence of early and late ST not to be statistically different between patients treated with BMS or DES, but most cases of very late ST were associated with DES [30]. This has been attributed to a host reaction in the vessel wall to durable polymers [32], which in general incite greater inflammation than the bare metal alternative [30]. Other causes of late-stage ST include

increased platelet aggregation or inflammation due to exposed stent struts [42]. Although these complications are still very rare (the annual incidence of very late ST is only 0.2-0.6%), their severity (with a 50% incidence of myocardial infarction and a 20% mortality rate as a consequence of ST) makes further improvements mandatory [31]. Thus, in order to enhance DES safety and long-term efficacy, various approaches aim at simultaneous promotion of endothelial proliferation and inhibition of neointimal proliferation [37]. The most recent generation of bioabsorbable stents is targeted especially towards younger patients, who are less likely to require procedural reintervention and thus will benefit most from such transient implants. A clinicial trial with the AMS (absorbable magnesium stent) platform has found that the stent was fully adsorbed after 4 months. This period might even be shortened in favor of restoration of vasomotor function, but the time over which stented arterial segments really need mechanical scaffolding has not yet been conclusively determined [37].

Despite the multitude of manufacturers and stent platforms on the market today, the drugs commonly used in DES all derive from two conventional anti-restenosis agents. The first is the immunosuppressive agent sirolimus, also known as rapamycin, which was discovered in *Streptomyces hygroscopicus* on the Pacific island Rapa Nui in 1964 [33] and originally developed as antifungal compound [16]. It prevents cell cycle transition from late G_1 into S phase by binding to the intracellular receptor Fk506-binding protein 12 (FKBP12) and inhibiting the kinase mammalian target of rapamycin (mTOR), in turn preventing degradation of the cyclin-dependent kinase inhibitor p27kip1. Therefore it acts as an unspecific inhibitor of mammalian cell proliferation, i.e. including all cells involved in vascular healing following stent implantation [29]. Consequently, the reendothelialization process of DES surfaces is delayed compared to BMS, where it is nearly complete about 3-4 months following implantation (**figure 1.5**). In contrast, a histological study found approximately 80% endothelialization of the sirolimus eluting Cypher stent 16 months after stenting [30]. Since 2003, sirolimus has been used in commercial DES and a number of sirolimus analogs have been developed to improve on safety and efficacy. For example, everolimus contains a side chain alkylated with a 2-hydroxyethy group, leading to 3-fold affinity to FKBP12 and 2- to 5-fold lower immunosuppressive activity than sirolimus [33]. Zotarolimus contains a tetrazole ring in the C_{40} position, giving it 3- to 4-fold lower immunosuppressive activity than sirolimus, with unchanged FKBP12 affinity and antiproliferative activity [33]. The semisynthetic sirolimus analog biolimus-A9 contains an extra alkoxy-alkyl group, making it highly lipophilic while maintaining the antiproliferative potency [33]. Other Limus derivatives are myolimus, pimecrolimus and tacrolimus, with the latter exerting its antiproliferative effects somewhat differentially on human vascular SMCs and endothelial cells [37].

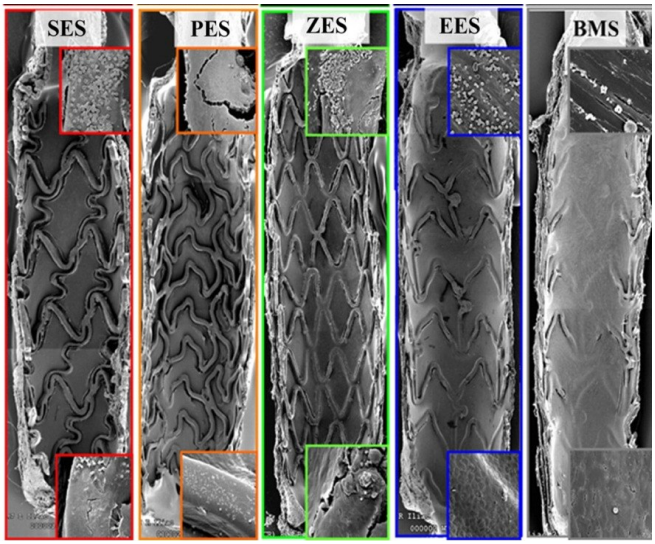

Figure 1.5.
Stent endothelialization by comparison. Representative SEM micrographs of 4 DES (eluting sirolimus (SES), paclitaxel (PES), zotarolimus (ZES) and everolimus (EES), respectively) and a BMS harvested from rabbit iliac arteries 14 days post stenting. Insets are 200× magnified. Modified from Joner et al. *J Am Coll Cardiol* 2008; 52(5):333-342 [43]

The other drug commonly used in DES is the cytostatic agent paclitaxel, first isolated from the bark of *Taxus brevifolia* in 1971. Unlike sirolimus, it arrests the cell cycle irreversibly in G_2/M phase, by binding to the β-subunit of tubulin heterodimers and thus interfering with mitotic spindle formation [33] and blocking cell proliferation. Sustained release of paclitaxel has been used in commercial DES since 2004 and has been shown to reduce neointima formation by about 50%, compared to paclitaxel-free stents [30]. At present, paclitaxel is also the only cytostatic drug used in drug eluting balloons (DEB), devices used on patients unable to be stented. The clinical success rate of DEB has been found to lie between that of BMS and DES [38].

Table 1.1 gives an overview of commercially available drug eluting stents and the particular drugs incorporated into them.

Drug	Drug eluting stents (manufacturer)
Sirolimus	AMS 4.0 (Biotronik), Cypher, Cypher Select (Cordis), Excel (JW Medical Systems), Nevo (Johnson & Johnson), Ideal Biostent (Xenogenics)
Biolimus-A9	Axxess Plus (Devax), Biofreedom (Biosensors), Biomatrix (Biosensors), Nobori (Terumo)
Everolimus	BVS (Abbott), Promus Element (Boston Scientific), Xience-V (Abbott)
Zotarolimus	Endeavor, Endeavor Resolute (Medtronic)
Paclitaxel	AMS 3.0 (Biotronik), Conor (Conor Medsystems), Taxus, Taxus Express, Taxus Liberté (Boston Scientific)

Table 1.1. Antiproliferative drugs and corresponding DES commonly used in current clinical practice.

Unfortunately, while the immunosuppressive activity, especially on T cells, has been successfully reduced with some sirolimus analogs, they still exert their antiproliferative effect on endothelial cells, too. The same is true for paclitaxel (PES in **figure 1.5**). Because of their detrimental side effect on endothelial function, antiproliferative drugs as well as permanent polymers are likely causes of late ST and adverse cardiac events [30, 37]. Ongoing efforts to improve DES performance include the development of new polymers and polymer blends, optimization of drug release through coating architecture (intra-strut wells) and combination of antiproliferative agents with other drugs, for example sirolimus and triflusal (inhibitor of platelet cyclooxigenase, i.e. antithrombotic) or zotarolimus and dexamethasone.

While no selective inhibitor of SMC proliferation has been found yet, novel drugs are under investigation that efficiently inhibit these cells without compromising endothelial cell function.

1.3.3.3. Vascular grafts

In aortic and iliac surgery, where segments of relatively wide (diameter > 7 mm) blood vessels are replaced, synthetic vascular grafts rather than stents are widely used. Smaller diameter grafts are also available but their use is limited because of problems with intimal hyperplasia and surface thrombogenicity, resulting in comparatively poor long-term performance [44]. In the short term, there is practically no spontaneous endothelialization of small diameter synthetic grafts [45]. That is why autologous vein grafts are currently the best treatment option for small diameter applications [46].

Artifical blood vessels for tissue engineering are mostly made up of expanded polytetrafluoroethylene (ePTFE, teflon), polyethylene terephthalate (PET, Dacron) or polyurethane, i.e. polymers that are well suited mechanically to withstand shear stress and blood pressure, but that are also characterized by their tendency to act prothrombogenic [47]. Especially for the larger diameters, an attempt to overcome such complications was made with the introduction of fully bioresorbably scaffolds [32]. They safeguard the mechanical compliance of the affected vessel by initially providing scaffolding and then restoring physiologic function by disappearing altogether. Properties of existing synthetic materials that are detrimental to cell adhesion can also be overcome by coatings with ECM proteins or peptides derived from them [48, 49]. For example, the cysteine-alanine-glycine (CAG) trimer found in collagen type IV, mixed in with PCL, provides small-caliber grafts with patency for over 2 years *in vivo* [50].

1.4. Polymers as biomaterials

1.4.1. General characteristics

Polymers are made up of repetitive monomers. The monomers form chains that can be either crosslinked, branched, star-shaped or linear [51]. Depending on the arrangement of the monomers, the polymer as a whole is either amorphous or crystal-like. Chemical properties are also decisive in determining whether a polymer is biostable or biodegradable. Chemical bonds in biodegradable polymers can be cleaved under *in vivo* conditions, often enzymatically or by hydrolysis [52]. For physiological elimination of the degradation products, an important consideration in polymer selection is that the breakdown process sets in once those products have been reduced to a molecular weight of less than 50,000 g/mol [51].

The use of biomaterials for clinical applications is very widespread, as they are part of wound covers, dental and bone implants, cardiovascular stents and artificial organs.

Biopolymers are derived from natural sources (e.g. collagen, chitosan, hyaluronic acid) as opposed to synthetically produced polymers.

Biostable polymers will not be degraded under physiological conditions and are therefore regarded as inert. There are, however, problems with temperature dependent deformation and long-term hydrolysis and oxidative degeneration of these polymers. Examples include polymethyl methacrylate (PMMA) used in dental fillings, artificial teeth or as bone cement, polyetheretherketone (PEEK) used in spinal devices, hip prostheses, heart valves and stents, polysiloxane used in breast implants, artificial tendons and joints and PTFE used in artificial blood vessels [53].

Biodegradable polymers are commonly employed in suture material, tissue engineering scaffolds and as carriers in drug delivery systems. Conceptually, their use avoids the problem of long-term inflammation, as they become gradually replaced by host tissue. This also enables their use in children without compromising growth processes [51].

1.4.2. Foreign body reaction to biomaterials

In general, the insertion of implants or implant-related material into a living organism is associated with an immune response to that foreign body. This foreign body reaction (FBR) is sometimes described as encompassing the whole series of host reactions initiated by the implantation process [54], and sometimes referred to only as the end stage of those responses [55]. In any event, before host cells interact with an implanted device, the latter initially acquires a layer of host proteins. Local injury and contact with blood lead to unspecific adsorption of proteins such as fibrinogen on the implant surface [52, 55]. This

deposition of plasma protein equals the formation of a blood based provisional matrix, from which bioactive agents such as cytokines and other soluble mediators are released to modulate the subsequent wound healing response [55]. The provisional matrix at the tissue/material interface is the initial thrombus to which monocytes will trigger an acute inflammatory response: mediated by mast cells secreting IL-4 and IL-13, neutrophils are attracted to the implant site and monocytes will adhere [55, 56]. Depending on the extent of implantation-induced injury and the tissue involved, acute inflammation resolves within minutes to days [54, 55].

The early stage of FBR is followed by a chronic inflammatory stage, during which lymphocytes and plasma cells are transiently present [55, 56]. Under the influence of IL-4 and IL-13 derived from mast cells and T lymphocytes, the adherent monocytes differentiate to macrophages [55–57]. Maximum infiltration with macrophages, the principle cellular player in FBR, occurs within three days [54]. The cytokine stimulus activates them such that the mannose receptor, important for mediating phagocytosis and endocytosis, becomes upregulated and the monocyte-derived macrophages fuse to form multinucleated foreign body giant cells (FBGCs) [55–57]. This process occurs from seven to 14 days following implantation [55]. Regardless of implant durability, the first two to four weeks of its presence are the period in which the FBR is influenced by material properties [55]. Once inflammation is resolved, the wound healing response progresses with infiltration of fibroblasts and the separation of a one- to two-cell layer of macrophages and FBGCs from the implant: granulation tissue develops [55]. This is the precursor to fibrotic encapsulation of the implant [55, 57]. Fibrous capsule formation can seriously compromise implant function. The other major FBR-associated deleterious effect is biomaterial degradation through release of esterases, lipases, oxidants and other bioreactive intermediates by macrophages and FBGCs [55, 57]. Depending on the implant material, this degradation can impair function or result in device failure [55, 57].

Depending on the severity of the foreign body reaction, the following categorization of biomaterials has been established: 1. toxic materials, which promote cell death in the surrounding tissue, 2. inert materials, which become encapsulated by a fibrotic reaction, 3. bioactive materials, which allow for extensive interaction with and integration into the surrounding tissue and 4. biodegradable materials, which become replaced by autologous tissue and allow complete tissue regeneration [58].

1.4.3. Surface modification of polymers

In order to reduce inflammatory reactions to biomaterials and improve their interaction with the surrounding tissue, the surface is commonly altered, leaving the bulk characteristics of

the material mostly unchanged. Chemical activation of the polymer surface involves the generation of functional groups. These can interact with chemical motifs present on the cell surface much more readily than the otherwise inert polymer itself [59]. Depending on the type of the functional group, different bonds with extracellular molecules can be formed. Ester bonds that are formed upon the previous generation of hydroxyl groups, for example, are easily cleaved, whereas generation of amino groups allows the formation of physiologically more stable amid bonds [51]. Functional groups are also necessary to couple biomolecules (e.g. amino acids, polysaccharids, enzymes) to the polymer, and they can be generated by plasma chemical, wet chemical or photochemical modification.

Plasma activation means modification with ionized gas. Practically all polymers can be modified this way, and the kind of modification can be controlled by the gas employed. For example, oxygen plasma will generate hydroxyl groups, while nitrogen plasma will generate amino groups on the polymer surface. The depth of plasma activation is limited to about 5 nm [60].

Wet chemical modification potentially reaches further down into the polymer bulk, depending on reaction conditions, e.g. solvents used in the process. For example, sodium hydroxide can be used to break ester bonds and increase the number of functional groups on the polymer surface.

Targeted local modification is possible through photochemical modification, where the polymer is subjected to high-energy ultraviolet radiation. This breaks chemical bonds and releases free radicals which in turn leads to crosslinking or generation of functional groups [61].

Another form of surface functionalization is the concept of biomimetic coatings. Here adverse host responses are avoided by the generation of 3D scaffolds supporting cell adhesion, growth and differentiation [62]. Whereas biomimetic materials can be made up entirely of ceramics, metal or synthetic polymers, biomimetic coatings utilize biological substances such as fibronectin, collagen, vitronectin or other macromolecules from the extracellular matrix to cover non-biological materials [62]. They are applied in vascular stents, tooth or bone implants.

1.5. Concept of biocompatibility

Biocompatibility is the ability of a material to perform with an appropriate host response in a specific application, marked by the absence of adverse effects [63]. More precisely, it is the sum of all material characteristics that relate to tissue integration and direct interaction with cells and their adhesion, growth, and differentiation [62].

For any implant material, it is essential that it is well tolerated by the receiving organism. Material-induced complications such as inflammation need to be minimized as much as possible. This can be achieved through a multitude of manipulations of the material in question, such as coating with ECM proteins or surface roughening by mechanical or chemical methods [62]. Therefore a multi-stage testing process must be undergone by new materials in which *in vitro* testing precedes animal and clinical testing. In cell culture experiments, viability and proliferation tests are proven methods to assess cytotoxicity and biocompatibility of new materials. For cell viability, several assays are available in which enzymatic activity can be assessed by comparison to appropriate controls. Often aided by changes in fluorescence patterns, the reaction of enzyme and substrate can be reliably measured on the premise that the more viable the cells are, the more metabolic activity there will be to detect.

1.6. VEGF and angiogenesis

1.6.1. Molecular variety of the VEGF family

Vascular endothelial growth factor (VEGF) is specific for endothelial cells. Its two major biological effects are the control of vascular development during embryogenesis and the control of blood and lymph vessel function in the adult [64]. The family of five mammalian VEGFs (types A, B, C, D and placental growth factor, PlGF) is multiplied further by alternative splicing and processing [65]. As a result of 14 alternative splicing events, combined with two polyadenylation signals, two promoters and eight exons, the human VEGF-A gene can give rise to 56 potential mRNAs [66]. Because it contains the largest variety of regulatory elements, VEGF-A mRNA has been coined a paradigm for complex regulation of gene expression at the post-transcriptional level [66]. The various mRNAs are translated into either free soluble proteins that primarily act as endothelial mitogens, or heparin-binding surface proteins that control vascular permeability [67]. VEGF family members regulate all types of vascular growth, i.e. sprouting of capillaries from pre-existing capillaries (angiogenesis), generation of muscular collateral vessels form arteriolar anastomoses (aretiogenesis) and lymph vessel growth from pre-existing lymphatic vessels (lymphangiogenesis) [68]. During embryonic development of the vasculature, VEGF-B, VEGF-D and PlGF seem to not be required, whereas VEGF-A and VEGF-C are essential [68]. How critical a factor in vascular development VEGF really is is illustrated by the fact that targeted inactivation of a single murine VEGF allele results in early embryonic lethality [69]. Apart from being essential and rate-limiting in physiological angiogenesis [70], VEGF also facilitates re-endothelialization of the lining of vessels that get inevitably damaged during stent implantation [71]. VEGF-A expression becomes progressively increased in

atherosclerosis and in-stent restenosis, which is thought to be a secondary effect of local hypoxia and inflammation [68]. Upregulation of VEGF-A is also important for tissue repair and for angiogenesis in skeletal muscle induced by physical exercise [68]. The angiogenic effect of VEGF is mediated first and foremost by the production of nitric oxide [7].

1.6.2. VEGF receptors

The various isoforms of VEGF exert their effects through three structurally related receptor tyrosine kinases and affinity-increasing coreceptors (such as neuropilins 1 and 2 and integrins). VEGF receptor-1 (VEGFR-1, also called Flt-1) as a receptor for PlGF and VEGF-B is important for recruitment of myelomonocytic cells in inflammatory responses [64]. VEGFR-2, also called Flk-1 or kinase-insert domain-containing receptor (KDR), mediates the mitogenic function of VEGF-A, as well as its effects on endothelial cell migration, invasion and microvascular permeability [72]. VEGFR-3 only binds the large precursors and proteolytically cleaved forms of VEGF-C and -D, with the processed forms having increased receptor affinity and more angiogenic potential, while the unprocessed precursors mainly promote lymphangiogenesis [68, 72]. Differential ECM-binding properties and proteolytic processing of its multiple isoforms drive an interplay between diffusible and ECM-bound VEGF that is the basis for angiogenic gradients shaping the vascular system [65]. The chemotactic effect of VEGF on endothelial cell migration is mediated through VEGFR-2 and phosphorylation of eNOS by the protein kinase Akt [73]. Other molecules required for VEGF signal transmission include VE-cadherin, β-catenin, PI3 kinase and Bcl-2 [69]. This signalling pathway induces lamellipodia formation in endothelial cells [74].

1.6.3. Animal models

In animal models, VEGF has been reported to reduce neointimal area [75]. Suppression of SMC proliferation, as well as antithrombotic and vasodilative effects appear to be mediated through low local concentrations of VEGF-A [68]. However, intimal hyperplasia can also be induced by VEGF when released from ePTFE grafts [76]. Medium concentrations (150 ng/d) of VEGF induce a constant increase in vascularisation even after VEGF supply ceases, as opposed to transient (if higher) vessel growth into porous scaffolds with high concentrations (1.5 µg/d) of VEGF [70].

Among the widespread effects of VEGF is the upregulation of endothelial NO synthase (eNOS) [70] as well as inhibition of platelet and leukocyte activation and of smooth muscle cell proliferation [28]. All of these are desirable outcomes in the context of vascular stent implantation, which served as motivation here to test the effects of VEGF stimulation on human umbilical vein endothelial cells (HUVECs) growing on a functionalized biopolymer.

1.7. The extracellular matrix

1.7.1. Molecular composition

The extracellular matrix (ECM) is a highly complex mesh made up of fibrous proteins, proteoglycans, hyaluronic acid and other glycosaminoglycans. The proteoglycans, consisting of a protein at the core and up to 95% carbohydrate, form a hydrogel in which fibrous proteins are embedded [77]. Proteoglycans also act as growth factor carriers and regulators of matrix assembly [62] and, by virtue of their highly sulfated, negatively charged glycosaminoglycan side chains, are responsible for turgor, elasticity and biomechanical pressure resistance of many tissues [62]. Abundant proteins of the ECM include elastin, collagen, fibrillin, vitronectin, laminin and fibronectin. These are mostly glycoproteins in which the carbohydrate content is less than 60% [77]. Abundant proteoglycans are versican in the skin and aggrecan in cartilage, present mostly in large complexes with hyaluronic acid. The exact biochemical composition, geometry and density of the ECM varies greatly from tissue to tissue, but in every instance provides a reservoir of signaling molecules and structural support that determine the anchorage and behavior of cells [76]. Moreover, the ECM has an impact on the metabolism of cells, their shape, development, migration, and proliferation [77]. Integrins on the cell surface and peptide epitopes contained in ECM molecules are crucial in mediating signals between cells and the ECM.

Most of the ECM proteins can be crosslinked through adapter molecules such as heparin sulphate, or can form complex heterodimers and heterotrimers [78]. For example, the laminin family consists of about 20 different heterotrimeric glycoproteins [62]. Fibronectin consists of two very large subunits (each almost 2,500 amino acids long) that each contain domains for binding heparin, integrin and collagen [77]. The three-dimensional makeup of the ECM molecules, its density, stiffness and other physical properties are more indirect cues for cell growth, differentiation and migration [62].

The synthesis of ECM components is also a hallmark of tissue inflammation. In the context of atherosclerosis, the arterial wall produces fibrils and fibers that entrap lipoproteins which can then associate with matrix components – the beginning of plaque formation. Further growth of the plaque involves an enormous upregulation of collagen production, up to a point where it constitutes 60% of the plaque itself [24].

1.7.2. The role of the ECM in implant biology

Molecules from the ECM or cell adhesive peptides derived from such molecules are widely used in implants and tissue engineering to functionalize synthetic surfaces, as they promote adhesion and proliferation of endothelial cells [48, 76]. The ECM itself has become a therapeutic target for inflammatory diseases in general: so-called protective ECM mimetics

are under development as therapeutic devices [24]. Coating with adhesive molecules from the extracellular matrix is one of three basic strategies to design biomimetic materials [62]. Because of the reported pro-endothelialization effects, this study includes the coating of a polymer with three different matrix proteins.

1.8. PCL as biomaterial

In the context of tissue engineering and artificial heart valves, polycaprolactone (PCL) is well investigated and distinguished by its biodegradability [79] and comparatively fast endothelialization [19], along with a lack of toxicity [46]. Degradation of this biodegradable aliphatic polyester happens predominantly through nonenzymatic hydrolytic cleavage [80]. *In vivo*, this leads to a breakdown of the PCL chain structure (figure 1.6) into low molecular weight fragments, which eventually can be phagocytosed. In rats, degradation studies of implanted PCL have found the molecular weight of the polymer reduced by 20-30% over three to six months, depending on arterial pressure and blood flow (reviewed in [81]).

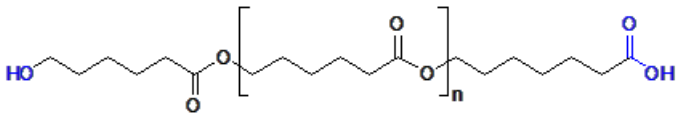

Figure 1.6. Chemical structure of poly(ε-caprolactone)

PCL was initially developed to be used in bioabsorbable surgical threads for bone sutures [62], but, interestingly, has also been used as a long-term contraceptive device [19]. In the cardiovascular setting, PCL is currently under investigation as scaffold material for small diameter vascular grafts in the treatment of CAD. Compared to the standard ePTFE used in large diameter grafts, it has been found to allow faster ECM formation and endothelialization and to facilitate the vascular healing process better: in a study where electrospun PCL nanofiber grafts (inner diameter 2 mm) were implanted into rat infrarenal abdominal aorta, the luminal surface of the prostheses showed 97% endothelial coverage 6 weeks later, and 100% at 12 weeks after implantation [81]. Concurrently, only a thin layer of neointima formed that stopped growing around 18 weeks after implantation. Another favorable PCL graft healing characteristic demonstrated in that study was low level chronic foreign body reaction, as evidenced by 50-60% transmural cellular infiltration of the graft body by macrophages and fibroblasts after 12 weeks, without any signs of chronic inflammation [81].

Another example for the biomedical use of PCL is the sirolimus loaded Xinsorb bioresorbable scaffold, where PCL is part of the polymer blend and which in an

experimental *in vivo* study in the porcine coronary artery model was shown to cause less restenosis (in terms of percentage of the implanted segment's diameter) than the sirolimus eluting Excel stent (reviewed in [32], see table 1). Moreover, electrospinning as the means of PCL scaffold production was reported to convey additional benefits for directional mechanical properties through engineered complex nanofiber orientation architecture with ECM-mimicking structures [46].

Here different morphologies and differently activated surfaces of PCL are systemically examined, as well as the impact of a growth factor stimulus, with respect to its potential as implant material with optimized properties for endothelialization.

1.9. Research aims and motivation

Taking the clinical experience with currently used cardiovascular stents and grafts into account, enhancing the stent surface for colonization with endothelial cells is a prerequisite for the accelerated formation of an intact endothelium at the implant site. Although numerous approaches in that regard have been made and in part even been transferred to the clinical practice, no solution has yet been found that yields smooth and quick endothelialization of the implant. Creating a truly endothelial-friendly implant surface is one of the biggest challenges in designing new vascular devices. Once the effect of a certain stimulus is established, the question arises how to best incorporate the molecule of interest into a biomaterial. The luminal surface is where the interaction with the patient's blood and immune system occurs, making it the target point for biomaterial designers to exert the bulk of mechanical and chemical engineering. Singling out PCL as a model polymer, this thesis is therefore concerned with a systematic study of the effect of a multitude of polymer surface modifications on the behavior of endothelial cells *in vitro*.

In addition, surface coating of the modified polymer with ECM proteins and cell stimulation with a specific growth factor are applied in an attempt to make use of biomolecules to facilitate the growth of endothelial cells on the biomaterials under investigation. It is clear that the *in vitro* examination of molecules responsible for interendothelial contact (and hence for barrier function) is useful for determining a biomaterial's endothelial cell compatibility [82]. Yet there are comparatively few studies looking at the molecular crossroads of signal transduction that becomes modulated by modification of the surface the signaling cells adhere to. Therefore important marker molecules for endothelial function have been selected here for quantitative gene expression analysis, to gain insight into what mechanisms on the molecular level might be at the root of differential cell behavior.

After establishing a suitable *in vitro* model for the evaluation of specific surface modifications of a model polymer and their effects on polymer endothelialization, the work undertaken during the course of this thesis is to provide answers to the following questions:

1. Which PCL modification increases endothelial cell adhesion the most?
2. Are there additional benefits to be had by endothelial cell stimulation with VEGF?
3. Can cumulative pro-endothelialization effects be achieved by PCL coating with ECM proteins?
4. In what way will the different polymer modifications alter mRNA expression of selected endothelial cell marker molecules?

2. Materials and Methods

2.1. Reagents and materials

2.1.1. Chemicals

All chemicals were of p. a. quality or higher and ordered from one of the following suppliers: Boehringer Ingelheim (Ingelheim), GibcoBRL (Life Technologies, Carlsbad, U.S.), Invitrogen (Life Technologies, Carlsbad, U.S.), Roche Molecular Biochemicals (Grenzach-Wyhlen), Sigma-Aldrich (Seelze), Mallinckrodt Baker (Griesheim), Serva Feinbiochemica (Heidelberg), Thermo Fisher Scientific (Karlsruhe) or Merck (Darmstadt). Industrial grade poly(ϵ-caprolactone) (PCL, CAPA 6800, M = 80,000 g/mol) was from Perstorp Holding AB (Warrington, U. K.).

2.1.2. Culture media and solutions

The following were prepared from commercially available ingredients:

Name	Ingredients
human umbilical vein endothelial cell (HUVEC) growth medium	10% (v/v) fetal calf serum (FCS; GibcoBRL), 0.1 ng/ml epidermal growth factor (EGF; Biomol, Hamburg), 1 ng/ml basic fibroblast growth factor (bFGF; Biomol, Hamburg), 5 U/ml heparin (Biochrom/Merck Millipore, Berlin), 1 µg/ml hydrocortisone (Sigma-Aldrich), 0.4% (v/v) endothelial cell growth supplement (ECGS; PromoCell, Heidelberg), 100 µg/ml penicillin (GibcoBRL), 100 µg/ml streptomycin (GibcoBRL), 2 mM L-glutamine (GibcoBRL) in MCDB131 reduced serum supplemented medium (PAN Biotech, Aidenbach)
HUVEC arrest medium	0.5% (v/v) FCS, 0.1 ng/ml EGF, 1 ng/ml bFGF, 5 U/ml heparin, 1 µg/ml hydrocortisone, 0.4% (v/v) ECGS, 100 µg/ml penicillin, 100 µg/ml streptomycin, 2 mM L-glutamine in MCDB131 reduced serum supplemented medium
EC basal medium	2.5% (v/v) FCS, 100 µg/ml penicillin, 100 µg/ml streptomycin, 2 mM L-glutamine in MCDB131 reduced serum supplemented medium

Name	Ingredients
human coronary artery endothelial cell (HCAEC) growth medium	5% (v/v) FCS, 0.4% (v/v) ECGS, 10 ng/ml recombinant human EGF, 1 µg/ml hydrocortisone, 22.5 µg/ml heparin in endothelial cell growth medium (PromoCell, Heidelberg)
10× phosphate buffered saline (PBS)	1.5 M sodium chloride, 100 mM sodium hydrogenorthophosphate, 40 mM potassium dihydrogen orthophosphate, adjusted to pH 7.4
Live/dead stain solution	0.00125% (v/v) calcein AM (Invitrogen), 0.0025% (v/v) ethidium homodimer (Invitrogen) in PBS (pH 7.4)
Phalloidin stain solution	Phalloidin-FITC (1 µg/ml; Sigma-Aldrich), 0.0025% (v/v) ethidium homodimer (Invitrogen)

Table 2.1. Culture media and solutions.

2.1.3. Primers for quantitative real-time PCR

primer name	gene name	primer sequence	PCR product size	NCBI reference sequence
eNOS qFwd	nitric oxide synthase 3 (endothelial cell) (NOS3)	GAG ACT TCC GAA TCT GGA ACAG	102 bp	NM_000603.4
eNOS qRev	nitric oxide synthase 3 (endothelial cell) (NOS3)	GCT CGG TGA TCT CCA CGTT	102 bp	NM_000603.4
ICAM-1 qFwd	intercellular adhesion molecule 1	TTG AAC CCC ACA GTC ACC TAT	190 bp	NM_000201.2
ICAM-1 qRev	intercellular adhesion molecule 1	CCT CTG GCT TCG TCA GAA TCA	190 bp	NM_000201.2

primer name	gene name	primer sequence	PCR product size	NCBI reference sequence
IL-8 qFwd	interleukin 8	CTC TTG GCA GCC TTC CTG ATT	147 bp	NM_000584.3
IL-8 qRev	interleukin 8	ACT CTC AAT CAC TCT CAG TTCT	147 bp	NM_000584.3
PECAM-1 qFwd	platelet/ endothelial cell adhesion molecule 1	CAA CGA GAA AAT GTC AGA	259 bp	NM_000442.5
PECAM-1 qRev	platelet/ endothelial cell adhesion molecule 1	GGA GCC TTC CGT TCT AGAGT	259 bp	NM_000442.5
VCAM-1 qFwd	vascular cell adhesion molecule 1	GCT GCT CAG ATT GGA GAC TCA	100 bp	NM_001078.3
VCAM-1 qRev	vascular cell adhesion molecule 1	CGC TCA GAG GGC TGT CTATC	100 bp	NM_001078.3
18SrRNA qFwd	18S ribosomal RNA rDNA	GGT TCG AAGACG ATC AGA TACC	344 bp	NR_003286.1
18SrRNA qRev	18S ribosomal RNA rDNA	TCG TTC GTT ATC GGA ATT AACC	344 bp	NR_003286.1

Table 2.2. Primers for real-time PCR. The 18S rRNA primers were established in the laboratory as qPCR reference for endothelial cells and were designed with Primer 3 software [83]. The sequences for PECAM-1 were taken from Kirschbaum et al. [84], and the remaining primer sequences were taken from Tersteeg et al [85]. Primers were ordered from Eurofins Genomics (Ebersberg).

2.2. Preparation of polymer and chemical activation

Work on this thesis was conducted in conjunction with another doctoral thesis [51] that was carried out in the chemistry group of the Institut für Biomedizinische Technik at the University of Rostock. All methods relating to the chemical preparation of the examined materials that were performed by chemists have therefore been separated from the material and methods section and can be found in the appendix.

2.3. Electron microscopy of PCL surface modifications

PCL samples were imaged without the need for precoating in an XL-30 field emission environmental scanning electron microscope (Philips, Eindhoven, NL) at 1.07-1.33 mbar and high voltage of up to 10 kV.

2.4. Isolation of endothelial cells

Umbilical cords were obtained from donors with their informed consent (University of Rostock ethics committee approved protocols II HV 09/2000 and II HV 38/2004). HUVECs were isolated through enzymatic digestion protocol (10 min with 0.05% collagenase II at 37°C, rinsing, 10 min centrifugation at 50 g) and identified by their characteristic polygonal shape and cobblestone growth pattern *in vitro*. Then they were cultured as primary cells in MCDB131-based optimized endothelial cell medium (see below) at 37°C, 95% humidity and 5% CO_2 through to passage 6. MCDB131 base medium was from PAN Biotech (Aidenbach).

2.5. Endothelial cell culture

HUVECs were cultured as primary cells in MCDB131-based optimized endothelial cell medium (0.1 ml/ml fetal calf serum, lowered to 0.025 ml/ml during VEGF stimulation, 0.1 ng/ml EGF, 1 ng/ml bFGF, 100 U/ml penicillin, 100 µg/ml streptomycin, 2 mM L-glutamine; different concentrations were applied during the series of optimization experiments) at 37°C, 95% humidity and 5% CO_2 through to passage 6. Human coronary artery endothelial cells (HCAECs) were cultured in endothelial cell medium (PromoCell). Cells were passaged as follows: wash cells for 15 s with 3 ml 4-(2-hydroxyethyl)-1-piperazineethanesulfonic acid (HEPES), remove HEPES, add 2 ml of trypsin, monitor cell detachment at room temperature under a TS100 light microscope (Nikon, Düsseldorf), add 4 ml trypsin neutralising solution (TNS), transfer cells into a 15 ml tube, pellet in a Universal 32 R centrifuge (Andreas Hettich GmbH & Co. KG, Tuttlingen) at 1100 rpm for 3 min, resuspend cells in 6 ml medium. Under the light microscope, cells were counted in a hemocytometer. Cells were seeded in 75 cm^2 tissue culture flasks at a density of about 1×10^4 cells/cm^2.
In experiments with cell cycle arrest, the endothelial cells were starved for 24 h in arresting medium (0.005 ml/ml fetal calf serum, 0.1 ng/ml EGF, 1 ng/ml bFGF, 100 U/ml penicillin, 100 µg/ml streptomycin, 2 mM L-glutamine).

2.6. VEGF stimulation of HUVECs and HCAECs

$VEGF_{165}$ was purchased from Pepro Tech Inc. (Rocky Hill, USA) and dissolved in sterile water to prepare a stock solution of 0.1 mg/ml. For stimulation of primary cells, working solutions were prepared in optimized endothelial cell medium. Endothelial cells were cultured until passage 3 and 24 h before stimulation, their cell cycle was reversibly arrested by depletion of growth factors and fetal calf serum from the culture medium. For direct VEGF stimulation, the culture medium was deprived of a number of growth factors and additives, including epidermal growth factor, basic fibroblast growth factor, and an 'endothelial cell growth supplement' (ECGS) of unknown content by a commercial provider (PromoCell). In the case of qPCR analysis (see sections 2.10-2.12), VEGF stimulation was for 24 h. One passage prior to the polymer tests, their response to VEGF was tested as follows: 3000 cells were seeded per well in a 96-well microtiter plate (Greiner BIO-ONE, Frickenhausen) and then stimulated for 96 h with 0.5, 1, 10, 25, 50,75 or 100 ng/ml VEGF. After 96 h, cell viability and proliferation was quantified.

2.7. Biocompatibility assays

All experiments included untreated cells as a control, polystyrene as control substrate, and a cell treatment control with 10^{-4} M tetraethylthiuram disulfide (TETD). This cytotoxic substance was used to demonstrate cell susceptibility to poisoning, as it drastically reduces the readouts in biocompatibility assays. Where polymer films were involved, circular discs (Ø = 6 mm; in the case of subsequent qPCR analysis: Ø = 10 mm) were punched, washed three times and fastened at the bottom of microtiter wells with the aid of teflon rings. These held the samples in place while allowing cells to be seeded and grown on the disc surface, i.e. the rings served to standardize growth conditions. To exclude potential bias introduced by the presence of the rings during the biocompatibility assay measurements, identically treated cells were allowed to adhere to the films in the presence of slightly differently shaped teflon rings and subjected to the standard measurements. Depending on the wall thickness of the rings, all measurements were skewed towards higher absolute readings compared to those without the rings **(appendix A.6).** Therefore, in obtaining the data presented here, all teflon rings had to be removed before the actual tests, or the CQB medium was transferred onto a fresh microplate before fluorescence readings.

As both PCL films and microwells are circular, the cell density is calculated by the following formula: $D=\pi/\pi \times r^2$, with n=number of cells seeded per well and r=substrate radius.

2.7.1. Cell viability assay

Cell viability was determined with the CellQuanti-Blue (CQB) assay (BioAssay Systems, Hayward, USA), a test detecting metabolic activity in living cells. Specifically, this assay measures the activity of intracellular reductases reducing resazurin substrate to resorufin. Cells were seeded in a 96-well microtiter plate. CQB medium was added to each well including the blank wells (wells without cells) after 96 h incubation, and the plates were returned to the incubator at 37°C for 2 h. Fluorescence signals were measured in a Fluostar Optima plate reader (BMG Labtech, Ortenberg) using an excitation wavelength of 542 nm and an emission wavelength of 590 nm. The fluorescence intensity obtained is directly dependent on the activity of the cells.

2.7.2. Cell proliferation assay

For measuring cell proliferation, 5-bromo-2'-deoxyuridine (BrdU) was added to the cells 18 h prior to testing and the incubation at 37°C continued. Then the medium was removed, cell fixation solution (200 µl per well) from the chemiluminescent BrdU-based cell proliferation assay (Roche Diagnostics GmbH, Mannheim) was added to the cells for 30 min at room temperature, then removed. Anti-BrdU antibody (HRP-conjugated) was diluted 1:100 and added to each well (100 µl) before a 90 min incubation period at room temperature. After removing the antibody solution, the samples were washed three times, and 100 µl substrate were added to each well, followed by 5 min shaking at 500 rpm. Luminescence was read in the Fluostar Optima plate reader within 10 min of adding the substrate.

2.7.3. Eluate test

Untreated plain PCL, PCL/HMDA, PCL/MDI/NH_3, PCL/O_2 plasma and thermanox as reference polymer were tested for their effect on HUVEC growth. The test materials were eluted (6 cm^2/ml) at 37°C in serum-free HUVEC growth medium for 24 h with vigorous shaking according to DIN 10993-12. 2000 cells per well were seeded and allowed to adhere to the microtiter plate for 24 h. Then a dilution series of the eluates was prepared (down to 1:32), the growth medium was removed from the cells and replaced with eluate in the different dilutions. HUVECs were incubated with the respective eluates for 48 h under standard culture conditions and then cell viability and proliferation was measured as described above.

2.8. ECM protein precoating

Fibronectin (cat.no. F2006), collagen I (cat.no. C7661) and laminin (cat.no. L2020) were all purchased from Sigma-Aldrich. Stock solution (1 mg/ml) was diluted in cell culture medium directly prior to coating. PCL films (6 mm discs), thermanox discs (6 mm) and polystyrene wells of 96-well microtiter plates were all treated equally for coating purposes, with 40 µl protein solution per microwell. Pure culture medium was used for non-coating controls. Coating conditions were 60 min at 37°C, followed by aspiration of the coating solution and two 10 min washes with sterile water. Homogeneity of the protein layer was confirmed by fluorescent labeling of amino groups and subsequent CLSM.

2.9. Confocal laser scanning microscopy

In parallel to biocompatibility testing, identically treated samples were stained using the Live/Dead viability/cytotoxicity kit (Invitrogen). For Live/Dead staining the reagents calcein AM and ethidium homodimer were diluted (1:800 and 1:400, respectively) in phosphate buffered saline (PBS, pH 7.4), mixed and 200 µl of the mixture was applied to the cells, followed by incubation at room temperature for one hour. Calcein AM is a precursor molecule that is taken up by viable cells and cleaved by intracellular esterases to form the fluorescent green cytosolic marker calcein. Ethidum homodimer is a fluorescent dye that cannot permeate intact cell membranes and therefore accumulates in non-viable cells. There its high affinity for DNA causes the labeling of these cells via emission of red fluorescent light. For phalloidin staining the cells were fixed in 4% formalin and incubated for 30 minutes with fluorescein isothiocyanate (FITC) labeled phalloidin (1 µg/ml) at room temperature. Phalloidin binds to actin filaments and therefore stains the cytoskeleton.

Confocal micrographs were obtained using a Fluoview FV1000 (Olympus, Hamburg) system.

2.10. Isolation and purification of RNA

For the purpose of mRNA expression analysis, endothelial cells were seeded onto 10 mm polymer discs at 15,000 cells/cm^2 in a 48-well microtiter plate and allowed to adhere for 24 h. Then a 24 h stimulation period with 25 ng/ml VEGF followed. After these two days of growth, the medium was drained from the cells, 300 µl Trizol reagent were added to the wells containing substrate and cells, and the suspension was collected in 2 ml RNase-free reaction tubes. After adding 30 µl chloroform, the samples were homogenized by thorough shaking for 1 min, then incubated for 5 min at room temperature. After 5 min, the mix was

centrifuged at 4°C and 12,000 g for 5 min, yielding three separated phases. The aqueous upper phase containing RNA was transferred to a new RNase-free microtube and another 200 µl Trizol (Invitrogen) and 20 µl chloroform were added. After vigorous shaking and 3 minutes incubation at room temperature, the samples were centrifuged again at 12,000 g for 2 min. Then the aqueous upper phase was transferred to a new RNase-free microtube and an equal volume of 70% ethanol was added. After thorough shaking, this mix was transferred onto an RNeasy spin column (Qiagen, Hilden), then centrifuged at 12,000 g for 15 s. The flow-through was discarded and 350 µl wash buffer RW1 (Qiagen) was pipetted onto the column, which was then centrifuged at 12,000 g for 15 s. The flow-through was again discarded. To exclude DNA contamination of the RNA, the sample was digested with DNase I for 15 min at room temperature. Again 350 µl wash buffer RW1 was applied to the spin column, and after 15 s centrifuging at 12,000 g the flow-through was discarded. The column was inserted into a new RNase-free collection tube, 500 µl wash buffer RPE (Qiagen) were applied, and after 15 s centrifuging at 12,000 g the flow-through was discarded. After adding another 500 µl buffer RPE, the samples were centrifuged at 12,000 g for 2 min and after discarding the flow-through again for 1 min, to dry the column. Finally the purified RNA was eluted with 30 µl RNase free water and 2× centrifugation at 12,000 g for 1 min. RNA concentration was measured with an Ultrospec 2000 photometer and RNA quality assessed by the ratio (absorbance at 260 nm): (absorbance at 280 nm).

2.11. Reverse Transcriptase-PCR

RNA was transcribed into cDNA using the RevertAid First Strand cDNA Synthesis Kit (Thermo Fisher Scientific) as follows: total RNA (200 ng per sample) was first primed with 275 ng of random hexamers at 70°C for 5 min. After the addition of first strand buffer (final concentration 50 mM Tris-HCl, 50 mM KCl, 4 mM $MgCl_2$, 10 mM DTT), ribonuclease inhibitor (0.5 U/µl) and dNTPs (1 mM), a 5 min incubation at room temperature was followed by the addition of M-MuLV reverse transcriptase (2 U/µl of final reaction volume). Reverse transcription was performed for 90 min at 37°C, followed by 10 min heat inactivation of the enzyme at 70°C. A control of total RNA in the absence of reverse transcriptase was included to exclude genomic contamination of the RNA samples. The resulting cDNA was diluted 1:7 in sterile water and stored at -20°C.

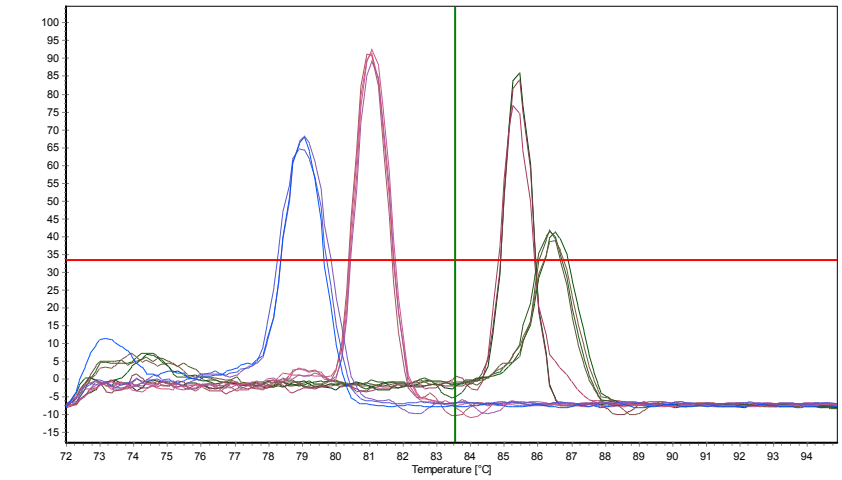

Figure 2.1.
Melting curve analysis of HCAEC/PCL/NH_3 plasma/fibronectin (C7) qPCR on IL-8 (blue), PECAM-1 (purple), ICAM-1 (brown) and eNOS (green) showing specificity of PCR products.

2.12. Quantitative PCR

In twintec 96-well source plates (Eppendorf), 7.5 µl Platinum SYBR Green qPCR Supermix containing *Thermus brockianus* DNA polymerase (Invitrogen), 3.0 µl primer mix (containing 1 pmol/µl each of fwd and rev primers) and 4.5 µl diluted cDNAs were pipetted per well. No-template controls were also performed to ensure specificity of the PCR amplification. The plates were sealed with adhesive optical film (BZO Seal Film, Biozym Scientific GmbH). In an Eppendorf Mastercycler, PCRs were done as 15 µl reactions with the following cycle conditions: 15 min initial denaturation at 95°C, 40 PCR cycles (12 s denaturation at 94°C, 25 s annealing at 56°C, 30 s extension at 72°C), 5 min final extension at 72°C, followed by 15 s at 72°C, a 20 min ramp to 95°C, 15 s at 95°C and 1 min at 20°C for melting curve analysis of the PCR products (**figure 2.1**). Results were quality controlled (figures 2.1 and 2.2) with realplex software (Eppendorf) and analysed with the $2^{-\Delta\Delta Ct}$ method [86].

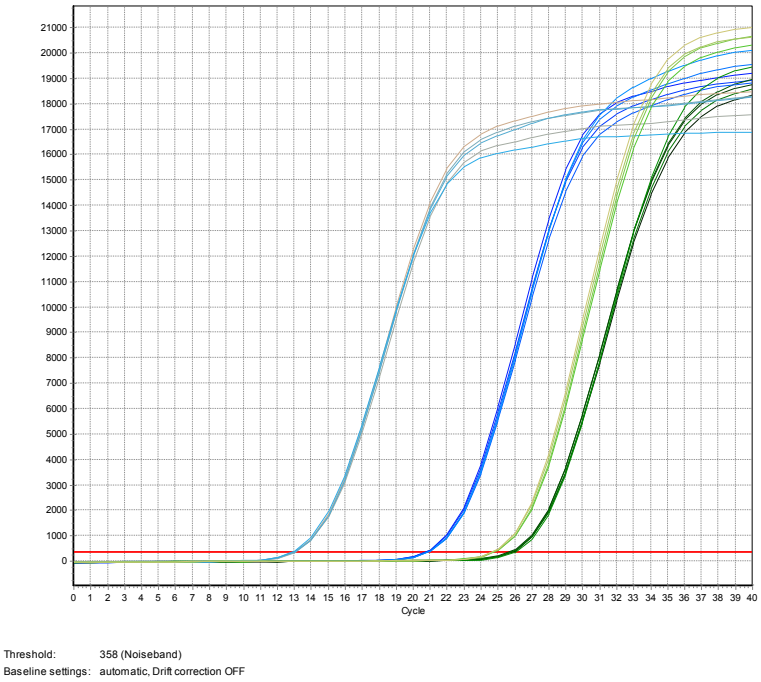

Figure 2.2.

Amplification plots of cDNA from HUVECs grown on PCL/O_2 plasma and stimulated with VEGF. PCR on 18S rRNA (grey), ICAM-1 (olive), PECAM-1 (blue) and IL-8 (green) showing reproducibility of single-well reactions.

2.13. Statistical analysis

Data were analyzed using the SPSS statistical package 21.0 (SPSS Inc., Chicago, Illinois, USA). Descriptive statistics were computed for continuous and categorical variables. The statistics computed included mean and standard deviations (SD) of continuous variables and are presented as mean±SD and percentage frequencies of categorical factors. For cell culture experiments, means and standard deviations were calculated from 8 individual measurements per condition. For differences between individual values, the square root of the sum of the squares of the two individual SD values yielded the SD of the difference. For normalization purposes, the raw data were standardized prior to analysis as follows: the microtiter plate-specific mean of the blank values (cell culture medium only) was divided by a ratio R, with R = (mean of untreated control cells on polystyrene) : (mean of blanks). This normalized blank value was then subtracted from all raw data of each microtiter plate, such that values from individual experiments became comparable. A two-directional t test was also used for statistical analysis. Generally, to evaluate statistical significance between groups, a two-way or one-way analysis of variance (ANOVA) was used to examine the influence of categorical, independent variables on one dependent variable. All p-values <0.05 which resulted from two-sided statistical tests were considered to be statistically significant. Over the series of PCL testing with HUVECs from three different donors, a univariate analysis of variance was used to evaluate statistical significance.

2.13.1. Nalimov test for outliers

The Nalimov test is particularly suited to test for outliers in small to medium sample sizes [87]. It is based upon the assumption of normality. A particular value x_1 is identified as an outlier if the statistic q

$$q = \left| \frac{x_1 - \bar{x}}{s} \right| \sqrt{\frac{n}{n-1}}$$

$\bar{x}$.... *mean of all values (incl. the value* x_1*)*
s .... standard deviation of all values
n .... number of values

exceeds the critical threshold q_{crit} for a given level of significance. If the calculated value of q is greater than the critical threshold, then the corresponding data value x_1 is regarded to be an outlier. The threshold values and corresponding levels of significance are listed in appendix table A1.

3. Results

3.1. Morphology of the polymer samples

Plain PCL presented with an overall wavy and cobblestone-like surface under the environmental scanning electron microscope (**figure 3.1**a). Electrospun PCL showed a pattern of irregularly interwoven PCL fibers that are approximately 5 µm wide (figure 3.1b). PCL etching with NaOH resulted in surface roughening with elongated cracks and cavities (figure 3.1c). Salt leaching produced cavities in the polymer that are 8 to 30 µm wide and make for a highly irregular surface structure (figure 3.1d). Neither chemical activation with O_2 plasma (figure 3.1e) nor with NH_3 plasma (figure 3.1f) nor with aminopropyltriethoxysilane (APTES, figure 3.1g) nor with hexane-1,6-diamine (HMDA, figure 3.1h) resulted in morphological changes of the plain polymer surface. The surface reaction of PCL with 4,4′-methylenebis(phenyl-isocyanate) (MDI) produced very fine cracks of up to 300 µm in length in the otherwise preserved wavy surface (figure 3.1i). All changes to the polymer surface, including manipulation of the morphology, wet chemical and plasma chemical activation, were verified by contact angle measurement. The corresponding figure can be found in the appendix.

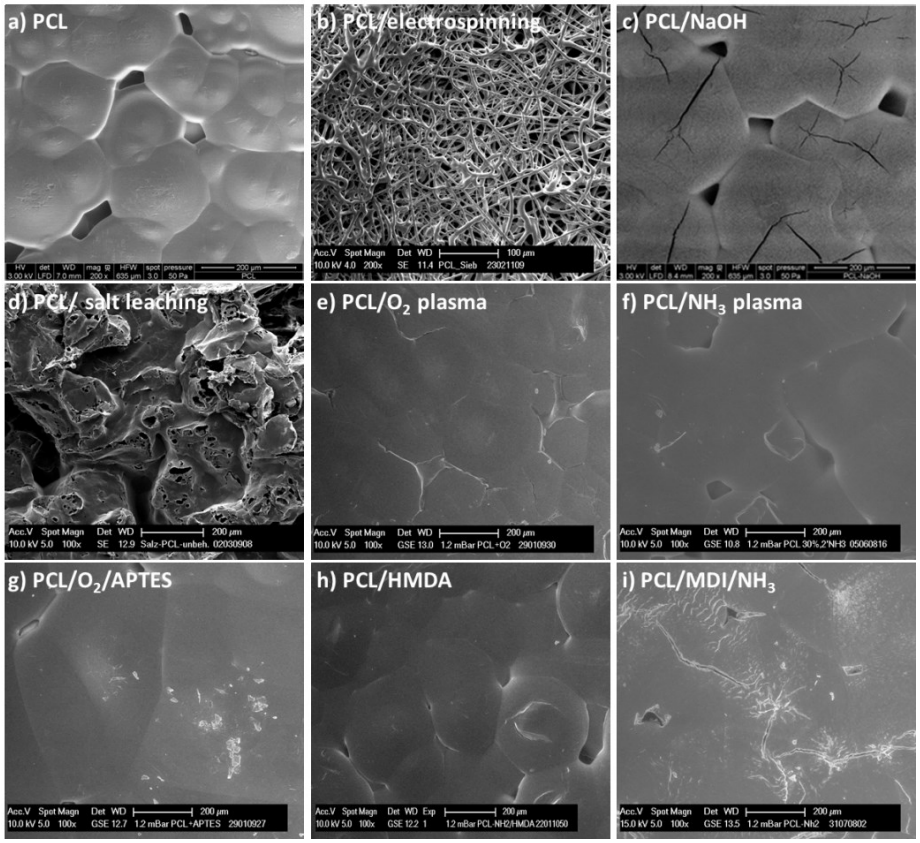

Figure 3.1. ESEM micrographs of the morphology of the variously functionalized PCL surfaces. Magnification 200× (a-c) and 100× (d-i), respectively.

3.2. Biocompatibility of functionalized polymers

When biomaterials are assessed for their biocompatibility, a fairly obvious prerequisite is that they should not possess any cytotoxic potential. In order to test for possible cytotoxic effects of the polymer, Human umbilical vein endothelial cells (HUVECs) were subjected to eluates from PCL and three exemplary modifications. Two reference materials were used here: thermanox (Thermo Scientific), a proprietary polymer that is highly resistant to most chemicals and treated for optimum cell attachment and growth *in vitro*, and polystyrene. Relative cell viability decreased with increasing concentration of the eluate. When compared to polystyrene, cell viability on differentially modified PCL fell below the reference line only in the samples exposed to the undiluted eluates (**figure 3.2**a), a situation that would not occur under physiological circumstances with constant blood flow. Twelve out of twenty diluted PCL eluates even led to significantly higher HUVEC viability than the pure culture medium. HUVECs on plain PCL as well as on O_2 plasma activated PCL showed lower proliferation rates compared to control cells on polystyrene (figure 3.2b). However, when the various PCL eluates were diluted, all HUVECs incubated in those samples showed proliferation rates that were significantly higher ($p<0.01$) than the rate seen in cells subjected to the undiluted thermanox eluate.

As can be seen in figure 3.2c and d, the various PCL eluates do not compromise HUVECs as much as undiluted thermanox eluate in terms of biocompatibility, as measured in both proliferation rate and viability of HUVECs growing in them. The highest viability of the cells was seen on plain PCL, but the differences between the individual PCL eluates were not significant. The respective values of the culture medium/polystyrene control fell in the same range as the cells incubated with the most diluted eluates, and on PCL/HMDA the cells incubated with up to 50% eluate concentration even showed higher relative viability and proliferation than the control cells. Of the PCL modifications, the oxygen plasma-activated form (PCL/O_2 plasma) was the one giving the lowest values for both viability and proliferation. None of these differences reached statisitical significance, whereas all dilutions of the different PCL eluates produced significantly higher viability and proliferation rates in HUVECs than thermanox as the reference material. Thus, regardless of surface modification, obvious cytotoxic properties of PCL could be excluded.

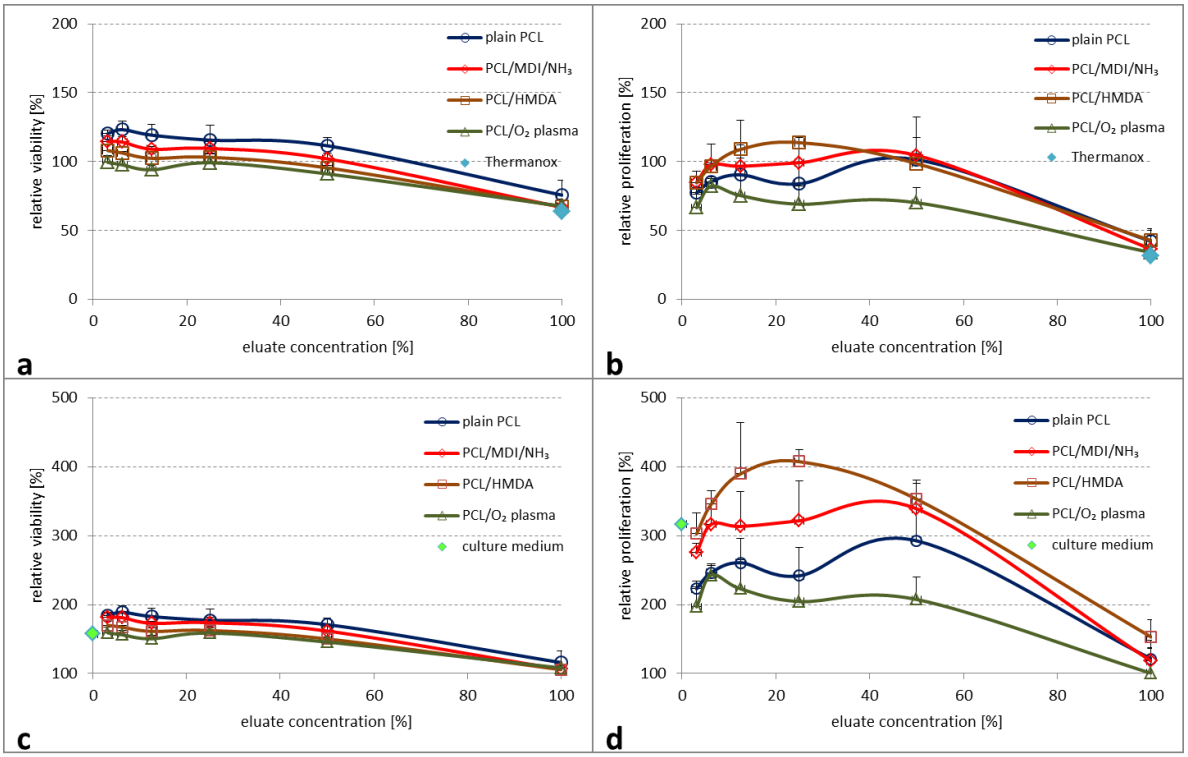

Figure 3.2. Biocompatibility of PCL and three functionalized varieties. The samples were eluted in cell culture medium for 24 h and then, in a dilution series, applied to pre-seeded HUVECs for 48 h before viability and proliferation testing. The reference (100%) used is polystyrene (for a and b) and undiluted thermanox polymer eluate (for c and d), respectively.

3.3. Optimization of VEGF stimulation

Primary endothelial cells can be isolated with relative ease and can then be cultured *in vitro*. Depending on the scientific question, the parameters for cell culture must be adapted. Here, the media composition, seeding density, number of passages, incubation time, cell cycle arrest and concentration of stimulating factors all had to be optimized before experiments on biomaterials could be conducted.

This part of the thesis is aimed at establishing a reliable *in vitro* model for the endothelialization of vascular implants, and then using this model to characterize the response of human primary endothelial cells on numerous PCL modifications in terms of biocompatibility, cell adhesion and morphology, and changes in gene expression.

3.3.1. Parameter 1: media composition

Ingredients of cell culture medium can have potent and potentially biasing effects on the behavior of cells and therefore need to be scrupulously controlled. The initial culture

medium composition contained a number of growth factors and additives, including epidermal growth factor, basic fibroblast growth factor, and an 'endothelial cell growth supplement' (ECGS) of unknown content by a commercial provider. HUVECs from that provider as well as self-isolated ones were cultured in the recommended medium for up to 5 days. The application of VEGF to endothelial cells incubated for 1 day and for 5 days with this complete medium yielded no stimulation of their viability or proliferation, regardless of VEGF concentration and cell source (**figure 3.3**).

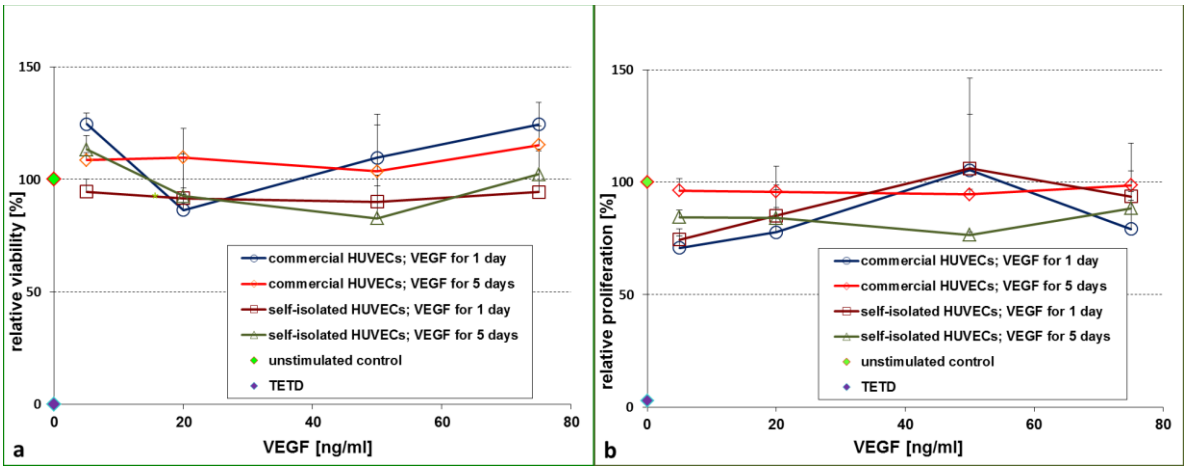

Figure 3.3. Effect of VEGF on HUVECs grown for 5 days in endothelial cell culture medium containing 0.1 ng/ml EGF, 1 ng/ml bFG and 4% endothelial cell growth supplement.

This result pointed to a probable masking of the stimulatory effect of the specific growth factor in the presence of other growth factors. Consequently, the cell culture medium was deprived of those factors and the endothelial cells stimulated with VEGF alone. As a result, the relative viability and proliferation of HUVECs were found to be stimulated (see figures 3.4 to 3.7).

As the complete medium contained 10% fetal calf serum, an experiment was done to test the effect of substantially lowered serum content. The comparison was between HUVECs growing in endothelial cell culture medium containing 2.5% fetal calf serum (in accordance with [67]) and HUVECs growing in that medium without any serum. **Figure 3.4** shows that serum is required for the stimulatory effect of VEGF to take hold, and that 2.5% serum is sufficient to achieve significant stimulation at two different doses of VEGF. It also shows that in the absence of serum the viability of HUVECs decreases with time.

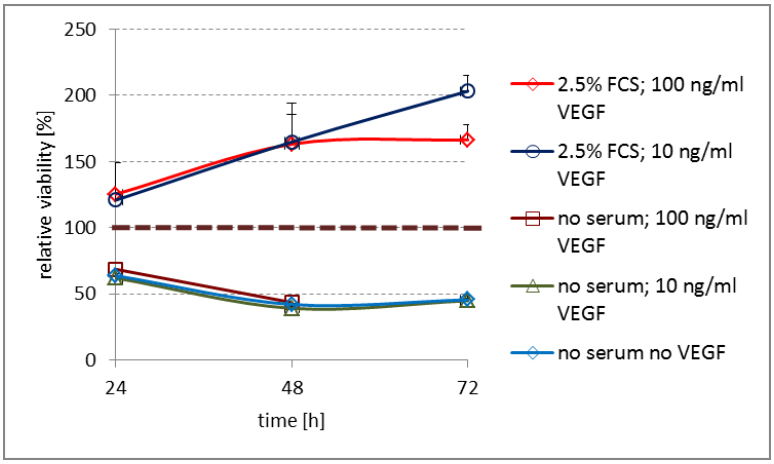

Figure 3.4. Impact of serum content and VEGF on relative viability of HUVECs over three days. Reference (100%; dashed line) is HUVECs viability in medium with 2.5% FCS in the absence of VEGF (measured in 24 h intervals).

3.3.2. Parameter 2: number of cell passages

It is known that primary cells tend to lose certain characteristics of their phenotype over time, i.e. after undergoing a number of mitotic cell divisions in culture [10]. Most researchers working with endothelial cells restrict experiments to <10 passages. In order to get information on the impact of this methodological factor, direct comparisons of different passages of cells from the same batch were performed. The responsiveness of HUVECs to VEGF generally decreased as the number of passages increased (**figure 3.5**). For cell viability, these differences were statistically significant at 1, 5 and 50 ng/ml VEGF. For relative proliferation rates, these differences were significant at 25 and 100 ng/ml VEGF, with VEGF stimulation at 25 ng/ml VEGF the only instance where relative proliferation in passage 7 was higher than in passage 3. As a consequence of these results, all experiments thereafter were performed with cells in passages 3 to 6.

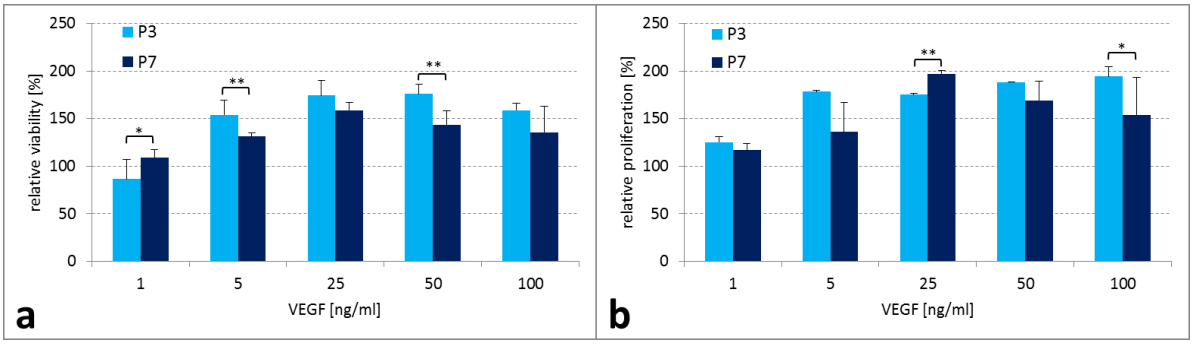

Figure 3.5. Extent of VEGF responsiveness varies with cell passage. Cell viability (a) and proliferation rates (b) of same-batch HUVECs in passages 3 and 7 after 72 h of stimulation with VEGF relative to unstimulated control. Asterisks denote statistical significance of difference between passage numbers (* $p<0.05$, ** $p<0.01$).

3.3.3. Parameter 3: VEGF concentration, time and duration of stimulation

Once cell growth is stimulated, the difference to an unstimulated control is expected to increase with time. Therefore the cell response to VEGF was monitored in 24 h intervals up to 96 h. To test for a possible concentration-dependent effect, eight different concentrations of VEGF were included in the experiments. The first set of experiments involved testing VEGF concentrations from 0.5 ng/ml to 100 ng/ml. Moreover, the VEGF stimulus was applied at two different time points: 1. immediately after cell seeding and 2. 24 h after cell seeding. Figures 3.6 and 3.7 show that after 24 h of stimulation, there were no significant differences between stimulated and unstimulated cells (there was no separate measurement of the cells that first received VEGF at this time point). After 48 h, the differences were significant at all eight concentrations, regardless of the time of VEGF application. **Figure 3.6** shows how the HUVEC response to VEGF differed between the two groups: the relative viability of the immediately stimulated cells reached 116.9±8.7% (at 0.5 ng/ml) to 172.2±12.9% (at 5 ng/ml), and in the cells receiving the late stimulus viability increased between 115.8±5.5% (at 0.5 ng/ml) and 148.1±12.5% (at 5 ng/ml) compared to the unstimulated control cells. The extent of stimulation in both groups increased overall with dose and time, and reached 400.8±17.8% (with 75 ng/ml VEGF immediately after cell seeding; figure 3.6a) and 378.3±30.1% (with 75 ng/ml VEGF 24 h after cell seeding; figure 3.6b) at 96 h after seeding.

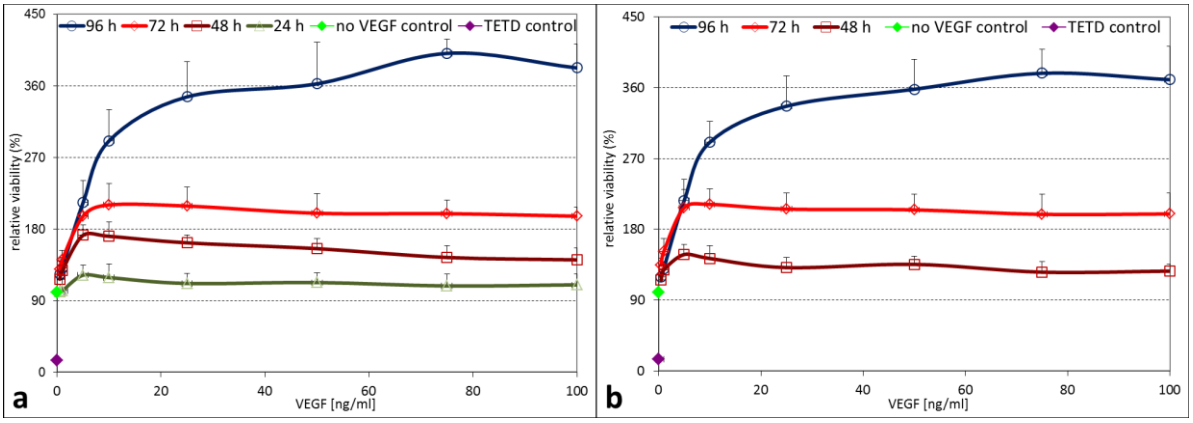

Figure 3.6. Effect of VEGF concentration and stimulation time on the viability of HUVECs. Cells were seeded, stimulated with VEGF (a) immediately after seeding or (b) 24 h after seeding at the concentrations indicated and incubated in 24 h intervals for up to 96 h along with non-stimulated controls (100%) before viability testing. Another control was subjected to 10^{-4} M TETD to demonstrate susceptibility of the cells to cytotoxic substances.

In addition, cell proliferation was measured under the same conditions, and the results (**figure 3.7**) showed a high degree of similarity to the viability testing (figure 3.6). When VEGF was administered immediately upon cell seeding, no significant stimulatory effect on cell proliferation could be seen 24 h later (maximum of 108.9±5.8% relative proliferation at 5 ng/ml VEGF; figure 3.7a) at all 8 concentrations. When the growth factor was given with a 24 h delay (figure 3.7b), the stimulation on the second day was slightly less than with those cells that had been exposed to VEGF for the whole 48 h period, but in both cases the differences to the control cells were highly significant ($p<0.01$) at all 8 VEGF concentrations. On the third day, the VEGF effect on the cells with late VEGF administration was slightly higher than on those with early VEGF administration (e.g. 250.6±14.5% vs 241.8±14.5% at 100 ng/ml). The outlying value at 10 ng/ml in the second group (180.5±79.6%, figure 3.7b) was in all likelihood due to experimental error, for it was the only result from 48 h to 96 h cell growth with a p-value larger than 0.01 in terms of difference to the unstimulated control. Its true value is probably at the upper end of the standard deviation and thus closer to the 221.3±14.0% relative viability measured in the immediately stimulated cells after 72 h. At the 96 h time point after cell seeding, the differences in proliferation rate between the two cell sets virtually disappeared, reaching up to 446.0±22.7% (VEGF directly after cell seeding, at 75 ng/ml; figure 3.7a) and 441.1±30.0% (VEGF after 24 h, at 50 ng/ml; figure 3.7b) of the unstimulated control, respectively.

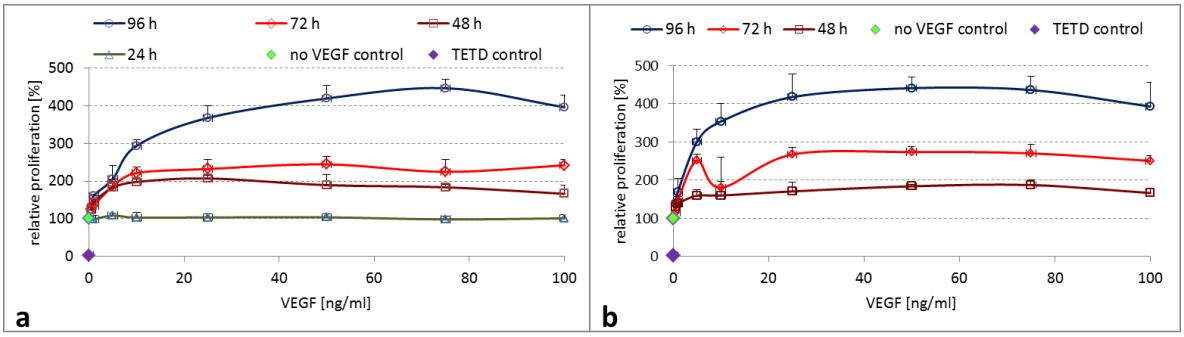

Figure 3.7. Effect of VEGF concentration and stimulation time on the proliferation of HUVECs. Cells were seeded, stimulated with VEGF (a) directly or (b) after 24 h at the concentrations indicated and incubated in 24 h intervals for up to 96 h along with non-stimulated controls (100%) before proliferation testing. Another control was subjected to 10^{-4} M TETD to demonstrate susceptibility of the cells to cytotoxic substances.

There was virtually no stimulation seen at the 24 h incubation time point, and this was true for both cell viability and proliferation. From 48 h onwards, the stimulatory effect leveled off around 50 ng/ml and sometimes was slightly reduced again at the maximum VEGF concentration (100 ng/ml). While marked stimulation generally could be achieved with 5 ng/ml, the positive correlation of VEGF dose and relative proliferation tended to drop off at all timepoints at the highest doses (>50 ng/ml). On the other hand, very distinct differences in the extent of stimulation from one day to the next could already be seen at 10 ng/ml. The series of experiments showed a concentration of 25 ng/ml to be effective for reliable and reproducible stimulation of HUVECs (figures 3.6 and 3.7), For reliable and reproducible stimulation of HUVECs, the concentration of 25 ng/ml was used as the standard in all subsequent experiments, with stimulation of the cells immediately after seeding and 96 h as the standard incubation time.

3.3.4. Parameter 4: initial cell density

A range of different cell seeding densities was sampled to test which one is optimal for VEGF stimulation, as seeding density is known to crucially affect results of endothelial cell testing *in vitro* [88]. At first, the cells were tested in the absence of VEGF. There was a linear correlation: the more cells were seeded, the higher their measured viability and proliferation rates were after 5 days (**figure 3.8**). When standardized to the lowest number of seeded cells (11,000/cm^2), the relative readings for 21,000 cells/cm^2 reached 143.9±5.0% (viability) and 268.5±13.2% (proliferation). With the exception of relative

proliferation at 14,000 cells/cm^2 (p=0.08), all differences to the minimum density were highly significant (p<0.0025).

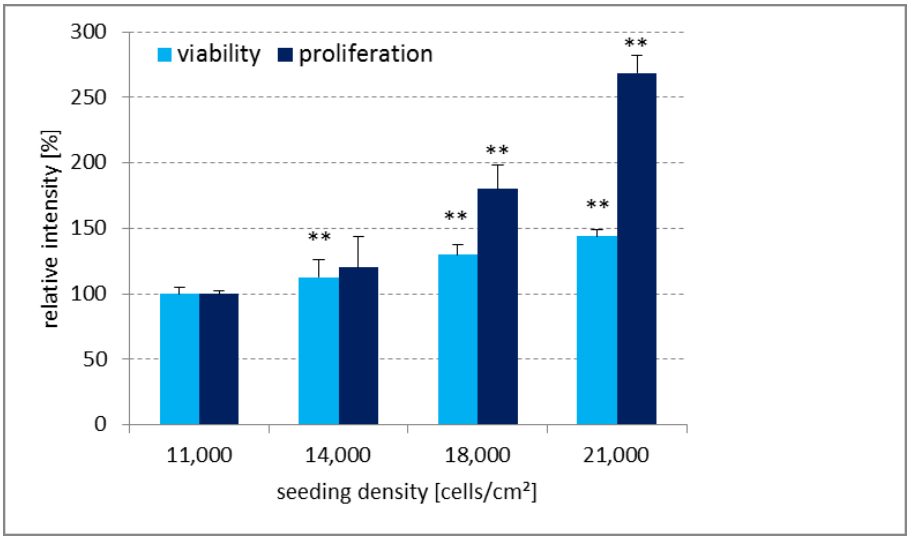

Figure 3.8. Effect of seeding density of HUVECs on magnitude of fluorescence (viability) and luminescence (proliferation) readings in routine biocompatibility assays. Shown is the relative intensity compared to 11,000 cells/cm^2 (100%) after 5 days of growth. Asterisks denote statistical significance of difference to that 100% control (* p<0.05, ** p<0.01).

In the next step, an experiment was set up to test whether initial cell density had an impact on VEGF responsiveness of HUVECs. As the experiments were done over a period of five days, it had to be ensured that the cells did not reach confluence, a state where contact inhibition comes into play and a growth factor can no longer stimulate cell growth. Cell viability and proliferation rate were separately measured at the four different densities and as expected, the relative stimulatory effect of VEGF decreased with increasing cell seeding density (**figure 3.9**). At 21,000 cells/cm^2, the effect upon cell proliferation disappeared altogether (figure 3.9b) At 11,000 cells/cm^2, the cells' viability increased to 176.2±7.4% in the presence of VEGF compared to the unstimulated control, whereas at 21,000 cells/cm^2 it only reached 150.9±6.6%. (The comparison between stimulated and unstimulated cells had to be done separately for each cell density, because of the confounding effect of seeding density described above.)

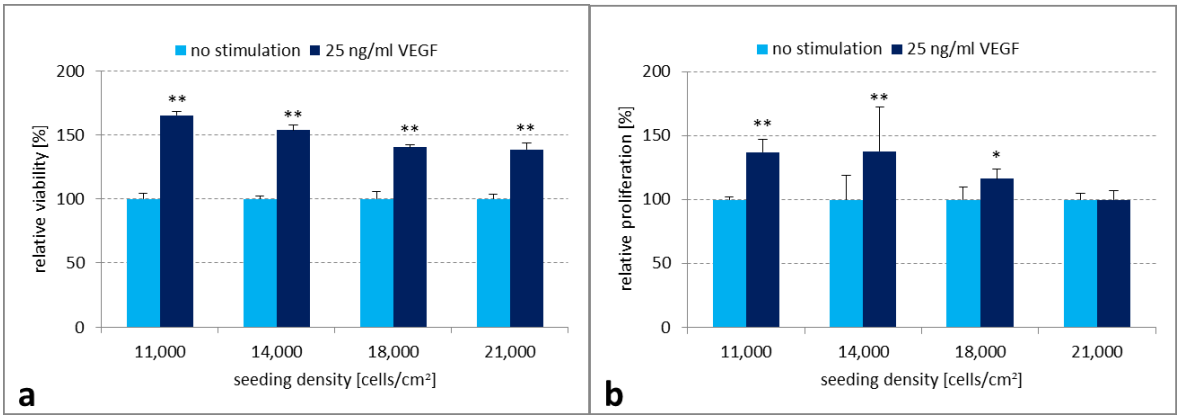

Figure 3.9. Effect of seeding density of HUVECs on magnitude of VEGF stimulation in terms of a) cell viability and b) proliferation rate readings in routine biocompatibility assays. Shown is the relative stimulation compared to the unstimulated control (set at 100% for each cell density) after 5 days. Asterisks denote statistical significance of VEGF effect at the respective seeding density (* $p<0.05$, ** $p<0.01$).

Because of the oppositional factors seeding density and relative stimulatory effect, a compromise needed to be found where enough cells grew to give fluorescence readings well above background levels, yet the density was not so high as to mask the growth factor induced stimulation. This was set at 11,000 cells/cm^2.

3.3.5. Parameter 5: cell cycle arrest

Arresting the cell cycle is a commonly used manipulation of cells *in vitro* that harmonizes them in a specific stage of the cell cycle (G_0, G_1 or G_2 phase). This arrest is transient and can be induced, for example, by medium depletion [89]. While only cells in G phase respond to growth inhibition, the remaining cells will complete the cell cycle but not enter a second one [90]. After release of cellular arrest, the cells generally spontaneously revert from the arrested state and proceed with the cell cycle [91]. Here cell cycle arrest was achieved by nutrient depletion for 24 h. Subsequently the cells were stimulated with 25 ng/ml VEGF in medium that was rich in nutrients but otherwise deprived of mitogenic factors (see section 2.10). **Figure 3.10** illustrates that at identical seeding densities, cell cycle arrest prior to VEGF stimulation enhances the VEGF responsiveness of HUVECs. While for relative viability the effect was detected at all seeding densities, it was statistically significant only at 11,000 cells/cm^2 (192% vs 176% stimulation) and 21,000 cells/cm^2 (201% vs 151% stimulation). For relative cell proliferation, the enhanced VEGF response through cell cycle arrest was much more pronounced and highly significant ($p<0.01$) at all seeding densities, reaching a maximum of 863% stimulation (compared to 169% at the same

seeding density without cell cycle arrest) at the lowest initial cell density (11,000 cells/cm^2), confirming the previous results on magnitude of VEGF stimulation (compare figure 3.9).

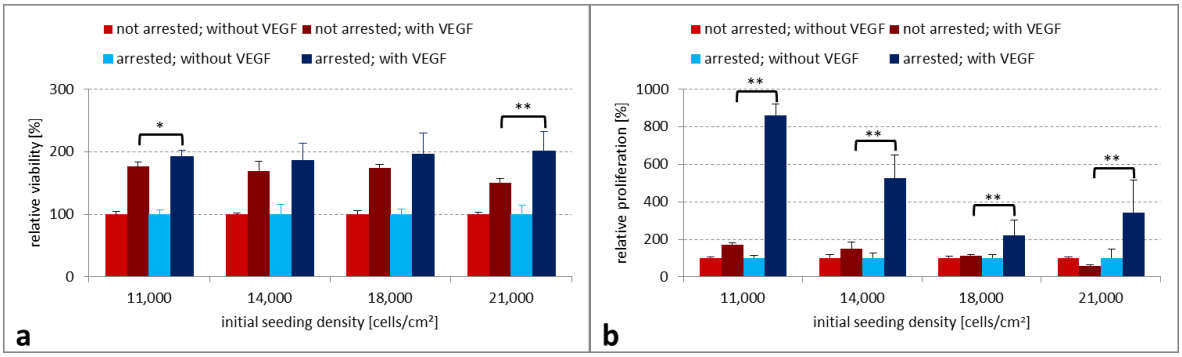

Figure 3.10. Cell cycle arrest prior to stimulation greatly enhances the effect of VEGF on HUVECs. Shown is (a) the relative viability and (b) relative proliferation rate compared to the unstimulated control (set at 100% for each cell density and separately for 'not arrested' and 'arrested'). Cells were seeded 24 h before VEGF stimulation, which then lasted 96 h. Arrested cells had been seeded and incubated in arresting medium for 24 h. Asterisks denote statistical significance of difference with/without cell cycle arrest (* $p<0.05$, ** $p<0.01$).

3.4. Reproducibility of VEGF response

The first tests of the effect of VEGF on HUVECs with three different reference materials produced a wide range of relative stimulation (**figure 3.11**). Of 64 individual measurements of cell viability in total, 53 (i.e. 82.8%) yielded a VEGF-induced stimulation of more than 130% (arbitrary threshold) compared to unstimulated cells. The degree of variability is independent of the substrate presented to the cells, but failure of stimulation (i.e. <100% relative viability) is most frequently associated with thermanox (4.7% of tests on this substrate). In contrast, 91% of all measurements on polystyrene and 95% of those on glass lay above the 130% threshold. This threshold was chosen to exclude random deviations and ensure that the detected range of responses was due to biological variability.

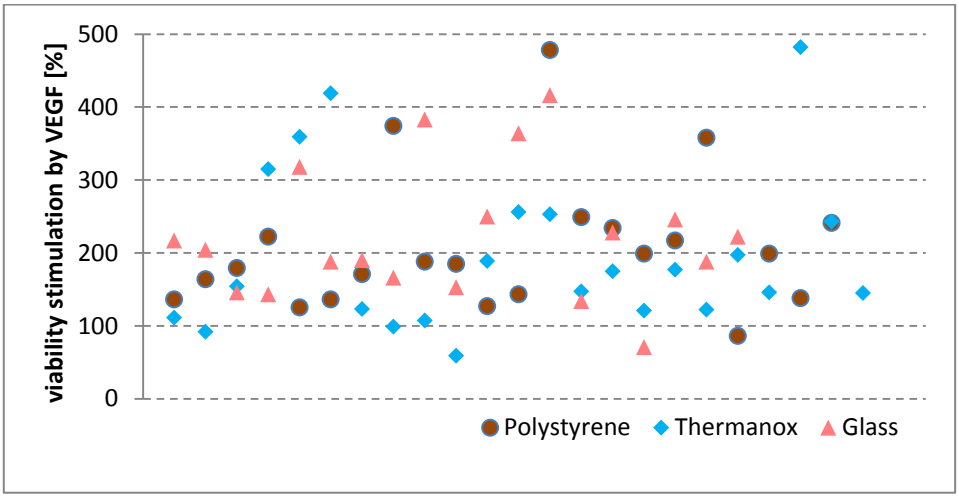

Figure 3.11. Scatter plot of 64 viability measurements with VEGF-stimulated HUVECs from 11 different donors growing on 3 different reference substrates. VEGF was given immediately after cell seeding at 25 ng/ml. Shown is only the mean viability of cells relative to the unstimulated control, without standard deviation.

In order to ascertain that all primary cells grown on polymers were susceptible to VEGF stimulation, from then on every batch of HUVECS was routinely pre-stimulated on glass, thermanox and polystyrene. **Figure 3.12** shows five representative examples. The extent of stimulation varied considerably with cell donor and VEGF concentration, but had to exceed said threshold for polymer experiments to proceed (leading to the exclusion of batch 5 in figure 3.12, for example).

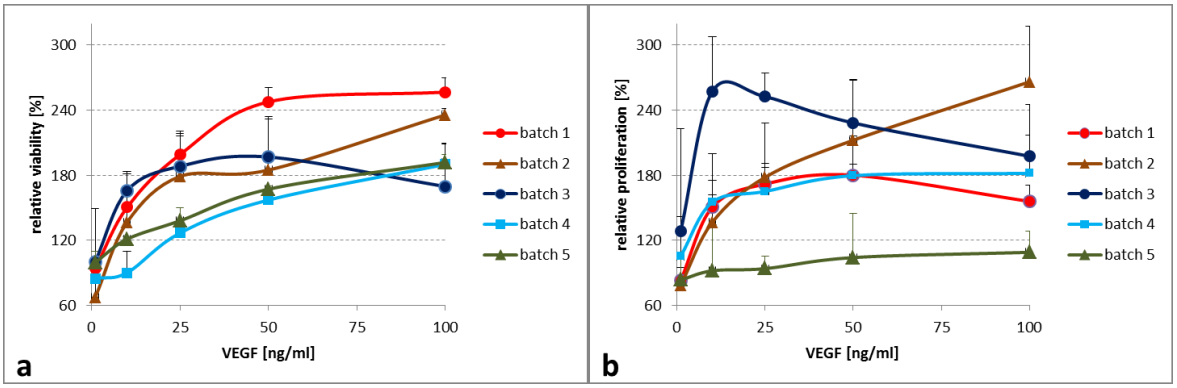

Figure 3.12. Pre-stimulation of different batches of HUVECs with VEGF. HUVECs at passage 3 were seeded on polystyrene at 11,000 cells/cm^2 and stimulated for 96 h with VEGF at the concentrations depicted. Shown is (a) their relative viability and (b) proliferation rate on polystyrene as compared to the non-stimulated control (set at 100%).

3.5. Viability of endothelial cells on PCL

3.5.1. Influence of PCL morphology on cell adhesion and viability

An important aspect in implant material selection is whether the morphology of its surface has an impact on the viability of cells adhering to it. From the experiments with PCL eluates it was already clear that HUVECs adhering to PCL are less viable than on the reference material polystyrene (see figure 3.1). Therefore plain PCL was used as the reference in the subsequent experiments on the effects of polymer surface modification. While salt leaching was the only treatment that allowed a slightly higher viability of both cell types (HUVECs: 103.5±13.0%, HCAECs: 112.4±17.8% relative to plain PCL), this increase was statistically not significant. This can be seen in **figure 3.13**.

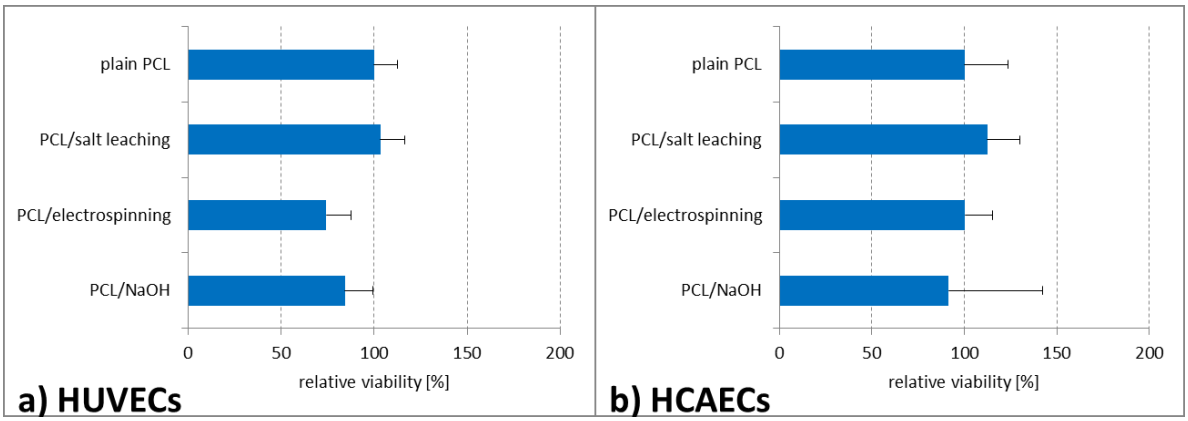

Figure 3.13. Relative cell viability of (a) HUVECs and (b) HCAECs after 96 h growth on modified PCL surfaces. Plain PCL was used as a reference and thus arbitrarily set at 100%. n=3 donors á 8 replicates

3.5.2. Influence of PCL surface activation on cell adhesion and viability

As the different PCL surface morphologies did not show marked effects on the viability of adherent cells, only plain PCL films were used for chemical activation and subsequent biocompatibility testing. Cell viability was measured after 96 h in relation to plain PCL. As can be seen in **figure 3.14**, for both cell types surface activation by itself did not greatly improve cell viability. For HUVECs, the changes were not significant when compared to plain PCL (figure 3.14a), with the values ranging from 80.8±19.8% (MDI/ NH_3 activation) to 129.0±27.0% (NH_3 plasma activation). However, the differences in viability of HUVECs reached statistical significance when different forms of PCL activation (plasma vs. wet chemical) were directly compared. Relative viability on PCL/O_2 plasma was significantly higher than on PCL/MDI/NH_3 and PCL/O_2/APTES, while relative viability on PCL/NH_3 plasma was significantly higher than on PCL/MDI/NH_3, PCL/O_2/APTES and PCL/HMDA.

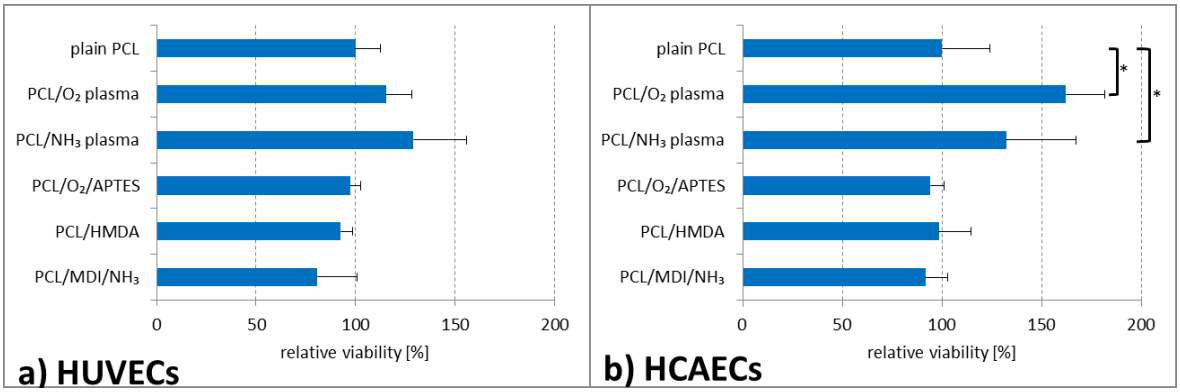

Figure 3.14. Relative cell viability of (a) HUVECs and (b) HCAECs after 96 h growth on activated PCL. Plain PCL was used as a reference and thus arbitrarily set at 100%. Asterisks denote statistical significance of difference to the reference (* $p<0.006$). n=3 donors á 8 replicates

In the case of HCAECs, the increase in viability on O_2 plasma activated PCL (162.0±19.6%; p=0.0000000004) and NH_3 plasma activated PCL (132.2±34.7%; p=0.0058) was highly significant compared to that seen on plain PCL (**figure 3.14b**). At the same time, HCAEC viability on all wet chemically activated forms of PCL was less (PCL/MDI/NH_3: 91.5±11.2%, PCL/O_2/APTES: 94.0±6.9% and PCL/HMDA: 98.3±16.0%) than on plain PCL (100±22.2%). By far the highest viability of HCAECs was seen on PCL/O_2 plasma.

3.5.3. VEGF response of endothelial cells on PCL

When the viability of HUVECs is standardized to that seen on unmodified PCL without VEGF, it becomes apparent that alterations of the polymer morphology (**figure 3.15**) result in lower effects of growth factor stimulation than chemical activation (**figure 3.16**). For example, electrospinning of PCL combined with the VEGF stimulus resulted in 101.6±18.0% viability compared to unstimulated HUVECs on plain PCL (figure 3.15a). Over all modifications of the polymer, only treatment with APTES (140.9±6.7%), salt leaching (140.4±37.7%), O_2 plasma (186.8±56.0%) and NH_3 plasma (214.9±86.9%) exceeded the extent of VEGF stimulation seen on plain PCL (figure 3.16a). Amongst these surface modifications, plasma activation stood out as the method yielding by far the highest VEGF-induced increase in endothelial cell viability.

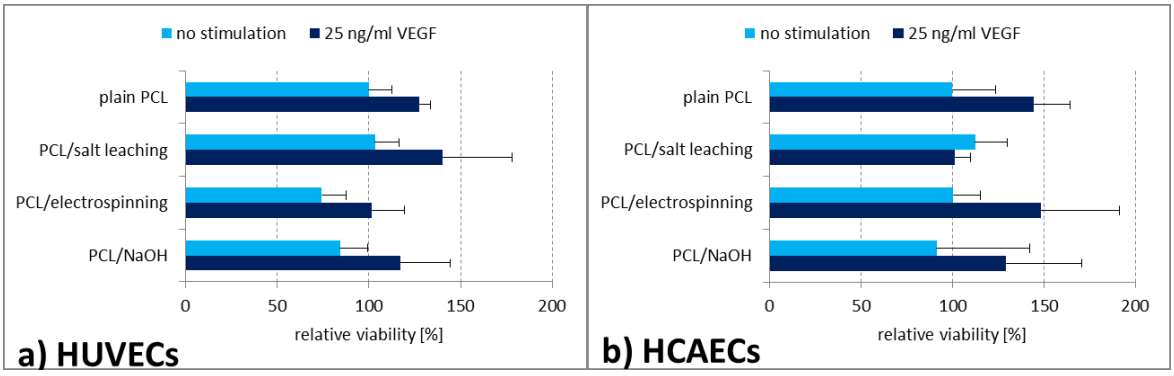

Figure 3.15. Relative cell viability of a) HUVECs and b) HCAECs after 96 h growth on various PCL morphologies with and without VEGF stimulation. Plain PCL was used as a reference and thus arbitrarily set at 100%. n=3 donors

For HCAECs, the pattern is very similar, especially with the chemically activated forms of PCL. Out of eight different modifications of PCL, five yielded higher VEGF-induced viability stimulation of HCAECs than plain PCL (144.6±19.7% relative viability): electrospun PCL (148.3±43.2%; figure 3.15b), PCL/O_2/APTES (154.4±59.1%), PCL/HMDA (160.5±51.8%), PCL/NH_3 plasma (164.6±47.5%) and PCL/O_2 plasma (256.1±128.6%).

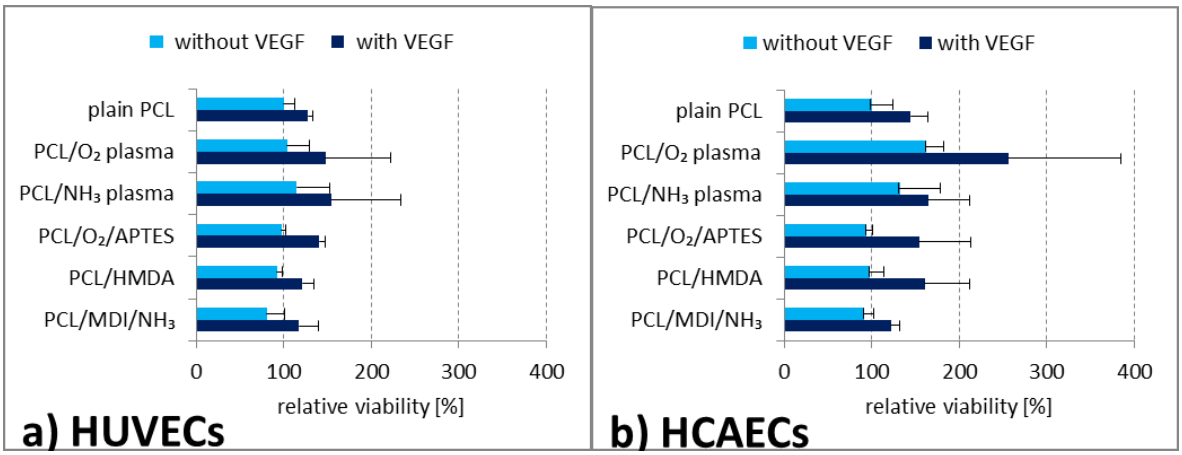

Figure 3.16. Relative cell viability of a) HUVECs and b) HCAECs after 96 h growth on activated PCL with and without VEGF stimulation. Plain PCL was used as a reference and thus arbitrarily set at 100%. n=3 donors

Confocal imaging revealed the stimulatory effect of the growth factor in a more pronounced manner than the CQB test. When HUVECs were labeled after 4 days of growth using the live/dead stain, their enhanced adhesion on various PCL surfaces became apparent (**figure**

3.17). The largest number of viable cells was seen on NH_3 plasma-activated PCL, while on the non-chemically activated forms of PCL (electrospinning and salt leaching), a high proportion of ethidium dimer stained, i.e.non-viable cells was prominent. Electrospun PCL presented with the highest ratio of dead vs. viable cells. Overall, adhesion of HUVECs on PCL in the absence of VEGF was poor, but was greatly augmented when VEGF was added directly after cell seeding.

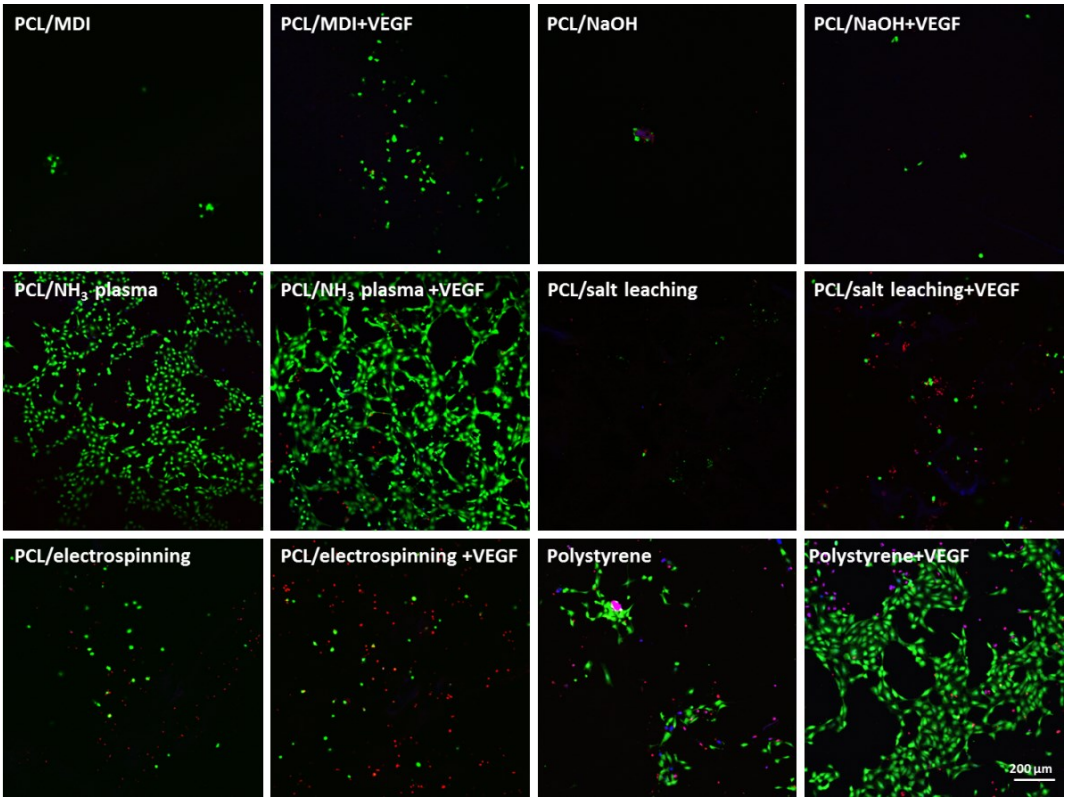

Figure 3.17. Confocal laser scanning micrographs of HUVEC attachment to PCL 96 h after seeding of 2×10^4 cells and live/dead staining. For each substrate cell adhesion without VEGF is shown on the left, in the presence of 25 ng/ml VEGF on the right. Scale bar for all images: 200 µm

The general picture of the VEGF effect on HCAECs was very similar to the one on HUVECs (**figure 3.18**). The substrate demonstrating the highest abundance of viable cells by way of live/dead staining was polystyrene, while NaOH-etched PCL was the PCL variety presenting with the most adherent cells compared to the other forms of PCL. Plasma activation of the polymer appeared to convey the highest stimulatory effect of VEGF on HCAECs. Again a large proportion of non-viable cells was evident on electrospun PCL. This prompted a later change of the staining method to phalloidin-FITC (see section 3.4.2).

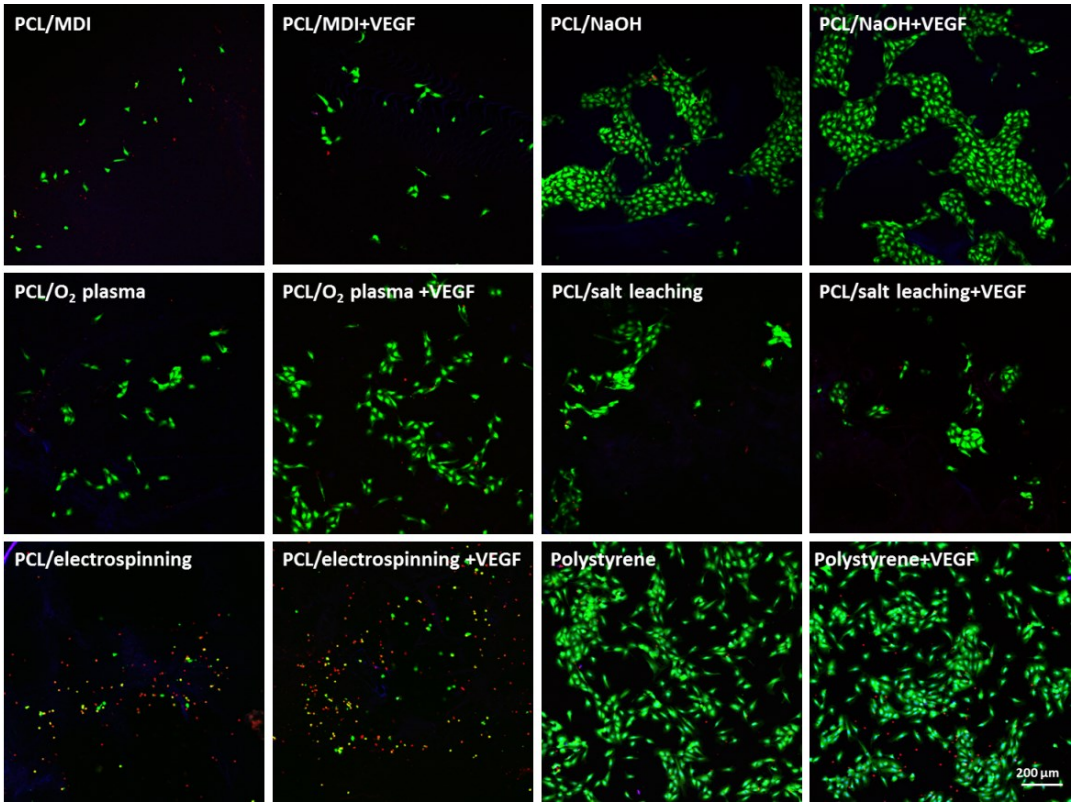

Figure 3.18. Confocal laser scanning micrographs of HCAEC attachment to PCL 96 h after seeding of 2×10^4 cells and live/dead staining. For each substrate cell adhesion without VEGF is shown on the left, in the presence of 25 ng/ml VEGF on the right. Scale bar for all images: 200 µm

The surface-specific analysis of the VEGF effect on HUVEC viability (**figure 3.19**a) revealed that all modifications of PCL resulted in greater viability of HUVECs adhering to them than on plain PCL (27.7±5.8% increase). Univariate analysis of variance showed that the gains were significant only for PCL/O_2/APTES ($p=0.03$), PCL/NH_3 plasma ($p<0.001$) and PCL/O_2 plasma ($p<0.001$). The highest stimulation was again seen on NH_3 plasma activated PCL, albeit with the highest standard deviation (164.1±55.2%). O_2 plasma activation of PCL resulted in the second-highest VEGF-induced viability stimulation (160.0±35.0%), while wet chemical activation with HMDA yielded the lowest effect (131.0±9.5%).

Stimulation of viability through VEGF on the individual surfaces was again very similar for HCAECs, despite overall larger standard deviations (figure 3.19b). Here the highest stimulation was detected on O_2 plasma activated PCL (168.1±69.8%) and electrospun PCL (168.4±81.7%), while on NH_3 plasma activated PCL VEGF led to only moderately increased viability (120.4±31.6%), even compared to plain PCL (44.6±19.7% increase). With PCL/salt leaching as the only exception, all VEGF-induced increases were statistically significant.

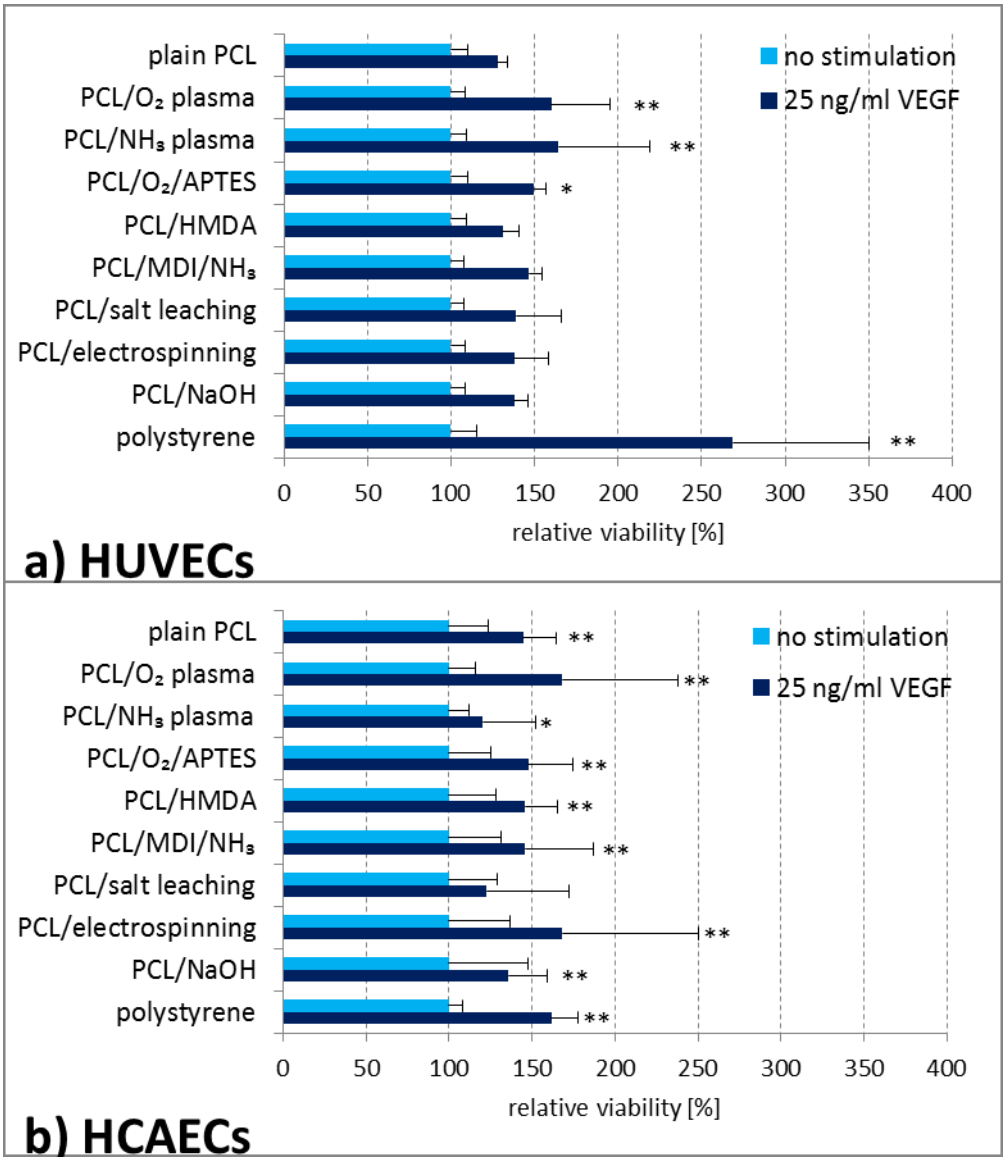

Figure 3.19. Stimulatory effect of VEGF on viability of (a) HUVECs and (b) HCAECs growing on modified PCL. Shown is the mean modification-specific effect of the growth factor relative to the unstimulated (100%) control on that same modification of PCL. Asterisks denote statistical significance of difference with/without VEGF on the same substrate. n=3 donors per cell type

3.5.4. Covalent coupling of VEGF to polymer

Covalent coupling of biomolecules is one important strategy to enhance the biocompatibility of polymers. Here 4-star-shaped poly(ε-caprolactone) with terminal acrylate groups (sPCL-A), a functionalized derivative of PCL [92], was used to couple VEGF, via adsorption and via crosslinkers (see appendix A.7). Then cell viability of HUVECs grown for 96 h on this substrate was compared to equally treated sPCL-A with VEGF directly added to the culture

medium and without VEGF altogether, so as to give information about the bioactivity of soluble vs immobilized VEGF.

When the growth factor was adsorbed onto the polymer (**figure 3.20**), the viability of HUVECs on plain sPCL-A as well as on sPCL-A/HMDA was significantly higher (56.0±8.6% and 53.8±6.6% relative to polystyrene, respectively) with VEGF than without it (46.5±5.8% and 45.6±5.0%, respectively). On sPCL-A/O_2 plasma the difference in viability was even higher, but not significantly so. On all three forms of sPCL-A, it made no significant difference whether VEGF was adsorbed onto the polymer or applied in soluble form.

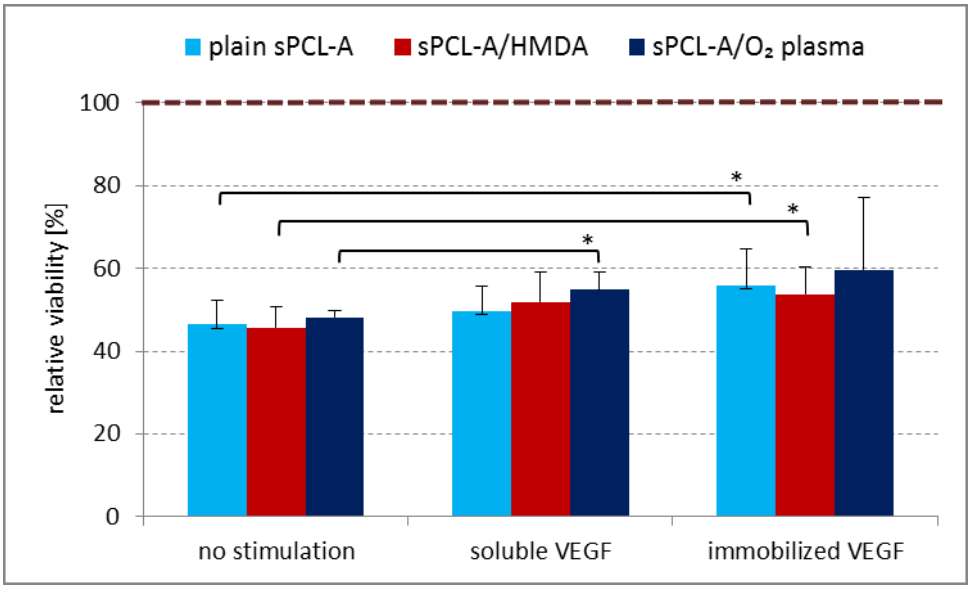

Figure 3.20. Impact of VEGF applied in two different ways on relative viability of HUVECs growing on sPCL-A with and without modification. Soluble growth factor was added at 25 ng/ml. Reference (100%; dashed line) is HUVECs viability on polystyrene in the absence of VEGF. Asterisks denote statistical significance of differences between bracketed groups (* $p<0.05$).

When VEGF was covalently coupled to sPCL-A via crosslinkers (**figure 3.21**), the only statistically significant differences were between absence and presence of VEGF. In the instance of highest relative viability (with VEGF coupled through the crosslinkers N-(3-dimethylaminopropyl)-N′-ethylcarbodiimide (EDC)/ (NHS) to otherwise unactivated sPCL-A; 80.0±14.9% viability relative to control HUVECs growing on polystyrene), however, the differences were not significant. There also were no statistically significant differences in HUVEC viability between the two different ways in which VEGF was presented to the cells (soluble vs covalently bound on the polymer). On sPCL-A activated with O_2 plasma, the

viability of HUVECs was significantly increased (to 63.2±2.0% relative to polystyrene) when VEGF was coupled to the polymer through the crosslinker DSC, compared to that on identically modified sPCL-A without the addition of VEGF (59.4±2.4% relative to polystyrene; p=0.012).

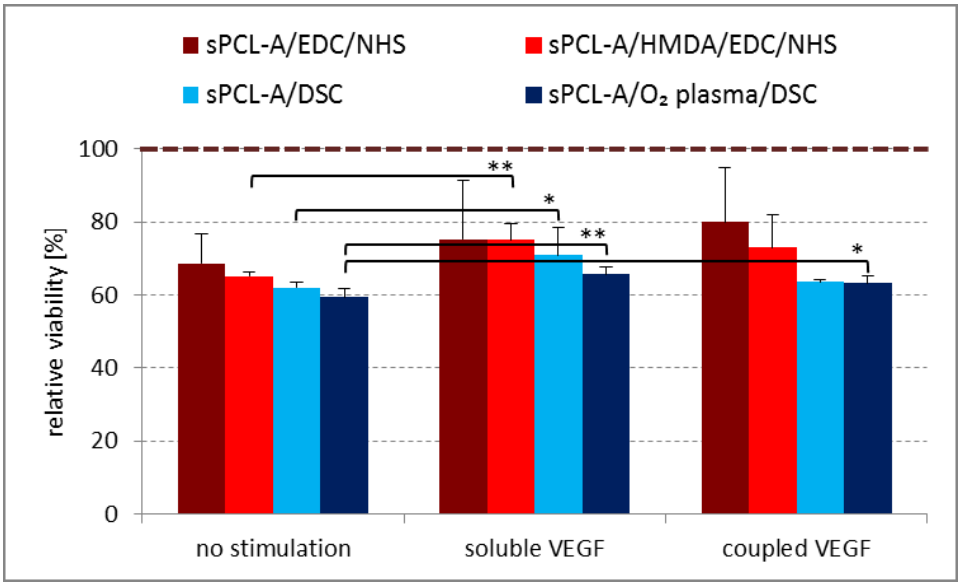

Figure 3.21. Influence of crosslinkers (EDC/NHS or DSC) and covalent coupling of VEGF on HUVEC growth on functionalized sPCL-A. Soluble growth factor was added at 25 ng/ml. Reference (100%; dashed line) is HUVECs viability on polystyrene in the absence of VEGF. Asterisks denote statistical significance of differences between bracketed groups (* $p<0.05$, ** $p<0.01$).

3.5.5. Influence of PCL functionalization with ECM protein

In order to promote endothelial cell adhesion on the polymer regardless of its surface properties, PCL was pre-coated with ECM proteins. For specific information on protein and dose, four different matrix proteins were screened at three different concentrations each: laminin, collagen type I, fibronectin and gelatin.

Figure 3.22 shows that uncoated PCL as a substrate for HUVECs compares poorly with polystyrene, but cell viability on PCL can be markedly improved by precoating it with protein. Gelatin gave the most inconsistent results, with the highest protein concentration (1 mg/ml) in the PCL coating yielding slightly lower cell viability than in the uncoated state. Collagen type I, laminin and fibronectin coats on PCL all cause highly significant increases in HUVEC viability at the highest concentration used (100 µg/ml). While this effect is directly

dose-dependent for collagen type I and laminin, coating PCL with fibronectin results in significantly higher cell viability at all three concentrations.

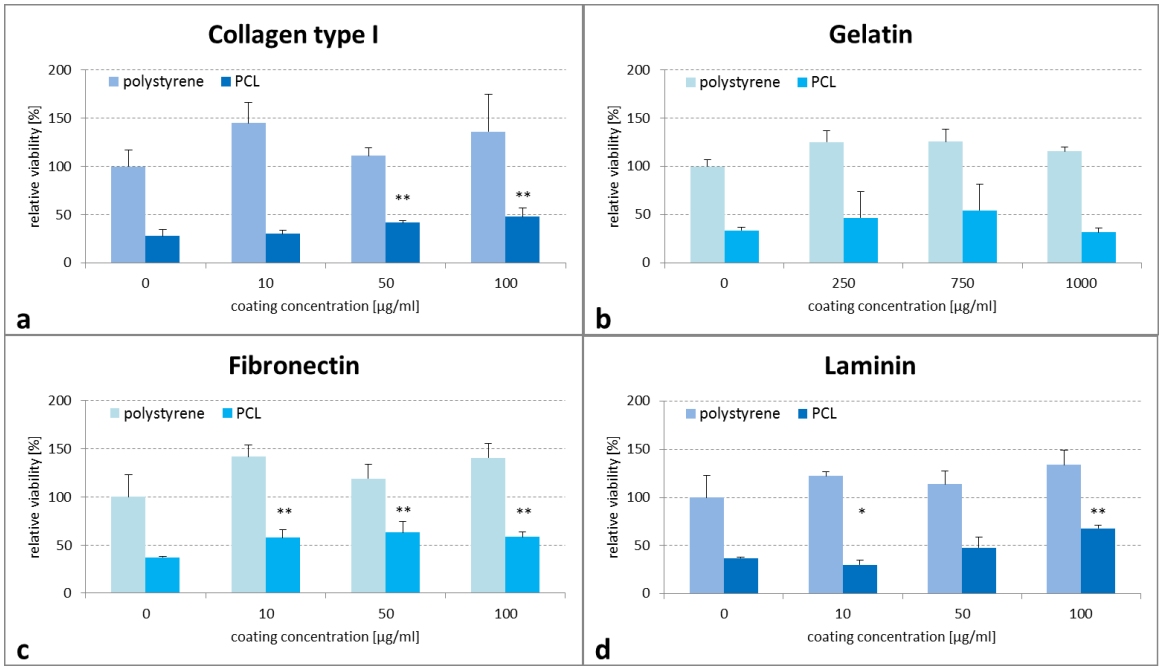

Figure 3.22. Relative increase in HUVEC viability on PCL through precoating with matrix proteins. Shown is the viability after 4 days of growth on PCL and polystyrene compared to that on uncoated polystyrene (0 µg/ml) as reference (100%). Asterisks denote statistical significance of differences between uncoated and coated PCL (* $p<0.05$, ** $p<0.01$).

The general stimulatory effect of protein precoating on HUVEC growth on PCL was confirmed with calcein AM staining and fluorescence microscopy (**figure 3.23** and **A.8**). In the case of collagen and laminin, however, the dosage dependence seen in viability testing could only be partially confirmed. For fibronectin, the dose-dependent effect on HUVECs adhesion on precoated PCL was clearly visible under the fluorescence microscope.

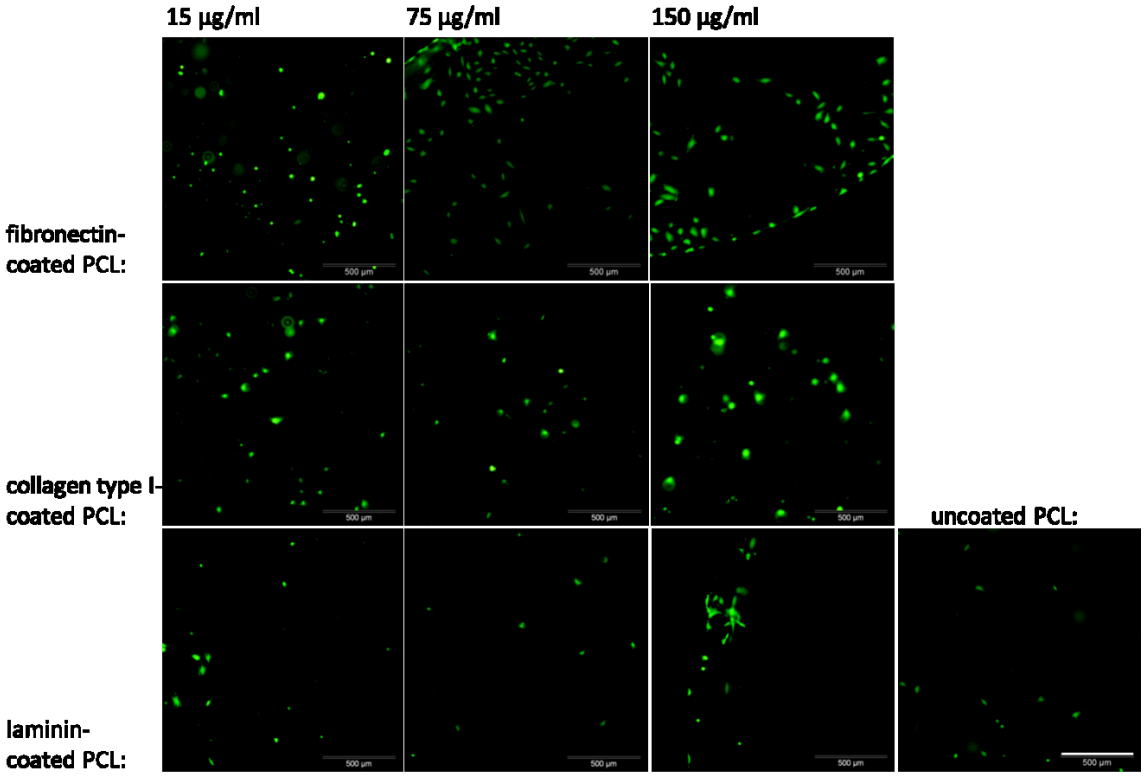

Figure 3.23. Fluorescent micrographs of calcein AM stained HUVECs grown for 48 h on PCL coated with fibronectin, collagen type I and laminin.
Scale bar for all images: 500 µm

Figure 3.24 shows that, with the exception of the lowest laminin concentration (10 ng/ml), at all concentrations tested, fibronectin, collagen I as well as laminin lead to increased cell viability after 96 h.

The highest relative increase was seen with 100 µg/ml laminin, at 182.1±9.4% compared to the uncoated PCL control (or from 37.2% to 67.7%, respectively, of uncoated polystyrene). In the case of fibronectin, all three concentrations resulted in more than 1.5-fold viability of HUVECs compared to their growth on uncoated PCL. The extent of stimulation achieved by coating with collagen type I or laminin was dose-dependent, but in the case of 10 µg/ml laminin, cell viability remained lower (80.8±12.8%) than on the uncoated control.

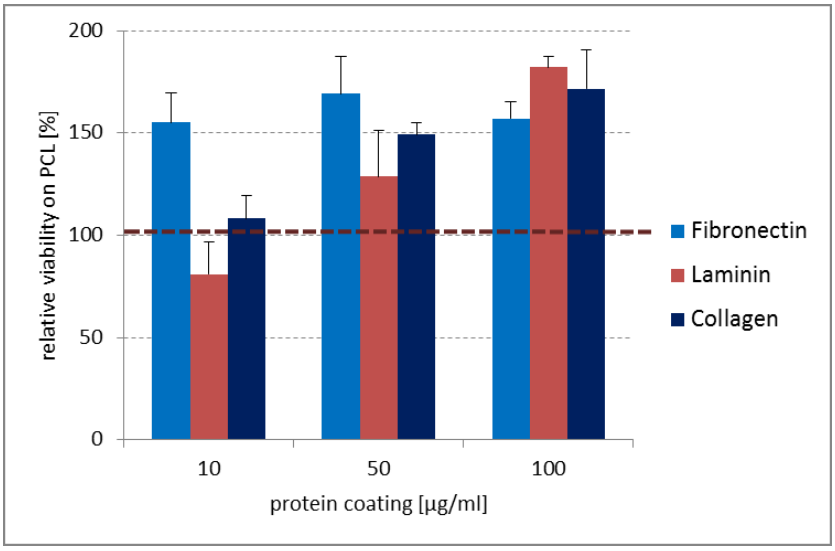

Figure 3.24. Relative increase in cell viability (HUVECs) through coating of PCL with extracellular matrix components. HUVECs were seeded immediately after coating PCL with the respective proteins and concentrations and allowed to adhere for 96 h. Reference (100%; dashed line) for relative viability is uncoated PCL.

3.6. Confounding methodological factors

3.6.1. Problem of proliferation testing on polymer films

When the biocompatibility assays were done with the cells growing on polymer films, the results for viability and cell proliferation did not correlate as they did in the preceding experiments on tissue culture plastic. While the viability readings for all forms of PCL were within a narrow range (35.9±1.6% to 57.8±4.2%) and all well below the value seen on polystyrene (**figure 3.25**a), proliferation testing of the same cells yielded a very wide range of 33.5±15.2% to 643.5±131.4%, with plain PCL, PCL/NaOH above polystyrene and PCL/MDI/NH_3, PCL/salt leaching and PCL/electrospinning even giving multitudes of the reading on the polystyrene reference (figure 3.25b). As the proliferation results could neither be aligned with those from the viability assay nor with confocal microscopy, methodological bias seemed likely.

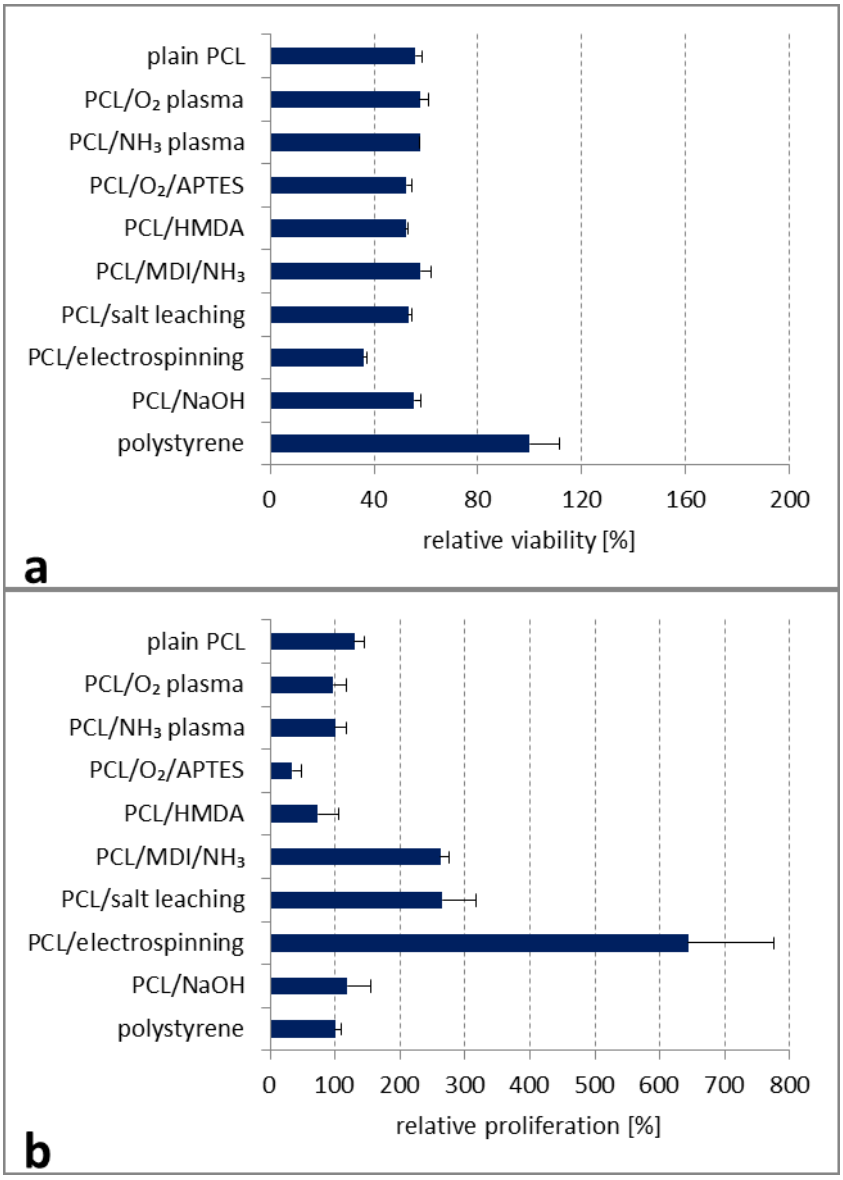

Figure 3.25. Absence of correlation between (a) viability and (b) proliferation testing of the same HUVECs growing on modified PCL films. Note the different scales of relative stimulation.

To analyse the apparent disparity, the BrdU assay was run on various polymers in the absence of cells. To test the possibility that there might be an issue with the anti-BrdU antibody unspecifically binding to the polymers, a subset of the samples was subjected to the test routine minus the antibody.

As can be seen in **figure 3.26**, the readings differed extremely, even in the absence of antibody. When normalized to polystyrene, all PCL varieties deviated from that baseline, from 105±17% (plain PCL) to 3350±1012% (sPCL-A). The differences were more

pronounced when the antibody was included, with sPCL-A again giving the maximum value (6613±2674%). In the presence of anti-BrdU, the only modifications that did not significantly differ from polystyrene were PCL/O_2 plasma and PCL/O_2/APTES.

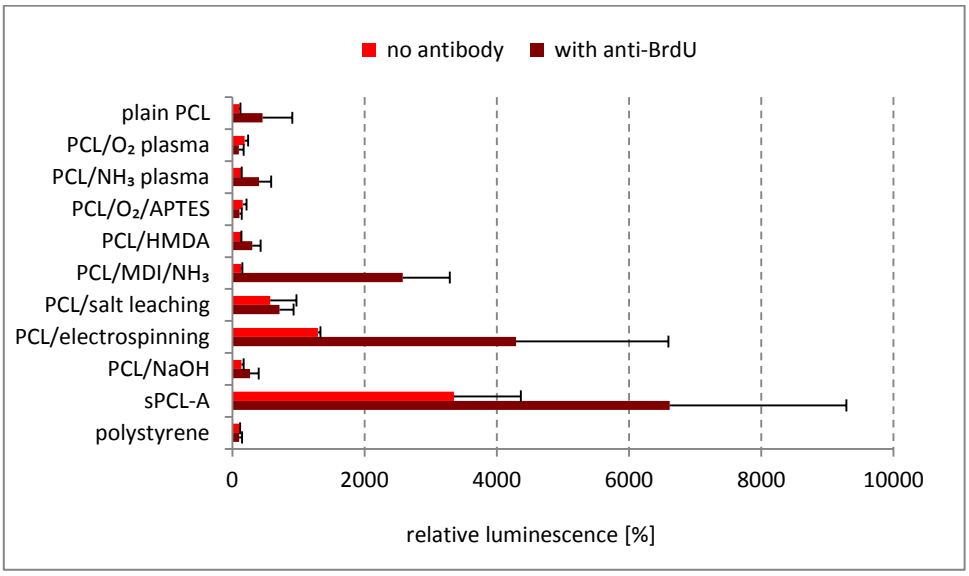

Figure 3.26. Results of BrdU testing on different varieties of PCL films in the absence of cells. The magnitude of measured luminescence changes greatly with type of modification.

This result can only be ascribed to unspecific effects of the polymers, constituting a severe bias for any measurement of cell proliferation on polymer films. As a consequence, the BrdU proliferation assay was no longer applied to cells growing on PCL films.

3.6.2. Fluorescent cell staining for CLSM

Because of the possibility that an experimental bias might be introduced through the manual transfer of the live/dead-stained cells from the microplate well onto glass slides immediately prior to CLSM, another staining method was tested where the adherent cells could be fixed on the PCL films. This was achieved with fixative and subsequent staining with FITC-conjugated phalloidin (**figure 3.27**).

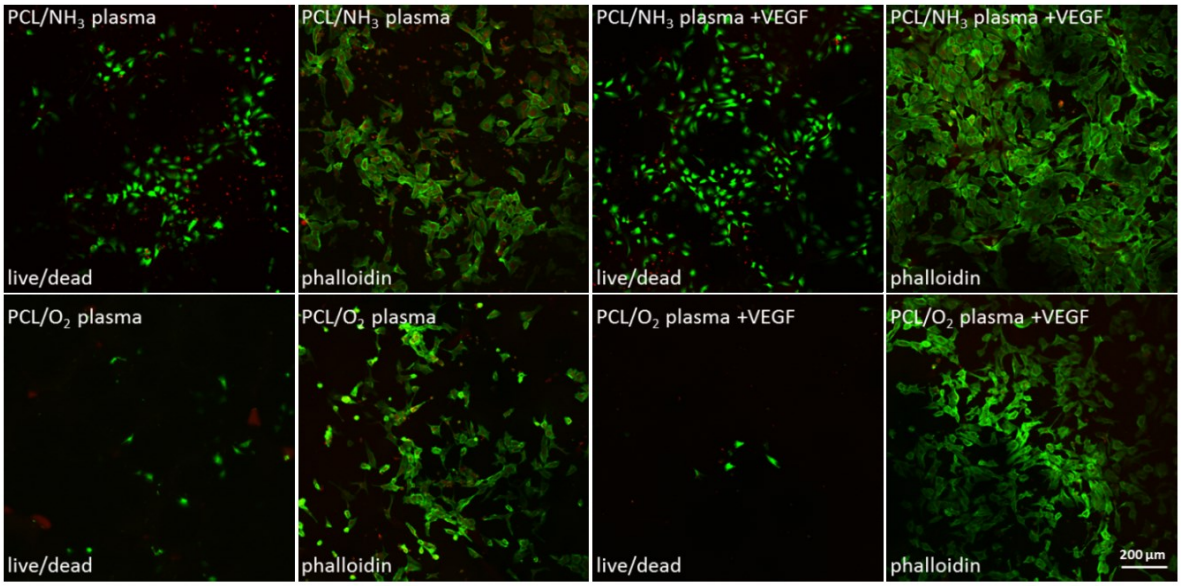

Figure 3.27. Comparison of live/dead and phalloidin-FITC staining of HUVECs. Per polymer film, 2×10^4 cells were seeded and incubated for 96 h. VEGF stimulation was with 25 ng/ml. Equally treated samples were subjected to either one of the two staining protocols and CLSM-imaged with the same fluorescence settings.

3.7. Combined stimulation of endothelial cells with fibronectin and VEGF

After finding that ECM protein coating could aid endothelial cell adhesion, the question arose whether a combined stimulation with VEGF would yield additional benefits for PCL endothelialization. For material selection, the previous results were assessed as to the most promising types of surface functionalization, and so both plasma chemical modifications and silanization with APTES as a representative for wet chemical modification were included, along with unactivated PCL.

When directly compared, precoating with 50 µg/ml fibronectin showed no increased viability for HUVECs grown on the four varieties of PCL (**figure 3.28**), while stimulation with the soluble growth factor significantly increased viability on PCL/O_2/APTES (p=0.00037; to 143.0±22.9%) and on PCL/NH_3 plasma (p=0.00007; to 129.3±11.7%). The combined treatment with fibronectin and VEGF on PCL/O_2/APTES led to a lower viability (109.4±45.2%) than the pure VEGF stimulus. On the other three varieties of PCL, the combination of fibronectin and 25 ng/ml soluble VEGF enhanced HUVEC viability relative to VEGF application alone (figure 3.28). The highest viability was seen on PCL/NH_3 plasma with combinatorial stimulation (147.5±29.3%) which was significantly higher (p=0.014) than with VEGF stimulation of HUVECs by itself.

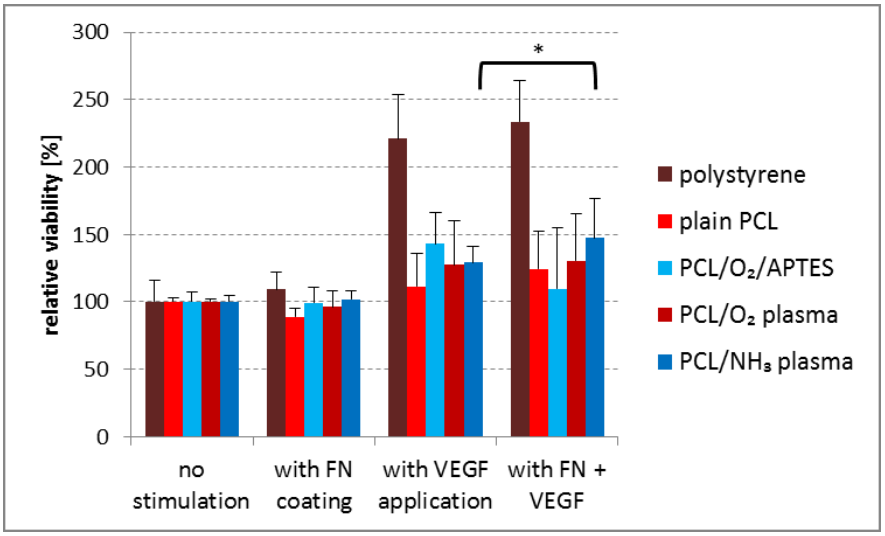

Figure 3.28. Separate and combinatorial stimulation of HUVECs growing on functionalized PCL varieties with fibronectin and VEGF. Shown is the modification-specific effect of stimulation of HUVECs for each substrate, i.e. normalized to the viability of HUVECs on the uncoated substrate without VEGF application (100%). Asterisk denotes statistical significance of difference between bracketed groups (* $p<0.05$).

3.8. Substrate induced changes in endothelial cell mRNA expression

Adhesion molecule expression on the cell surface is an important indicator for how intact the endothelium is. Some of these molecules even serve as biomarkers for the inflammatory risk of coronary artery disease [19]. Therefore the comparative analysis of gene expression in endothelial cells growing on differently modified substrates should provide information on the suitability of those substrates as potential implant material. Three such molecules, intercellular adhesion molecule 1 (ICAM-1), vascular cell adhesion molecule 1 (VCAM-1) and platelet/ endothelial cell adhesion molecule 1 (PECAM-1) were selected for qPCR analysis. In addition, eNOS was included as a marker for functional endothelia, and IL-8 as a representative for proinflammatory endothelial response to different substrates. The necessary standardization of gene expression was achieved through normalizing the amounts of individual transcripts to 18S rRNA, representing ribosomes which contain approximately 80% of all eukaryotic cellular RNA [77]. For normalization in comparative analyses of mRNA levels, 18S rRNA has been found to be superior to other housekeeping genes [93]. Taking the results from surface functionalization and protein precoating into account, each substrate was presented to the cells in four different conditions: 1. without added substances, 2. coated with fibronectin, 3. with soluble VEGF and 4. with fibronectin coating and soluble VEGF combined.

The amplification plots (figure 2.6) and melting curve analysis (figure 2.5) of the PCR products, together with the number of replicates per qPCR sample (table 3.1) demonstrate the reproducibility and reliability of the qPCR experiments.

Cell type	Substrate/treatment	cDNA code	ICAM-1	VCAM-1	PEC-AM-1	eNOS	IL-8
HUVEC	PCL	U1	3	4	4	3	4
HCAEC	PCL	C1	2	4	4	0	1
HUVEC	PCL/NH_3 plasma	U2	3	5	4	4	2
HCAEC	PCL/NH_3 plasma	C2	3	4	4	4	4
HUVEC	polystyrene	U3	4	4	4	4	3
HCAEC	polystyrene	C3	4	3	4	3	4
HUVEC	PCL/O_2/APTES	U4	4	4	4	4	4
HCAEC	PCL/O_2/APTES	C4	3	4	4	3	3
HUVEC	PCL/O_2 plasma	U5	4	3	4	4	4
HCAEC	PCL/O_2 plasma	C5	4	4	4	4	4
HUVEC	PCL/FN	U6	4	4	4	4	4
HCAEC	PCL/FN	C6	1	1	4	3	2
HUVEC	PCL/NH_3 plasma/FN	U7	4	3	4	4	4
HCAEC	PCL/NH_3 plasma/FN	C7	3	3	3	4	3
HUVEC	polystyrene/FN	U8	4	4	4	4	4
HCAEC	polystyrene/FN	C8	3	3	4	3	4
HUVEC	PCL/O_2/APTES/FN	U9	4	2	4	4	3
HCAEC	PCL/O_2/APTES/FN	C9	4	2	4	4	2
HUVEC	PCL/O_2 plasma/FN	U10	4	4	4	4	4
HCAEC	PCL/O_2 plasma/FN	C10	3	3	4	4	3
HUVEC	PCL+VEGF	U11	0	0	4	0	2
HCAEC	PCL+VEGF	C11	1	2	3	0	0
HUVEC	PCL/NH_3 plasma+VEGF	U12	4	4	4	4	4
HCAEC	PCL/NH_3 plasma+VEGF	C12	3	3	3	4	3
HUVEC	polystyrene+VEGF	U13	5	4	4	5	5
HCAEC	polystyrene+VEGF	C13	4	3	4	4	4
HUVEC	PCL/O_2/APTES+VEGF	U14	4	4	4	4	4
HCAEC	PCL/O_2/APTES+VEGF	C14	4	3	4	4	2

Cell type	Substrate/treatment	cDNA code	ICAM-1	VCAM-1	PEC-AM-1	eNOS	IL-8
HUVEC	PCL/O_2 plasma+VEGF	U15	5	5	5	5	5
HCAEC	PCL/O_2 plasma+VEGF	C15	2	3	3	1	1
HUVEC	PCL/FN+VEGF	U16	4	4	4	4	4
HCAEC	PCL/FN+VEGF	C16	1	1	0	0	1
HUVEC	PCL/NH_3 plasma/FN+VEGF	U17	4	4	4	4	4
HCAEC	PCL/NH_3 plasma/FN+VEGF	C17	1	2	1	1	1
HUVEC	polystyrene/FN+VEGF	U18	4	4	4	4	4
HCAEC	polystyrene/FN+VEGF	C18	3	2	2	4	4
HUVEC	PCL/O_2/APTES/FN+VEGF	U19	0	0	2	0	1
HCAEC	PCL/O_2/APTES/FN+VEGF	C19	0	0	2	0	1
HUVEC	PCL/O_2 plasma/FN+VEGF	U20	4	4	4	4	4
HCAEC	PCL/O_2 plasma/FN+VEGF	C20	2	2	4	1	3

Table 3.1. Overview of qPCR samples and reproducibility of mRNA specific results. Shown is the number of successful amplifications per mRNA and sample.

Only samples that gave single-peak melting curves were included in the final analysis. Data from unreplicated amplifications have been omitted from the following graphs. All qPCR results are presented as fold changes in mRNA abundance relative to cells of the same type growing on uncoated polystyrene without VEGF stimulation. The results are presented in blocks illustrating the effects of both polymer surface modification and external stimulation on mRNA quantity, with each of the examined genes documented separately for better comprehension of the multitude of data.

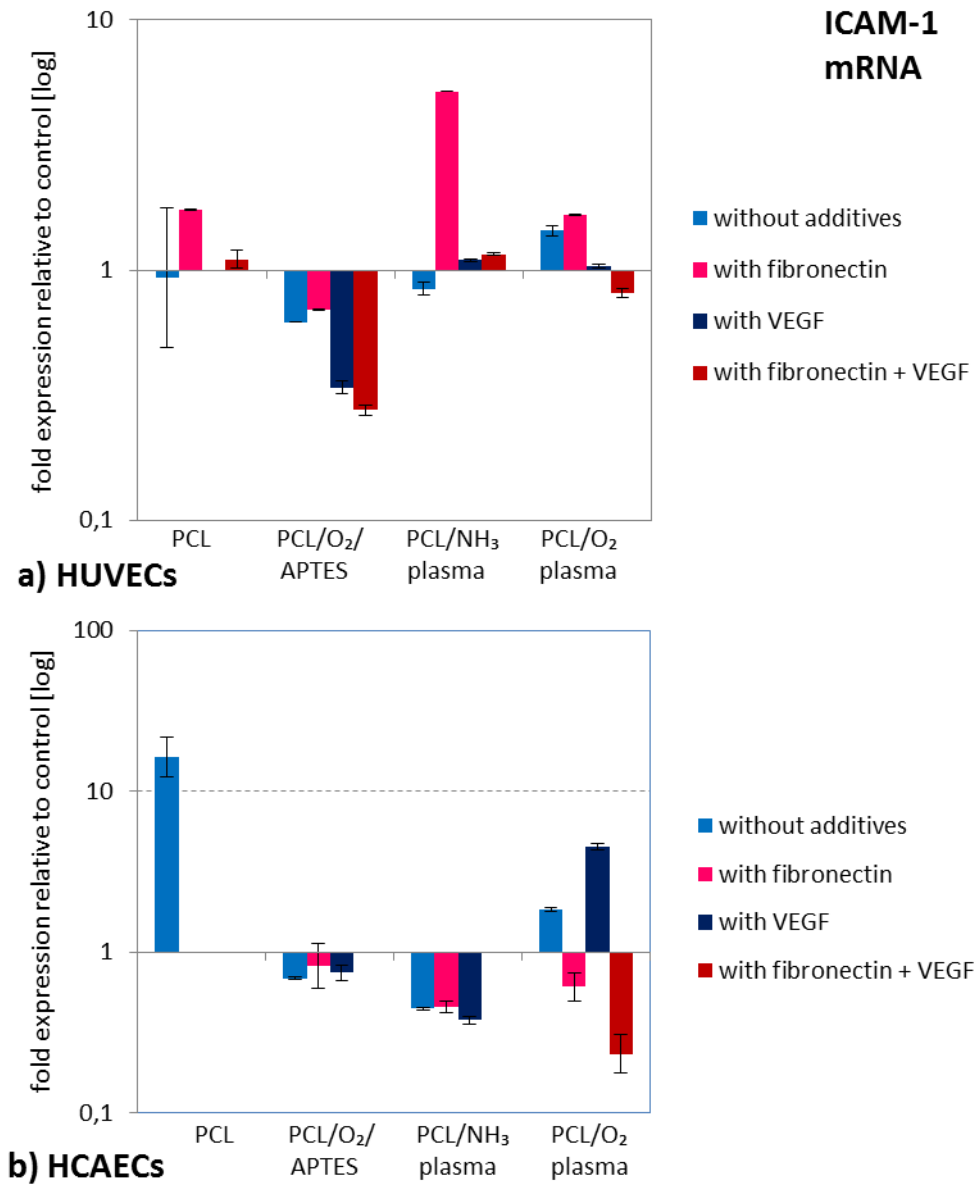

Figure 3.29. ICAM-1 expression in (a) HUVECs and (b) HCAECs as a function of PCL modification and presence of fibronectin (50 µg/ml) and/or VEGF (25 ng/ml). The untreated controls are HUVECs (for a) or HCAECs (for b) grown on polystyrene without additives. A fold-change of 0.4 is the same as 2.5-fold downregulation. Error bars denote the minimum and maximum of the standard error of the mean.

Because the three adhesion molecules as well as IL-8 are seen as indicators for the initial foreign body reaction to freshly implanted stents or grafts [9], the expectation was that their expression would be comparatively high in endothelial cells growing on untreated PCL, and that surface modification of PCL would alleviate the extent of such an increase. The effects of externally added stimuli such as fibronectin and VEGF are harder to predict, but in the afore described experiments they had already shown to be beneficial for PCL endothelialization, so it might be assumed that mRNA of a functional marker molecule such

as eNOS would be more abundant in cells that had received the extra stimulants compared to cells that had not.

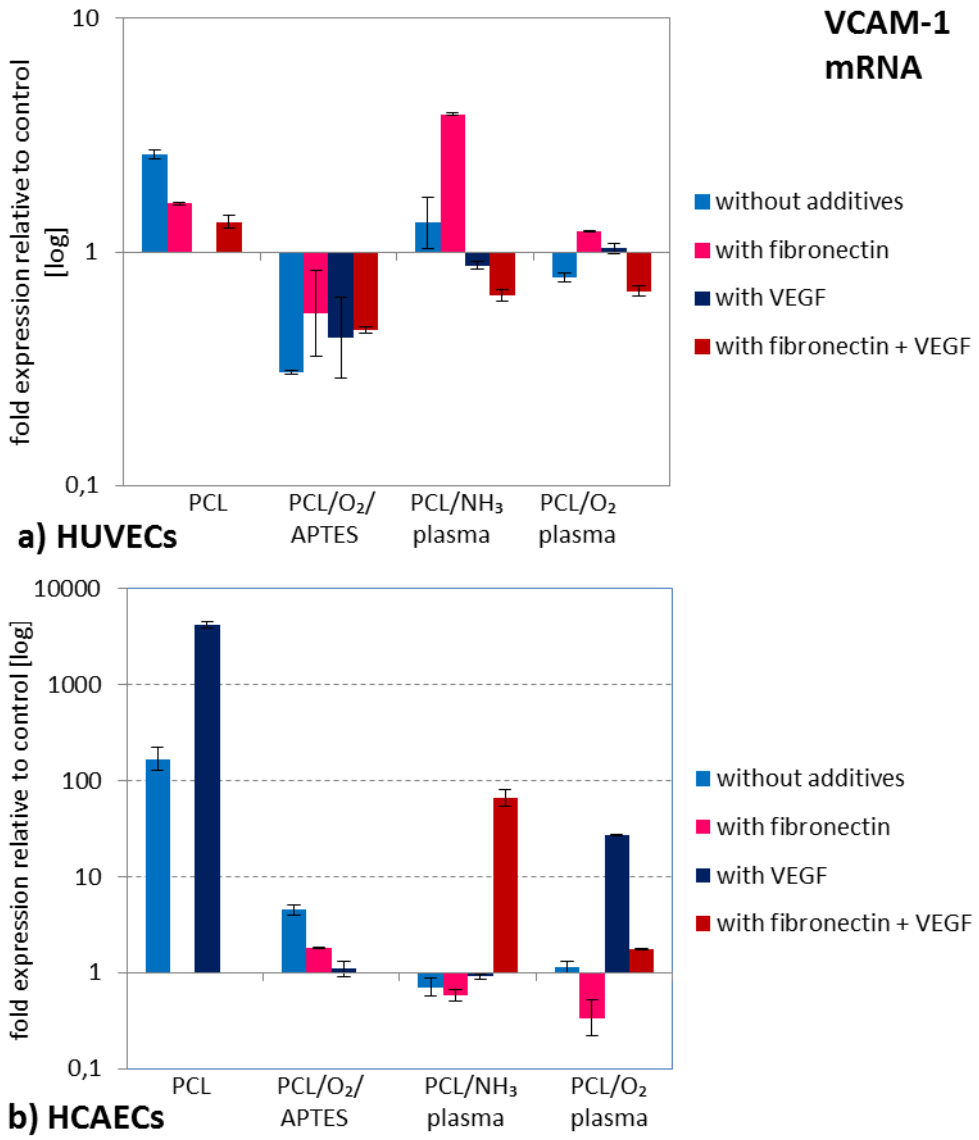

Figure 3.30. VCAM-1 expression in (a) HUVECs and (b) HCAECs as a function of PCL modification and presence of fibronectin (50 µg/ml) and/or VEGF (25 ng/ml). The untreated controls are HUVECs (for a) or HCAECs (for b) grown on polystyrene without additives. A fold-change of 0.4 is the same as 2.5-fold downregulation. Error bars denote the minimum and maximum of the standard error of the mean.

With respect to the three endothelial adhesion molecules, these expectations for quantitative changes in mRNA expression were met, particularly for HCAECs: regardless of external stimulation, all HCAECs on plain PCL showed a more than 5-fold increase of ICAM-1 (**figure 3.29**b), VCAM-1 (maximum 4211-fold VCAM-1 amount on plain PCL with VEGF; **figure 3.30**b), and PECAM-1 mRNAs (**figure 3.31**b) compared to the amounts

present in control cells growing on uncoated polystyrene. This large increase was considerably reduced on PCL surfaces that had been modified, either by APTES or plasma activation. It should also be noted here that the threshold cycles for 18S rRNA were unusually high for all HCAEC samples from unmodified PCL (22 to 26, compared to 11 to 17 for the other samples).

Such a clear trend was not seen in HUVECs. But the prominent decrease in both ICAM-1 and VCAM-1 mRNA amount exclusively in cells growing on APTES-modified PCL points to surface-dependent effects (figures 3.29a and 3.30a). In the case of ICAM-1, the APTES-specific decrease was seen in both cell types, albeit in HCAECs on a much smaller scale than in HUVECs.

For ICAM-1 and VCAM-1 transcripts, a 5.2-fold and 3.9-fold increase was detected in HUVECs growing on fibronectin-coated NH_3 plasma activated PCL. Compared with the lack of relevant changes in HUVECs growing on PCL/NH_3 plasma in the three remaining conditions, this result indicates an interplay between this particular surface and fibronectin that seems to be abolished in the presence of VEGF.

The quantitative changes seen in the amounts of PECAM-1 mRNA (**figure 3.31**) were altogether the least pronounced among the adhesion molecules. In HUVECs, PECAM-1 transcript remained virtually unchanged, with a maximum fold change of only 1.67 after stimulation with VEGF alone on PCL/O_2/APTES (figure 3.31a). HCAECs growing on PCL activated with APTES and NH_3 plasma, respectively, showed a pattern that very closely resembled the one seen in HUVECs. On O_2 plasma activated PCL, the only major change in the HCAEC PECAM-1 mRNA amount was with combined fibronectin and VEGF stimulation, which led to a 14.7-fold decrease (figure 3.31b). The biological meaning of this outlier result cannot be evaluated. Leaving that aside, the mRNA expression of PECAM-1 in HCAECs falls into the general pattern of overall increase that is much reduced in extent when the cells grow on surface activated PCL compared to regular PCL.

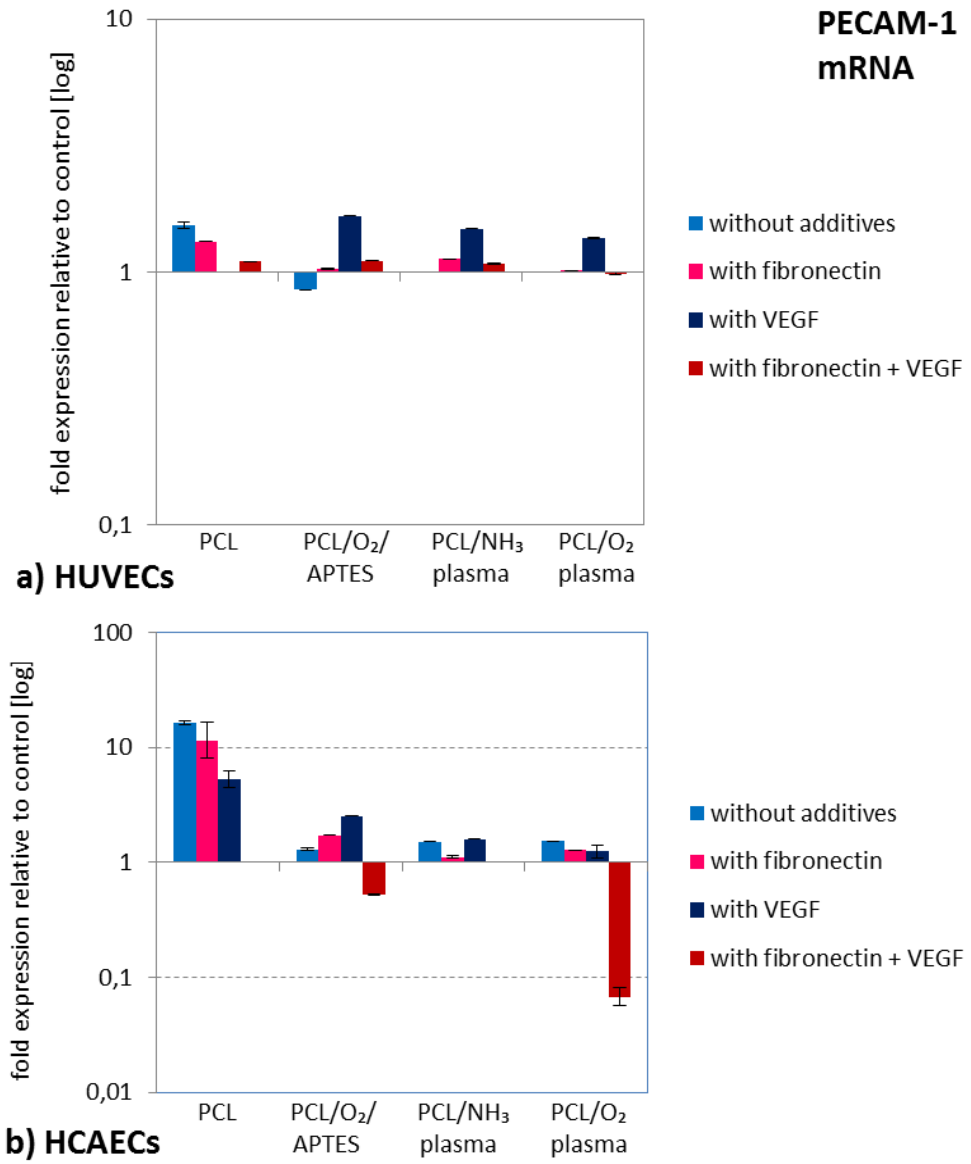

Figure 3.31. PECAM-1 expression in (a) HUVECs and (b) HCAECs as a function of PCL modification and presence of fibronectin (50 µg/ml) and/or VEGF (25 ng/ml). The untreated controls are HUVECs (for a) or HCAECs (for b) grown on polystyrene without additives. A fold-change of 0.4 is the same as 2.5-fold downregulation. Error bars denote the minimum and maximum of the standard error of the mean.

The amount of IL-8 mRNA was expected to increase in general, since IL-8 is a proinflammatory cytokine and the endothelial cells were only exposed to their respective substrate for 48 h before RNA isolation. Physiologically, this would equate to the initial phase of the foreign body reaction, in which IL-8 is involved. In HUVECs, IL-8 transcript amounts relative to control cells on tissue culture polystyrene were increased for all four substrates and conditions (**figure 3.32**a), with cells growing on plasma activated PCL demonstrating even higher amounts (up to 19.3-fold on fibronectin coated PCL/NH_3 plasma

relative to the control) than those growing on regular PCL (maximum 7.3-fold with fibronectin and VEGF treatment). Independent of external stimulation, the lowest relative amounts of HUVEC IL-8 mRNA were detected when the cells grew on APTES activated PCL.

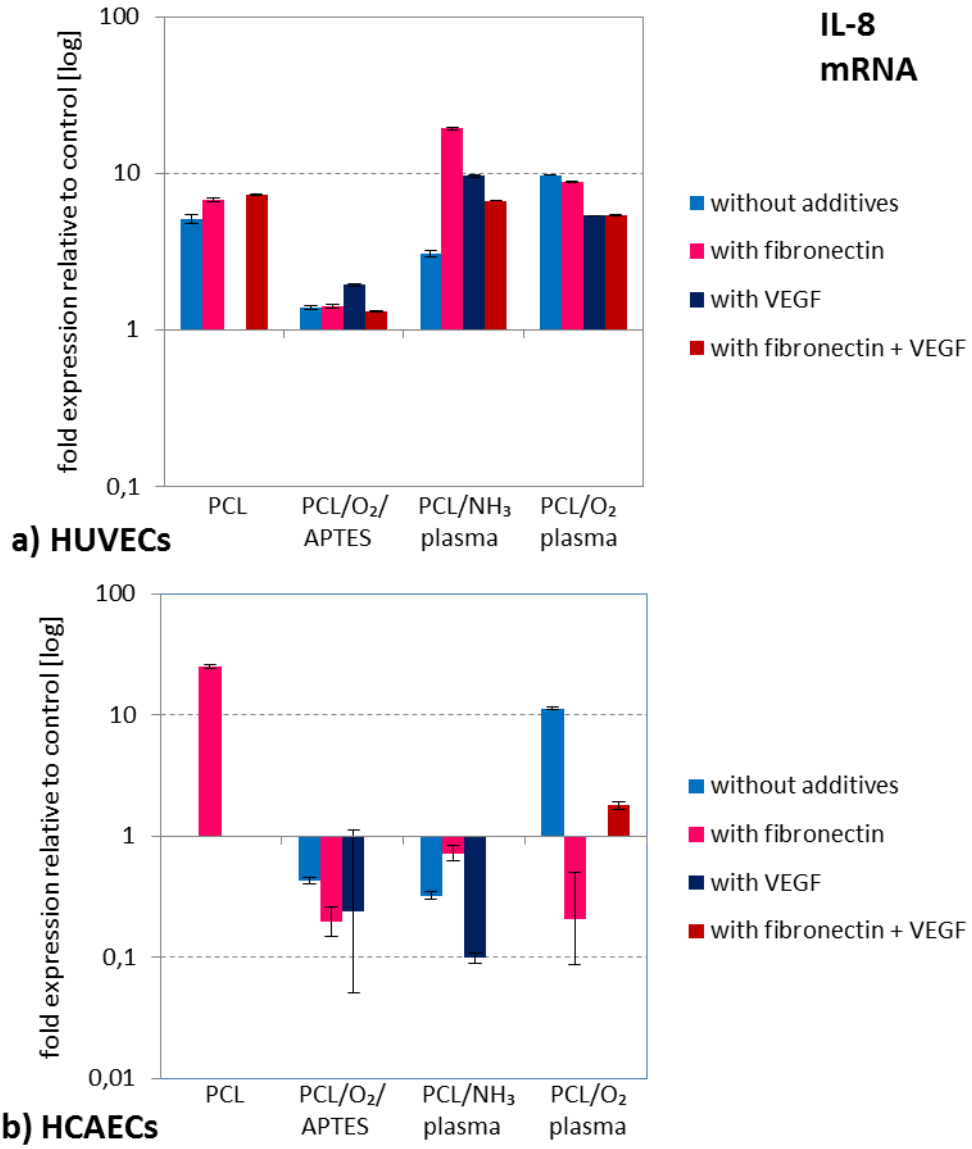

Figure 3.32. IL-8 expression in (a) HUVECs and (b) HCAECs s as a function of PCL modification and presence of fibronectin (50 µg/ml) and/or VEGF (25 ng/ml). The untreated controls are HUVECs (for a) or HCAECs (for b) grown on polystyrene without additives. A fold-change of 0.4 is the same as 2.5-fold downregulation. Error bars denote the minimum and maximum of the standard error of the mean.

The quantification of IL-8 transcript in HCAECs (figure 3.32b) yielded results that were not as unequivocal as in HUVECs, with relatively increased amounts only in cells grown on regular PCL and O_2 plasma activated PCL. In contrast, HCAECs on PCL activated with

either APTES or NH_3 plasma presented with reduced levels of IL-8 mRNA, down to a 10.2-fold decrease (in HCAECs on PCL/NH_3 plasma with VEGF stimulation). Once again, the highest increase in mRNA amount was seen on regular PCL (with fibronectin; 24.8-fold), compared to which all HCAECs on activated PCL surfaces produced less IL-8 transcript.

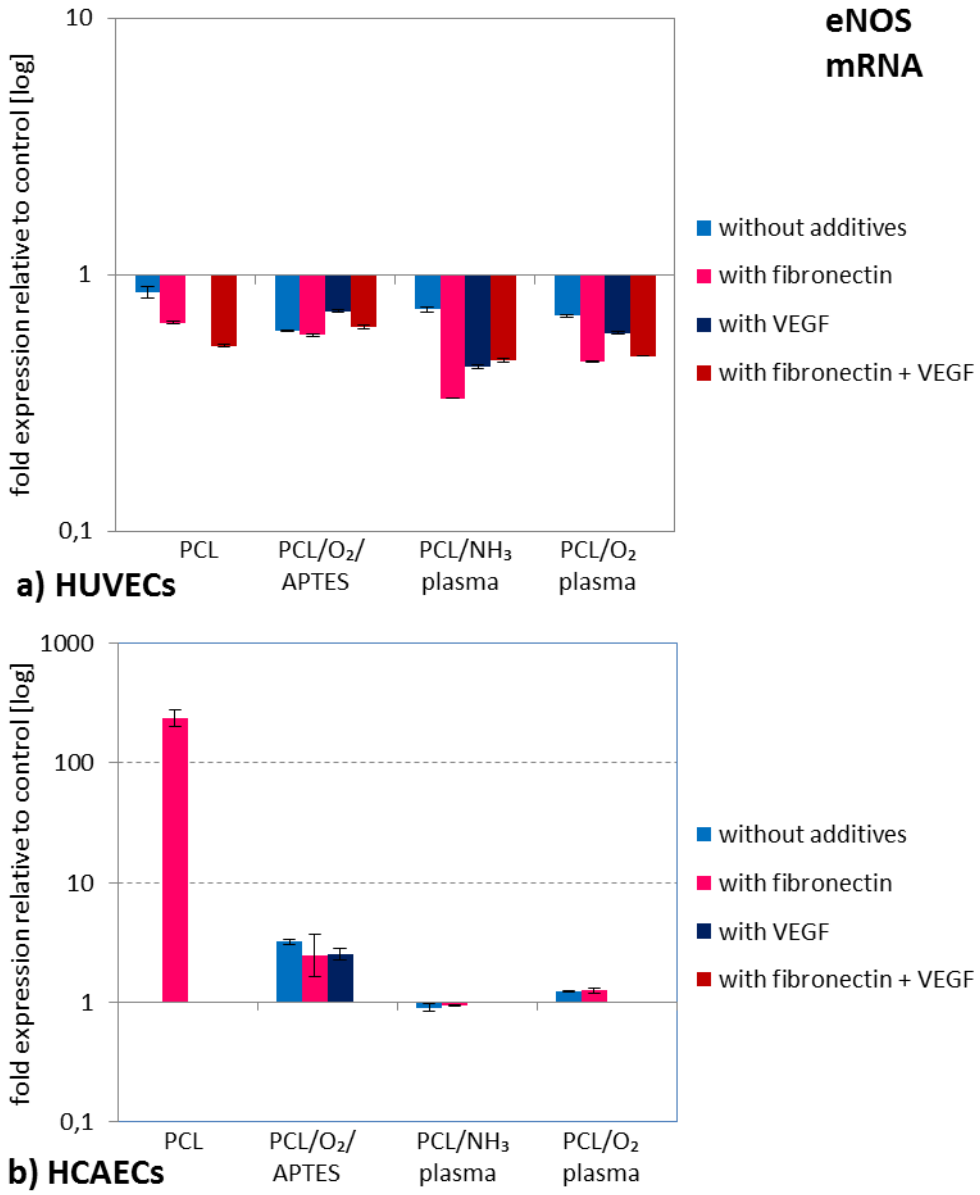

Figure 3.33. eNOS expression in (a) HUVECs and (b) HCAECs as a function of PCL modification and presence of fibronectin (50 µg/ml) and/or VEGF (25 ng/ml). The untreated controls are HUVECs (for a) or HCAECs (for b) grown on polystyrene without additives. A fold-change of 0.4 is the same as 2.5-fold downregulation. Error bars denote the minimum and maximum of the standard error of the mean.

The trend of marked increase in the amount of transcript in HCAECs grown on regular PCL and mitigated increase in HCAECs grown on activated PCL reappeared in the case of

eNOS (**figure 3.33**b). Compared to the control growing on uncoated polystyrene, eNOS mRNA remained practically unchanged on plasma activated PCL (maximum 1.3-fold increase in HCAECs grown on PCL/O_2 plasma/fibronectin), while on PCL/O_2/APTES the increase was higher (maximum 3.2-fold increase in HCAECs receiving no external stimulation). Why the gain was so much more extreme in cells on regular PCL with fibronectin coating (234-fold relative to the control) cannot be explained, but there were many unreplicated amplifications of eNOS transcript in the HCAEC samples. Overall, surface activation of PCL appears to mitigate mRNA abundance of cell adhesion molecules, IL-8 and eNOS in HCAECs.

The picture for HUVEC eNOS mRNA (figure 3.33a) was very different, with relative reduction found in every instance. While the observed decrease was only minor on regular and APTES activated PCL (minimum of 0.53 on fibronectin coated PCL with VEGF), it became more pronounced on the two plasma activated PCL varieties (minimum of 0.33 on fibronectin coated PCL/NH_3 plasma). That this functional endothelial marker should be consistently decreased in terms of mRNA expression was contrary to expectations, but is in line with the consistent upregulation of IL-8 expression in HUVECs on PCL.

4. Discussion

The scientific aim of this thesis was to examine endothelial cell adhesion to biomaterials subjected to different kinds of modification and functionalization, and to characterize cell behavior on the various materials differentially by means of biocompatibility testing, confocal microscopy and gene expression studies. This shall contribute to the body of knowledge on interaction between endothelial cells and implant materials, as endothelialization of vascular implant surfaces is one crucial aspect in the aftermath of medical intervention in patients with peripheral or coronary artery disease (CAD). The problem of endothelial injury during stent or graft implantation cannot be avoided and thus represents an inherent risk for later complications. A complex cascade of inflammatory processes may culminate in restenosis or thrombosis. Despite significant reductions in these complications that have been achieved with the development of DES and DEB, a serious risk for the patient remains. A truly safe and efficacious stent would have to minimize vessel trauma and inflammation, be mechanically sound yet biocompatible, facilitate endothelialization and positive remodeling of the vessel, be anti-restenotic and void the need for anti-platelet therapy [94].

Since the scope was limited to *in vitro* experiments, two different types of primary endothelial cells were examined and compared, for a better understanding of what range of response might occur when cells differing in their phenotypes are interacting with differentially modified biomaterials.

4.1. Optimization of *in vitro* stimulation parameters

The first series of experiments established an incubation and stimulation regime for primary endothelial cells. Firstly, PCL as the polymer of choice was tested for possible cytotoxic effects. These could be ruled out for untreated and activated forms of PCL (see figure 3.2.) While in undiluted form they performed significantly poorer than polystyrene, the relative viability and proliferation of human umbilical vein endothelial cells (HUVECs) incubated in the PCL eluates was still higher than of those exposed to thermanox, the other polymer tested. Besides, biocompatibility values of the diluted PCL eluates tended to excel those of polystyrene, and *in vivo* any substances detrimental to ECs would be strongly and rapidly diluted through the constant flow of blood. It was found that depletion of the endothelial cell culture medium of growth factors was essential, to exclude masking effects in the subsequent VEGF stimulation experiments (see figure 3.2). There a cumulative effect of the growth factor on both viability and proliferation of HUVECs was confirmed. As issues with dedifferentiation of primary cells that are experimented on for more than 4 days in a row are well documented [10], the general duration of the experiments was limited to 96 hours. This

assured avoidance of said problems, and at the same time it proved to be long enough for substantial effects on cell behavior to materialize. Similarly, same-batch cells were only employed in experiments between passages three to six, as their responsiveness to VEGF stimulation decreased significantly at passage 7 (see figure 3.5).

The seeding density was another factor that needed consideration. It was found that the extent of VEGF responsiveness was dependent on it, with greater increases in cell viability and proliferation at lower seeding densities. This is in good agreement with the published finding that cell seeding density and growth factor sensitivity are inversely correlated [67], as well as with previous studies on endothelial cell – biomaterial interaction, where high seeding densities correlated with extensive intercellular interaction that masked substrate dependent differences in cell adhesion [88]. Because endothelial cell density after implantation of blood contacting devices will initially always be low on the newly introduced surface, low seeding densities are recommended for *in vitro* studies of biomaterial applications, such as PCL in this case. Confluence should be avoided because contact inhibition will render the cells unresponsive to growth stimuli. For these reasons, HUVECs and human coronary artery endothelial cells (HCAECs) were generally seeded at 11,000 cells/cm^2 for biocompatibility testing of the various PCL substrates. In the context of endothelial cell culture with polymer, such a density has been successfully tried before [15].

Arresting the cell cycle prior to VEGF stimulation proved to greatly enhance the stimulatory effect of VEGF, especially on the proliferation rate of HUVECs (see figure 3.10). This result is in line with previous studies on growth factor effects on arrested cells [89], and therefore temporary cell cycle arrest was introduced as standard treatment of all endothelial cells tested on polymer substrates.

As primary cells can only be cultured for a limited time, the variability of cell responses across different cell sources also was an important issue to solve. Individual testing of each new batch of cells revealed that in terms of stimulation of proliferation and viability of endothelial cells, there is a considerable range. In some cases, a linear dose response to VEGF was seen, whereas in others the maximum stimulation was already reached at a medium VEGF concentration and above that dropped off (see figure 3.12). As a consequence, cells had to pass a quality control step where the stimulation by VEGF had to exceed 130% of the unstimulated state in order to be employed in subsequent growth experiments on the functionalized polymer. This was done to achieve better reproducibility of results.

In addition, confounding methodological factors were identified and subsequently controlled for, excluding a source of bias.

4.2. Polymer surface modification

One important step towards the development of an implant allowing rapid endothelialization is optimizing the polymer surface for adhesion of endothelial cells, which the present thesis has endeavored to do. While polymers are favored as stent coatings thanks to their degradation behavior [95], they are very hydrophobic as unmodified material and therefore difficult to colonize with the desired cells. Surface functionalization can reduce that hydrophobicity and will exert maximum effect *in vitro*, because cells are directly seeded onto functional groups [96]. This research demonstrates that changes in PCL morphology do not significantly increase the attraction of this material for HUVECs and HCAECs (see figure 3.13), and that there is a limited influence of chemical surface modification on the adhesion of the two types of endothelial cells *in vitro* (see figure 3.14). The number of accessible amino groups on the PCL surface plays a role, for example, since it is the highest with APTES modification and the lowest with plasma activation, and HUVECs as well as HCAECs seem to prefer the latter (see figure 3.14). Wulf and colleagues have shown that ammonia plasma activation of PCL generates up to 12% primary amines of the total nitrogen content, while PCL activation with APTES results in 26% primary amines [95]. It is possible that the intermediate silane layer (situated between the PCL and the amino group on the surface) generated by APTES modification contributes to the observed lower viability of the endothelial cells there.

Wet chemical modification can alter the surface topography, creating a surface that is rough and hydrophilic [95] and therefore easier to colonize. The modification solution is assumed to penetrate the polymer bulk, but associated changes in bulk properties can be minimized in optimal modification conditions. With plasma activation there is no such change in bulk properties of the material [97][Junkar et al. 2011]. Also in contrast to wet chemical treatments, plasma modification does not necessitate the use of solvents, hence there is no risk of the material roughening or degrading [98]. An early study reported enhanced growth of bovine aortic endothelial cells over 3 days as a result of the generation of oxygen-containing surface chemistries by plasma activation [99]. More recently, plasma-activated coating has been found to possess very low thrombogenicity *in vitro* and to be a feasible modification of stents with favourable endothelialization rate and neointimal response *in vivo* [26]. The results here point in the same direction, as amongst all modified forms of PCL, for HUVECs as well as for HCAECs, both types of plasma activated PCL were found to convey the highest relative viability. So despite the lack of significant differences, the observed trend is in accordance with previous research demonstrating that adhesion and growth of human endothelial cells can be enhanced by changing surface properties of polymer substrates [15]. Moreover, the remarkable similarity of the results for HUVECs and

HCAECs (see figures 3.13 and 3.14) is an indication for the applicability of these findings to endothelial cells in general.

4.3. Growth factor stimulation

In animal models, VEGF has been reported to reduce both neointimal growth [75] and neovascularisation. Among the effects of VEGF are the upregulation of endothelial NO synthase (eNOS) [100] as well as inhibition of platelet and leukocyte activation and of smooth muscle cell proliferation [28]. All of these are desirable outcomes in the context of vascular stent implantation, which motivated this research in terms of testing the effects of VEGF stimulation on endothelial cells growing on a functionalized biopolymer. It is demonstrated here that HUVEC and HCAEC proliferation and viability can be profoundly and reliably stimulated by VEGF *in vitro* (figures 3.6 and 3.7) and that the extent of that stimulation varies with the adhesion substrate (figures 3.15 to 3.20).

Previous studies [71, 101, 102] have highlighted the potential for VEGF to optimize the outcome of stent angioplasty, which is supported by the findings here because after stimulating the viability of HUVECs or HCAECs through plasma chemical activation of the substrate they adhere to (figure 3.14), the application of VEGF further increases their viability (figures 3.16 and 3.19). The observed magnitude of stimulation through VEGF is in good accordance with other studies. A 15% increase in human saphenous vein endothelial cell number after 2 days of 1 ng/ml VEGF stimulation has been reported with recombinant VEGF [70], while HUVECs exposed to VEGF-eluting stents showed an 11% increase in cell growth [71]. Walter et al. reported a 25% increase in re-endothelialization of rabbit external iliac artery 10 days after implantation of a VEGF gene-eluting stent compared to a control stent [103]. In rats, a single 30-minute application of 100 µg VEGF to the freshly denuded intima of the carotid artery resulted in nearly double re-endothelialization compared to controls, along with only one third of neointimal thickening 2 weeks after surgery [102]. In rabbits, delivery of 100 µg VEGF through a deployed stent to the underlying arterial wall accelerated re-endothelialization from 4 weeks post implantation in controls to 1 week, along with markedly reduced stent thrombosis [101]. In contrast, VEGF has also been found to induce intimal hyperplasia when released from ePTFE grafts [76].

Overall, in the present study treatment with VEGF achieved good stimulation of human endothelial cells on all substrates tested. It is evident that the type of PCL activation has an effect on the extent of VEGF-induced stimulation of HUVEC viability on PCL. A specific growth stimulus through VEGF may accelerate the colonization of the luminal stent surface with endothelial cells, and a confluent endothelium constitutes an antithrombogenic surface [104]. In this regard, there was again great congruence in the results obtained with

HUVECs and HCAECs, and this was true for cell viability testing as well as confocal laser scanning microscopy (see figures 3.13 to 3.19).

Recent and current strategies using DES to reduce restenosis focus primarily on antiproliferative approaches. Sirolimus and paclitaxel control restenosis through a cytostatic mode of action and are therefore the two most commonly used antiproliferative substances in DES coatings. Through intracellular signaling cascades, sirolimus and paclitaxel arrest the smooth muscle cells (SMCs) in G_1 and G_2 phase of the cell cycle, respectively. A major disadvantage of these antiproliferative drugs is that they are not cell type specific and arrest endothelial cell proliferation as well. Sirolimus is known to strongly inhibit VEGF expression and secretion, which then results in delayed re-endothelialization and can promote acute stent thrombosis [105]. Both sirolimus and paclitaxel, when incorporated into DES, produced significant reductions in re-endothelialization compared to bare metal stents, and the inhibitory effect of sirolimus was greater than that of paclitaxel [106]. Experimental and clinical studies have demonstrated that antiproliferative drugs released from DES delay stent re-endothelialization and favor a prothrombogenic environment that can cause late thrombosis [107, 108].

Generally, the initial absence of a functional endothelium is associated with neointimal hyperplasia and thrombosis alike [109]. A direct correlation between endothelial defects and neointimal thickening in terms of severity and extent was found early on in several rat models as well as in human coronary arteries explanted from transplant recipients [[100, 103]. Subsequent studies have suggested that accelerating re-endothelialization can attenuate restenosis and inhibit stent thrombosis. Jeremy and colleagues found that the presence of an intact endothelium can suffice to effectively inhibit the proliferation of the underlying medial SMCs [110]. This inhibition is mediated via release of vasodilators, i.e. NO and heparin sulphate, that keep SMCs in a quiescent state [111, 112]. A prerequisite for this is not only complete re-endothelialization but regained functional capacity of the endothelium, such that it can regulate vasodilators and thereby halt SMC hyperplasia. An in silico model of stent deployment and subsequent shear stress distribution on ECs and NO production by ECs revealed that if the endothelium can become functional very quickly (within two weeks post implantation), then in-stent restenosis can be avoided altogether [113].

Hence there is a need to use alternative drugs in vascular implant coatings which will facilitate the growth of endothelial cells and simultaneously inhibit the growth of SMCs. VEGF appears to be a good candidate, especially for combinatorial implant coatings (for example, with an antiproliferation drug), as it is specific for endothelial cells and also indirectly inhibits SMC proliferation by inducing endothelial NO synthase. Stent-based

delivery of naked plasmid DNA encoding human VEGF in rabbits resulted in expression of VEGF mRNA and protein for up to 10 days [103]. Interestingly, throughout this period the VEGF transcript was localized primarily to the outer media and adventitia of the vessel wall. Concurrently the endothelium recovered in terms of anatomy (confluent monolayer) as well as function (NO production), and it did so much more rapidly than in animals which had been implanted a control stent. This shows that VEGF may also modulate aspects of endothelial homeostasis that are more qualitative, apart from facilitating endothelial repair at the stent site [102]. At 3 months post procedure, neointimal proliferation in the VEGF-stented rabbits was also significantly reduced [103]. These findings indicate that VEGF incorporated into vascular implants may indirectly reduce the extent of neointimal hyperplasia while promoting endothelial recovery.

Suitability of VEGF is also demonstrated by the data obtained here when the growth factor was bound to the polymer surface. Whether it was through adsorption onto sPCL-A or by covalent coupling through crosslinkers, VEGF was able to significantly increase the viability of HUVECs adhering to sPCL-A. This result corresponds nicely with an animal study where PCL scaffolds were implanted in mice and after 7 and 14 days a significant pro-angiogenic effect was manifest when VEGF was bound to PCL through heparin [114]. In the sPCL-A experiments here, there was no significant difference in the bioactivity of immobilized and soluble VEGF. A new study has also found bioactivity of VEGF not to be impaired when it is dissolved in chloroform, as is necessary prior to its covalent coupling to polymers [115]. This is an important result, as such coupling is essential for long term release of VEGF from implants.

4.4. PCL coating with ECM proteins

All polymers discovered and used in the vascular implant setting so far have proven to be inferior to the native endothelium. Yet certain modifications can be very helpful in overcoming this general drawback. Polymer coating with proteins from the ECM provides cells with molecular cues for adhesion and so generally facilitates endothelial cell growth [76], which is one critical aspect of an implant's biocompatibility. Besides, it is known that the effectiveness of VEGF in inducing blood vessel formation is enhanced when it is bound to the ECM [114].

Here, the endothelialization facilitating effect of matrix proteins was dose-dependent for laminin, fibronectin, gelatin and collagen type I, with fibronectin stimulating the growth of HUVECs in the most consistent manner (figures 3.22 and 3.23). Because of this and the fact that fibronectin is the most adhesive of the ECM glycoproteins [62], the focus of the subsequent experiments was put on fibronectin coatings of PCL.

While protein coatings are common practice for biomaterials in a cell culture context [85], the fast degradation rate of ECM proteins is problematic [35], and it should be kept in mind that the ECM also promotes primary lesions and restenosis in humans [102]. This is hardly surprising, as the process of blood coagulation starts out with surface adhesion of serum protein [98], and the ECM meshwork constitutes a large protein-rich surface. While fibronectin possesses good affinity for binding endothelial cells, it also induces platelet activation [76]. Moreover, fibronectin not only promotes endothelial cell growth but also vascular SMC migration and proliferation as shown *in vitro* [85]. In that study, only a mixture of the ECM components fibronectin, fibrinogen and tropoelastin was able to minimize SMC migration whilst still promoting endothelial cell outgrowth. Increased ECM synthesis occurs, for example, in response to vascular intimal injury [18]. Arterial neointimal hyperplasia is a wound healing response to the significant mechanical trauma at the implant site. This process is associated with proliferation and migration of vascular SMCs and ECM deposition, which leads to restenosis. Furthermore, *in vitro* testing of enriched hematopoietic progenitor cell cultures revealed a mostly negative impact of collagen type I on cell growth [78]. This may be attributed to the fact that collagen I activates platelets, which also readily bind to it, resulting in thrombus formation [116]. Also, degraded collagen type I has been shown to induce an activated, proliferating SMC phenotype, whereas without degradation collagen promotes a quiescent and contractile vascular SMC phenotype [117]. Here, the general increase in endothelial colonization of ECM protein-coated PCL observed in the PCL coating experiments (figure 3.22) indicates that these cell-adhesive glycoproteins can adsorb onto the polymer without denaturing. This finding is in agreement with the literature [118].

In spite of the occasional reports on complications related to the use of ECM protein on biomaterials [85, 117], several approaches in tissue engineering make use of ECM proteins as carriers for bioactive compounds such as growth factors [35]. Furthermore, scaffolds designed to guide bone regeneration include collagen for its beneficial properties in wound repair, for example [35].

While it is known that protein adsorption (especially of cell adhesive glycoproteins present in serum) can mask the surface chemistry of implants [118], it appears to be advantageous when the desired protein (e.g. fibronectin) is intentionally adsorbed onto the surface. The results obtained in this thesis demonstrate that ECM protein precoating is clearly beneficial for subsequent adhesion of endothelial cells (figure 3.22). In patients, the increased endothelialization should then prevent the migration and proliferation of SMCs.

Certain combinations of alpha and beta integrin subunits are specific to matrix proteins such as fibronectin, laminin and collagen [78]. Through its integrin-binding amino acid

sequence arginine-glycine-asparagine (RGD), fibronectin can promote cell attachment, spreading and differentiation [119]. A pronounced stimulatory effect of fibronectin on cell adhesion and growth has been demonstrated for HUVECs [120] as well as for human aortic endothelial cells [121]. On hydrophobic surfaces, fibronectin is likely oriented in such a way that its integrin-binding sequences are most accessible [62]; this might account for enhanced endothelialization on fibronectin coated PCL (see figures 3.23 and 3.24), as PCL in itself is a hydrophobic material.

In line with previous studies [118], there is an increase in endothelial colonization of PCL when the polymer is precoated with ECM protein. When the polymer is coated with proteins by adsorption only, as was the case here, the strength of the polymer-protein bond can be assumed to be comparatively low. The lower the anchorage strength of fibronectin on the modified material, the more cell-matrix focal adhesions can be formed on that material [122].

Furthermore, proteins of the extracellular matrix are known to suppress HUVEC apoptosis [123]. Apoptotic HUVECs are procoagulant and bind platelets [123]. Apoptosis rates revealed through TUNEL staining of HUVECs could be reduced as much as 40% *in vivo* by coating collagen modules with fibronectin [123]. This is another beneficial impact of fibronectin coatings on endothelialization and might be the cause of the additional gain in HUVEC viability upon combined VEGF application and protein coating of plain PCL and NH_3 plasma activated PCL (see figure 3.28).

As plasma chemical activation of PCL and silanization with APTES consistently yielded the best results in terms of improved viability, proliferation and adhesion of endothelial cells, these modifications were selected for subsequent investigations into the effects of cell exposure to additional treatments found to be promoting the endothelialization of PCL. When ECM protein coating of PCL was combined with VEGF stimulation, the effects seen before with fibronectin alone were not reproduced (see figure 3.26). This was most likely due to the difference in cell origin, as throughout this study cell source proved to be the main cause of variability of cell responsiveness to adhesion promoting external stimuli. Another possible explanation is fast degradation of fibronectin. Nonetheless, the combination of surface activation, fibronectin coating of the polymer and VEGF produced an increase in cell viability that was greater than with VEGF alone. In the case of HUVECs growing on PCL/NH_3 plasma, this increase was significant, suggesting that the combined treatment may aid uniform and fast endothelialization of plasma activated PCL.

4.5. Substrate induced changes in endothelial cell mRNA expression

The pattern of adhesion molecule gene expression seen here has its value most likely with regard to the foreign body reaction the examined PCL surfaces might elicit *in vivo*. The results speak in favor of PCL/O_2/APTES, where upregulation of the proinflammatory genes was least pronounced. APTES modified PCL was included in the qPCR study because it emerged from the previous experiments as the most promising type of wet chemical activation for endothelialization. Across the four PCL surfaces and two cell types investigated, APTES modified PCL caused the least proinflammatory mRNA profile in the cells growing on it, with a pronounced relative decrease in HUVEC ICAM-1 and VCAM-1 mRNAs, and the smallest relative increase in HUVEC IL-8 mRNA. In HCAECs on PCL/O_2/APTES, ICAM-1 mRNA hardly changed relative to the control (see figure 3.29b), and the increase in VCAM-1 mRNA was smaller than on the other substrates (see figure 3.29b). However, as the experiments were performed with monocultures of endothelial cells, the molecular response of the cells to the different surfaces and stimulants at the mRNA level cannot be regarded as representative for physiological conditions, where gene regulation is substantially influenced by the interplay between different cell types. The adhesion molecules in particular are subject to feedback loops of regulation between endothelial cells, monocytes, platelets, neutrophils and other leukocytes. Therefore the degree and/or the direction of change in the amount of transcripts of the five genes investigated could well be different in experimental settings involving coculture with white blood cells, and different again in animal models.

A large proportion of the changes in the transcript amount of the five genes examined here was less than two-fold compared to the control and therefore in all likelihood not biologically relevant. In their thorough analysis of HUVEC and HCAEC adhesion molecule gene expression, Suna and colleagues considered only changes that were more than 2.6-fold as significant [17]. The finding here that the highest relative increase in a particular gene transcript was always seen in HCAECs corresponds well with their data, where the mRNA response to an inflammatory stimulus was generally significantly higher in HCAECs than in HUVECs [17].

ICAM-1 was the only gene for which the quantitative mRNA response to the different substrates and stimuli (see figure 3.29) was broadly similar in both HUVECs and HCAECs (e.g 0.62-fold for HUVECs and 0.44-fold for HCAECs on PCL/O_2/APTES without additives, 0.84-fold for HUVECs and 0.69-fold for HCAECs on PCL/NH_3 plasma without additives, 1.43-fold for HUVECs and 1.84-fold for HCAECs on PCL/O_2 plasma without additives), and even in this case the extent of regulation in some instances differed markedly (e.g. 2.95-fold downregulation for HUVECs compared with only 1.35-fold for HCAECs on PCL/O_2/APTES with VEGF). So while the results of cell viability for HUVECs and HCAECs

alike indicate that plasma activation of PCL is the most advantageous form of PCL modification and are in good accordance, the qPCR results show substantial differences in the way that surface modification and growth stimulation impact on gene expression in different cell types.

The observation that both ICAM-1 and VCAM-1 mRNA expression show the overall highest increase when HUVECs as well as HCAECs are grown on regular PCL is supported by the fact that the two molecules are induced at sites of inflammation [9]; PCL without adhesion-friendly surface activation was expected to yield the highest degree of foreign body response in endothelial cells. The extent of upregulation is in accordance with other findings: Suna and colleagues found VCAM-1 transcript in HUVECs and HCAECs increased 289-fold and 1141-fold, respectively, in response to 2 h stimulation with lymphotoxin-alpha (LTA; a member of the tumor necrosis factor family). Van der Zijpp and colleagues reported that fibronectin coating masks the influence of the underlying polymer surface on ICAM-1 expression in HUVECs [10]. This in contrast to the findings here, where the surface-dependent quantitative changes in ICAM-1 mRNA were also seen when the PCL surface was precoated with fibronectin.

In a few instances (HUVEC ICAM-1 and VCAM-1 on NH_3 plasma activated PCL, HCAEC IL-8 on O_2 plasma activated PCL), the general trend for change in transcript quantity on a particular PCL surface showed an aberration when fibronectin alone was added to that surface. A possible reason for this observation may lie in conformational changes that the underlying polymer surface induces in fibronectin, thus influencing its cell binding properties [10]. Such an effect seems likely to be overridden by the presence of VEGF, as indicated by the respective qPCR data here.

The qPCR results for PECAM-1 (see figure 3.31) are in line with those reported by Busch and colleagues, who also found that the expression of this adhesion molecule varies with polymer substrate [4]. Under static conditions, they saw higher upregulation than under flow. Here the most apparent outcome was that, taking both endothelial cell types into account, PCL activation with APTES or NH_3 plasma left the production of PECAM-1 transcript in the cells growing on those substrates almost unchanged (see figure 3.31). For HUVECs, the biggest factor influencing PECAM-1 mRNA seems to be stimulation with VEGF alone, which is in accordance with their adhesion on the various PCL surfaces observed by means of CLSM (see figure 3.17). Whether the observed changes indicate advantageous properties of activated PCL cannot be clearly assessed, because PECAM-1 expression in endothelial cells has been reported to be reduced or unchanged, respectively, at the protein level upon application of LPS and TNF-α, both strong proinflammatory stimuli [82].

The comparatively strong increase in IL-8 transcript amount in HUVECs on both nitrogen and oxygen plasma activated PCL (see figure 3.31) does not preclude these surfaces from further consideration. Firstly, they compared favorably in all the experiments on biocompatibility, and secondly, it is already known that resting HUVECs express high levels of IL-8 [11]. That this represents a cell type specific characteristic is supported by the overall reduced IL-8 response in HCAECs, where most of the samples grown on activated PCL demonstrated decreased levels of IL-8 mRNA compared to the unstimulated control grown on polystyrene (see figure 3.31b).

The consistent decrease in eNOS mRNA amount in HUVECs was surprising, because as an indicator for proper endothelial functional, more differential expression patterns could be expected, with surfaces that had proven beneficial for HUVEC adhesion to modified PCL allowing for increased eNOS transcription. The apparent downregulation observed in the experimental setup here suggests that HUVECs perhaps need more time to fully settle on the newly introduced adhesion substrate before qualitative differences between substrates will translate into differential eNOS expression.

The limitations of the qPCR data presented here are manifold: they were obtained 1. *in vitro* with endothelial cells only, 2. in a static setup, 3. with only one concentration of fibronectin and VEGF, and 4. at only one time point. While significant changes in mRNA amounts have been detected with only 2 hours of EC stimulation [17], it is possible that the expression, especially of target genes such as eNOS, might take longer than the 24 h used here to be altered significantly. One explanation for the consistent downregulation of eNOS in HUVECs might be that during the relatively short exposure of the cells to the polymer substrates, they are still preoccupied with the foreign body reaction. Another possibility, as has been speculated by van der Zijpp and colleagues [10], is that in the early phase of interaction with the biomaterial, the cells are channeling their energy to adhesion and growth on the polymer, and as a consequence transcription of eNOS would not increase until monolayer formation is completed.

The impact of blood flow on the cells is also considerable. There are many studies demonstrating that shear stress, as it is present in blood vessels *in vivo* due to constant blood flow, is a major factor influencing the behavior of endothelial cells. So it is feasible that the presence of shear stress might be a requirement for the characteristic pattern of endothelial gene expression. For example, it is known that eNOS is activated by blood shear stress [124] and that local changes in shear stress, which occur at arterial branching points and elsewhere, alter the mRNA expression of ICAM-1 and VCAM-1 [12]. The application of physiological shear stress, however, was not possible within the framework of this thesis. Thus it seems possible that the observed consistent downregulation of eNOS

mRNA in HUVECs growing on plain and activated PCL is a result of the absence of shear stress. In any event, it seems likely that the occasional drastic regulation of important endothelial genes seen here is an artefact, especially as there was no instance in which it was reproduced over the two cell types examined.

So while the qPCR experiments over the 16 conditions (four substrates in four different states of stimulation) and two cell types investigated yielded results that were much less unequivocal than expected, one important trend confirmed the findings from the studies on PCL endothelialization: overall expression of genes that are regarded as markers for inflammatory risk in atherosclerosis was substantially increased on PCL without surface activation, and these increases were much reduced after chemical activation of the PCL surface. Hence, such surface modification appears to be a treatment capable of counteracting proinflammatory properties of this polymer.

4.6. Conclusion

Re-endothelialization of luminal surfaces is the critical factor after implantation of cardiovascular prostheses or stents. This thesis has established an experimental model for polymer endothelialization *in vitro* and examined the potential of morphological, chemical and biological modifications of PCL in that regard. Of these, plasma chemical activation of the polymer surface yielded the largest increase in HUVEC and HCAEC growth, with remarkable similarity between the two cell types. In particular, PCL activated with NH_3 plasma was the material with the most pro-endothelialization properties, while APTES activated PCL appeared to induce the lowest extent of inflammatory response in terms of mRNA expression.

Endothelialization can be enhanced by VEGF, both in soluble form and after its immobilization on the polymer. There was a high degree of congruence between the two cell types in terms of VEGF responsiveness. To ensure endothelial cell stimulation, the concentration of VEGF at the substrate/endothelial interface should be equal to a range of 5 to 50 ng/ml *in vitro*.

Precoating of PCL with fibronectin can be beneficial, but in combination with VEGF there is no significant cumulative gain for HUVECs or HCAECs. Therefore, pending animal and preclinicial studies, it is proposed that the results presented in this thesis can contribute to alleviate the shortcomings of presently used cardiovascular implants. In particular, chemical and biological surface modification of polymers have the potential to reduce post-procedural restenosis and thrombosis risks that still remain for patients receiving such implants.

Abstract

Owing to the aging population in the developed world and increasing prevalence of atheroscleoris and cardiovascular disease, vascular implants for the treatment of diseased blood vessels are in high demand. While the practice of percutaneous transluminal coronary angioplasty (PTCA) with and without stenting has reached a high degree of clinical routine, a large number of coronary heart disease patients are still affected by post-operative complications such as restenosis and thrombosis. These often necessitate further medical intervention with open surgery, or in severe cases even cause fatal myocardiac arrest.

The crucial player at the interface of implant and patient is the endothelial cell layer, as it is situated on the vessel wall, separating the underlying tissue from the bloodstream. During the insertion of vascular implants, endothelial injury is inevitable. At the same time, functional recovery of the endothelium is imperative to the implant's success and the patient's wellbeing. The majority of clinically used implants today, however, have shortcomings in allowing the endothelium to recover. As a consequence, too many patients are still suffering the aforementioned post-implantation complications. This status quo creates a need for modern biomaterials that aid endothelial cells in their adhesion and functional recovery post-stenting. In this context, the present thesis systematically examines the potential of numerous chemical polymer modifications with regard to endothelialization. Human umbilical vein endothelial cells (HUVECs) and human coronary artery endothelial cells (HCAECs) are used to characterize endothelial cell responses in terms of *in vitro* viability, adhesion, growth and mRNA expression. As cell substrates, the biopolymer poly(ε-caprolactone) (PCL), three morphologically modified and five chemically activated forms of PCL are investigated in detail, as well as the impact of PCL precoating with proteins of the extracellular matrix and the effect of VEGF, an endothelium specific growth factor.

Firstly, a suitable *in vitro* model was established and optimized. A number of aspects had to be considered so as to exlude potential bias and bring the substrate effects to the fore. These included cell culture parameters as well as methodology-based factors such as unwanted interaction of the examined material with components of routine laboratory assays. Cytotoxicity of the modified polymer was excluded, and the standard experimental conditions were set to: exclusive use of cell passages 3 to 6, VEGF test stimulation of each cell batch, 24 h reversible arrest of the cell cycle before seeding, an initial cell seeding density of 11,000 cells/cm^2, VEGF stimulation immediately after cell seeding and for a total duration of 96 h at 25 ng/ml.

With the experimental setup optimized, primary endothelial cells were seeded on the various PCL surfaces and their biocompatibility assessed in a comparative approach. Cell viability assays demonstrated plasma activation of PCL to yield a substrate that presents both HUVECs and HCAECs with the best conditions for adhesion and growth. These results were confirmed by confocal laser scanning microscopy. Then the cells were subjected to additional stimulation by vascular endothelial growth factor, applied directly to the cell culture medium to boost endothelial cell proliferation on the polymer. For HUVECs, the maximum growth response, measured as cell viability and by confocal laser scanning microscopy, was again seen on the two plasma activated forms of PCL. For HCAECs, the highest stimulation of viability was detected on electrospun PCL and O_2 plasma activated PCL.

When, through crosslinkers, VEGF was covalently coupled to a PCL derivative, the viability of HUVECs adhering to this substrate was still increased, with no significant loss of the stimulatory effect compared to VEGF bound to PCL by surface adsorption.

In the next step, the various polymer surfaces were coated with extracellular matrix proteins, a method that is commonly used *in vitro* to promote cell adhesion. This proved to be beneficial for HUVECs, with fibronectin giving the most consistent benefit among four proteins tested. As a consequence, fibronectin precoating of PCL was investigated in combination with VEGF stimulation of HUVECs. A trend for additional advantageous effects on cell viability was seen, but the increase was significant only for NH_3 plasma activated PCL. Finally, mRNA expression in both cell types after 24 h stimulation with VEGF on four different PCL surfaces with and without fibronectin coating was analysed for eNOS, IL-8 and the endothelial adhesion molecules ICAM-1, PECAM-1 and VCAM-1. PCL activated with aminopropyltriethoxysilane (APTES) was the substrate on which HUVECs and HCAECs presented with the least proinflammatory mRNA expression pattern. The most notable difference between the two cell types here was that HCAECs always showed the highest relative increase in a given mRNA. Overall, however, the qPCR results were unequivocal, an outcome that is ascribed to experimental limitations such as the static setup and the snapshot sampling at only one time point.

By examining the impact of morphological, chemical and biological modifications of PCL, this thesis contributes towards the existing body of work on polymer endothelialization. It is concluded that NH_3 plasma chemical activation of PCL combined with VEGF stimulation best enhances *in vitro* endothelialization.

As an outlook for prospective studies, simulation of the blood vessel environment by application of shear stress and co-culture with smooth muscle cells or leukocytes are desirable, before the most favorably performing material can be transferred into animal studies and preclinical studies.

References

1. Thews, G., Mutschler, E., Vaupel, P.: Anatomie, Physiologie, Pathophysiologie des Menschen. 135 Tabellen. Wiss. Verl.-Ges., Stuttgart (1999)
2. Gutiérrez, E., Flammer, A.J., Lerman, L.O., Elízaga, J., Lerman, A., Fernández-Avilés, F.: Endothelial dysfunction over the course of coronary artery disease. Eur. Heart J. 34, 3175–3181 (2013)
3. Yin, M., Yuan, Y., Liu, C., Wang, J.: Combinatorial coating of adhesive polypeptide and anti-CD34 antibody for improved endothelial cell adhesion and proliferation. J Mater Sci Mater Med 20, 1513–1523 (2009)
4. Busch, R., Strohbach, A., Rethfeldt, S., Walz, S., Busch, M., Petersen, S., Felix, S., Sternberg, K.: New stent surface materials: the impact of polymer-dependent interactions of human endothelial cells, smooth muscle cells, and platelets. Acta Biomater 10, 688–700 (2014)
5. Stevens, H.Y., Melchior, B., Bell, K.S., Yun, S., Yeh, J.-C., Frangos, J.A.: PECAM-1 is a critical mediator of atherosclerosis. Dis Model Mech 1, 175-81; discussion 179 (2008)
6. Muller, W.A.: How endothelial cells regulate transmigration of leukocytes in the inflammatory response. Am. J. Pathol. 184, 886–896 (2014)
7. Park, S., DiMaio, T.A., Scheef, E.A., Sorenson, C.M., Sheibani, N.: PECAM-1 regulates proangiogenic properties of endothelial cells through modulation of cell-cell and cell-matrix interactions. Am. J. Physiol., Cell Physiol. 299, C1468-84 (2010)
8. Chacko, A.-M., Nayak, M., Greineder, C.F., Delisser, H.M., Muzykantov, V.R.: Collaborative enhancement of antibody binding to distinct PECAM-1 epitopes modulates endothelial targeting. PLoS ONE 7, e34958 (2012)
9. Hua, S.: Targeting sites of inflammation: intercellular adhesion molecule-1 as a target for novel inflammatory therapies. Front Pharmacol 4, 127 (2013)
10. van der Zijpp, Ype J T, Poot, A.A., Feijen, J.: ICAM-1 and VCAM-1 expression by endothelial cells grown on fibronectin-coated TCPS and PS. J Biomed Mater Res A 65, 51–59 (2003)
11. Yamaguchi, H., Ishii, E., Tashiro, K., Miyazaki, S.: Role of umbilical vein endothelial cells in hematopoiesis. Leuk Lymphoma 31, 61–69 (1998)
12. Rouleau, L., Rossi, J., Leask, R.L.: Concentration and time effects of dextran exposure on endothelial cell viability, attachment, and inflammatory marker expression in vitro. Ann Biomed Eng 38, 1451–1462 (2010)

13. Padfield, G.J., Newby, D.E., Mills, N.L.: Understanding the role of endothelial progenitor cells in percutaneous coronary intervention. J. Am. Coll. Cardiol. 55, 1553–1565 (2010)
14. Ma, X., Wu, T., Robich, M.P., Wang, X., Wu, H., Buchholz, B., McCarthy, S.: Drug-eluting stents. Int J Clin Exp Med 3, 192–201 (2010)
15. Nickson, C.M., Doherty, P.J., Williams, R.L.: Novel polymeric coatings with the potential to control in-stent restenosis--an in vitro study. J Biomater Appl 24, 437–452 (2010)
16. Head, S.J., Bogers, Ad J J C, Kappetein, A.P.: Drug-eluting stent implantation for coronary artery disease: current stents and a comparison with bypass surgery. Curr Opin Pharmacol 12, 147–154 (2012)
17. Suna, S., Sakata, Y., Sato, H., Mizuno, H., Nakatani, D., Shimizu, M., Usami, M., Takashima, S., Takeda, H., Hori, M.: Up-regulation of cell adhesion molecule genes in human endothelial cells stimulated by lymphotoxin alpha: DNA microarray analysis. J Atheroscler Thromb 15, 160–165 (2008)
18. Isenberg, B.C., Williams, C., Tranquillo, R.T.: Engineering of Small-Diameter Vessels. In: Principles of Regenerative Medicine, vol. 2nd edition 2011vol. , pp. 853–875
19. Hansson, G.K.: Inflammation, atherosclerosis, and coronary artery disease. N. Engl. J. Med. 352, 1685–1695 (2005)
20. Glagov, S., Weisenberg, E., Zarins, C.K., Stankunavicius, R., Kolettis, G.J.: Compensatory enlargement of human atherosclerotic coronary arteries. N Engl J Med 316, 1371–1375 (1987)
21. Farcas, M.A., Rouleau, L., Fraser, R., Leask, R.L.: The development of 3-D, in vitro, endothelial culture models for the study of coronary artery disease. Biomed Eng Online 8, 30 (2009)
22. Stary, H.C., Chandler, A.B., Dinsmore, R.E., Fuster, V., Glagov, S., Insull, W., JR, Rosenfeld, M.E., Schwartz, C.J., Wagner, W.D., Wissler, R.W.: A definition of advanced types of atherosclerotic lesions and a histological classification of atherosclerosis. A report from the Committee on Vascular Lesions of the Council on Arteriosclerosis, American Heart Association. Circulation 92, 1355–1374 (1995)
23. Hewing, B., Fisher, E.A.: Preclinical mouse models and methods for the discovery of the causes and treatments of atherosclerosis. Expert opinion on drug discovery 7, 207–216 (2012)
24. Padmanabhan, J., Gonzalez, A.L.: The Effects of Extracellular Matrix Proteins on Neutrophil-Endothelial Interaction - A Roadway To Multiple Therapeutic Opportunities. Yale J Biol Med 85, 167–185 (2012)

25. Grewe, P.H., Deneke, T., Holt, S.K., Machraoui, A., Barmeyer, J., Muller, K.M.: Scanning electron microscopic analysis of vessel wall reactions after coronary stenting. Z Kardiol 89, 21-27 (2000)
26. Waterhouse, A., Wise, S.G., Yin, Y., Wu, B., James, B., Zreiqat, H., McKenzie, D.R., Bao, S., Weiss, A.S., Ng, M.K., et al.: In vivo biocompatibility of a plasma-activated, coronary stent coating. Biomaterials 33, 7984–7992 (2012)
27. Zimmer, S., Nickenig, G.: Prediction and prevention by progenitors? Stent thrombosis and EPCs. European heart journal 31, 2569–2571 (2010)
28. Curcio, A., Torella, D., Indolfi, C.: Mechanisms of smooth muscle cell proliferation and endothelial regeneration after vascular injury and stenting: approach to therapy. Circ J 75, 1287–1296 (2011)
29. Granada, J.F., Inami, S., Aboodi, M.S., Tellez, A., Milewski, K., Wallace-Bradley, D., Parker, S., Rowland, S., Nakazawa, G., Vorpahl, M., et al.: Development of a novel prohealing stent designed to deliver sirolimus from a biodegradable abluminal matrix. Circ Cardiovasc Interv 3, 257–266 (2010)
30. Lanzer, P., Sternberg, K., Schmitz, K.-P., Kolodgie, F., Nakazawa, G., Virmani, R.: Drug-eluting coronary stent very late thrombosis revisited. Herz 33, 334–342 (2008)
31. Iqbal, J., Gunn, J., Serruys, P.W.: Coronary stents: historical development, current status and future directions. Br Med Bull 106, 193–211 (2013)
32. Zhang, Y., Bourantas, C.V., Farooq, V., Muramatsu, T., Diletti, R., Onuma, Y., Garcia-Garcia, H.M., Serruys, P.W.: Bioresorbable scaffolds in the treatment of coronary artery disease. Med Devices (Auckl) 6, 37–48 (2013)
33. Räber, L., Windecker, S.: Current status of drug-eluting stents. Cardiovasc Ther 29, 176–189 (2011)
34. Mani, G., Chandrasekar, B., Feldman, M.D., Patel, D., Agrawal, C.M.: Interaction of endothelial cells with self-assembled monolayers for potential use in drug-eluting coronary stents. J. Biomed. Mater. Res. Part B Appl. Biomater. 90, 789–801 (2009)
35. He, Q., Zhao, Y., Chen, B., Xiao, Z., Zhang, J., Chen, L., Chen, W., Deng, F., Dai, J.: Improved cellularization and angiogenesis using collagen scaffolds chemically conjugated with vascular endothelial growth factor. Acta Biomaterialia 7, 1084–1093 (2011)
36. Jukema, J.W., Verschuren, J.J.W., Ahmed, T.A.N., Quax, P.H.A.: Restenosis after PCI. Part 1: pathophysiology and risk factors. Nat Rev Cardiol 9, 53–62 (2011)
37. Sternberg, K., Grabow, N., Petersen, S., Weitschies, W., Harder, C., Ince, H., Kroemer, H.K., Schmitz, K.-P.: Advances in coronary stent technology--active drug-loaded stent surfaces for prevention of restenosis and improvement of biocompatibility. Curr Pharm Biotechnol 14, 76–90 (2013)

38. Fröhlich, G.M., Lansky, A.J., Ko, D.T., Archangelidi, O., Palma, R. de, Timmis, A., Meier, P.: Drug eluting balloons for de novo coronary lesions - a systematic review and meta-analysis. BMC medicine 11, 123 (2013)
39. Huang, K.N., Grandi, S.M., Filion, K.B., Eisenberg, M.J.: Late and Very Late Stent Thrombosis in Patients With Second-Generation Drug-Eluting Stents. Canadian Journal of Cardiology 29, 1488–1494 (2013)
40. Curfman, G.D., Morrissey, S., Jarcho, J.A., Drazen, J.M.: Drug-Eluting Coronary Stents — Promise and Uncertainty. N Engl J Med 356, 1059–1060 (2007)
41. Dangas, G.D., Claessen, B.E., Caixeta, A., Sanidas, E.A., Mintz, G.S., Mehran, R.: In-Stent Restenosis in the Drug-Eluting Stent Era. Journal of the American College of Cardiology 56, 1897–1907 (2010)
42. Huang, Y., Venkatraman, S.S., Boey, Freddy Y C, Lahti, E.M., Umashankar, P.R., Mohanty, M., Arumugam, S., Khanolkar, L., Vaishnav, S.: In vitro and in vivo performance of a dual drug-eluting stent (DDES). Biomaterials 31, 4382–4391 (2010)
43. Joner, M., Nakazawa, G., Finn, A.V., Quee, S.C., Coleman, L., Acampado, E., Wilson, P.S., Skorija, K., Cheng, Q., Xu, X., et al.: Endothelial cell recovery between comparator polymer-based drug-eluting stents. Journal of the American College of Cardiology 52, 333–342 (2008)
44. Zilla, P., Bezuidenhout, D., Human, P.: Prosthetic vascular grafts: wrong models, wrong questions and no healing. Biomaterials 28, 5009–5027 (2007)
45. Zheng, W., Wang, Z., Song, L., Zhao, Q., Zhang, J., Li, D., Wang, S., Han, J., Zheng, X.-L., Yang, Z., et al.: Endothelialization and patency of RGD-functionalized vascular grafts in a rabbit carotid artery model. Biomaterials 33, 2880–2891 (2012)
46. Wu, H., Fan, J., Chu, C.-C., Wu, J.: Electrospinning of small diameter 3-D nanofibrous tubular scaffolds with controllable nanofiber orientations for vascular grafts. J Mater Sci Mater Med 21, 3207–3215 (2010)
47. Teichmann, J., Morgenstern, A., Seebach, J., Schnittler, H.-J., Werner, C., Pompe, T.: The control of endothelial cell adhesion and migration by shear stress and matrix-substrate anchorage. Biomaterials 33, 1959–1969 (2012)
48. Lin, Q., Ding, X., Qiu, F., Song, X., Fu, G., Ji, J.: In situ endothelialization of intravascular stents coated with an anti-CD34 antibody functionalized heparin-collagen multilayer. Biomaterials 31, 4017–4025 (2010)
49. Unger, R.E., Peters, K., Huang, Q., Funk, A., Paul, D., Kirkpatrick, C.J.: Vascularization and gene regulation of human endothelial cells growing on porous polyethersulfone (PES) hollow fiber membranes. Biomaterials 26, 3461–3469 (2005)
50. Kuwabara, F., Narita, Y., Yamawaki-Ogata, A., Kanie, K., Kato, R., Satake, M., Kaneko, H., Oshima, H., Usui, A., Ueda, Y.: Novel small-caliber vascular grafts with

trimeric Peptide for acceleration of endothelialization. Ann. Thorac. Surg. 93, 156-63; discussion 163 (2012)

51. Teske, M.: Nass- und plasmachemische Oberflächenmodifizierung biodegradierbarer, polymerer Implantatwerkstoffe unter Immobilisierung von Wirkstoffen zur Optimierung der Zelle-Implantat-Interaktion [Dissertation]. Universität Rostock (2013)
52. Ratner, B.D.: Biomaterials science. An introduction to materials in medicine. Elsevier Academic Press, London, UK, 3rd edition (2013)
53. Wintermantel, E.: Biokompatible Werkstoffe und Bauweisen. Implantate für Medizin und Umwelt. Springer, Berlin (1998)
54. Wang, X., Lennartz, M.R., Loegering, D.J., Stenken, J.A.: Multiplexed cytokine detection of interstitial fluid collected from polymeric hollow tube implants—A feasibility study. Cytokine 43, 15–19 (2008)
55. Anderson, J.M., Rodriguez, A., Chang, D.T.: Foreign body reaction to biomaterials. Seminars in Immunology 20, 86–100 (2008)
56. Rodriguez, A., MacEwan, S.R., Meyerson, H., Kirk, J.T., Anderson, J.M.: The foreign body reaction in T-cell-deficient mice. J. Biomed. Mater. Res. 90A, 106–113 (2009)
57. Higgins, D.M., Basaraba, R.J., Hohnbaum, A.C., Lee, E.J., Grainger, D.W., Gonzalez-Juarrero, M.: Localized immunosuppressive environment in the foreign body response to implanted biomaterials. Am. J. Pathol. 175, 161–170 (2009)
58. Wintermantel, E., Ha, S.-W.: Medizintechnik. Life Science Engineering ; Interdisziplinarität, Biokompatibilität, Technologien, Implantate, Diagnostik, Werkstoffe, Zertifizierung, Business/ Erich Wintermantel; Suk-Woo Ha. Springer Berlin Heidelberg, Berlin, Heidelberg (2009)
59. Storm, T., Wulf, K., Teske, M., Löbler, M., Kundt, G., Luderer, F., Schmitz, K.-P., Sternberg, K., Hovakimyan, M.: Chemical activation and changes in surface morphology of poly(ε-caprolactone) modulate VEGF responsiveness of human endothelial cells. J Mater Sci Mater Med 25, 2003–2015 (2014)
60. Desmet, T., Morent, R., Geyter, N. de, Leys, C., Schacht, E., Dubruel, P.: Nonthermal plasma technology as a versatile strategy for polymeric biomaterials surface modification: a review. Biomacromolecules 10, 2351–2378 (2009)
61. Bremus-Köbberling, E.A.: Strukturierung und Modifizierung von Polymeren mit UV-Laserstrahlung für Life-science-Anwendungen [Dissertation]. Rheinisch-Westfälische Technische Hochschule, Mainz, Aachen (2004)
62. Mark, K. von der, Park, J., Bauer, S., Schmuki, P.: Nanoscale engineering of biomimetic surfaces: cues from the extracellular matrix. Cell Tissue Res 339, 131–153 (2010)

63. Gorbet, M.B., Sefton, M.V.: Biomaterial-associated thrombosis: roles of coagulation factors, complement, platelets and leukocytes. Biomaterials 25, 5681–5703 (2004)
64. Koch, S., Tugues, S., Li, X., Gualandi, L., Claesson-Welsh, L.: Signal transduction by vascular endothelial growth factor receptors. Biochem. J. 437, 169–183 (2011)
65. Ferrara, N.: Binding to the Extracellular Matrix and Proteolytic Processing: Two Key Mechanisms Regulating Vascular Endothelial Growth Factor Action. Molecular Biology of the Cell 21, 687–690 (2010)
66. Arcondéguy, T., Lacazette, E., Millevoi, S., Prats, H., Touriol, C.: VEGF-A mRNA processing, stability and translation: a paradigm for intricate regulation of gene expression at the post-transcriptional level. Nucleic Acids Res. 41, 7997–8010 (2013)
67. Lang, I., Hoffmann, C., Olip, H., Pabst, M.A., Hahn, T., Dohr, G., Desoye, G.: Differential mitogenic responses of human macrovascular and microvascular endothelial cells to cytokines underline their phenotypic heterogeneity. Cell Prolif 34, 143–155 (2001)
68. Ylä-Herttuala, S., Rissanen, T.T., Vajanto, I., Hartikainen, J.: Vascular endothelial growth factors: biology and current status of clinical applications in cardiovascular medicine. J. Am. Coll. Cardiol. 49, 1015–1026 (2007)
69. Ferrara, N.: VEGF: an update on biological and therapeutic aspects. Current Opinion in Biotechnology 11, 617–624 (2000)
70. Davies, N., Dobner, S., Bezuidenhout, D., Schmidt, C., Beck, M., Zisch, A.H., Zilla, P.: The dosage dependence of VEGF stimulation on scaffold neovascularisation. Biomaterials 29, 3531–3538 (2008)
71. Swanson, N., Hogrefe, K., Javed, Q., Gershlick, A.H.: In vitro evaluation of vascular endothelial growth factor (VEGF)-eluting stents. International Journal of Cardiology 92, 247–251 (2003)
72. Winder, T., Lenz, H.-J.: Vascular endothelial growth factor and epidermal growth factor signaling pathways as therapeutic targets for colorectal cancer. Gastroenterology 138, 2163–2176 (2010)
73. Dimmeler, S., Dernbach, E., Zeiher, A.M.: Phosphorylation of the endothelial nitric oxide synthase at Ser-1177 is required for VEGF-induced endothelial cell migration. FEBS Letters 477, 258–262 (2000)
74. Garrett, T.A., Van Buul, Jaap D, Burridge, K.: VEGF-induced Rac1 activation in endothelial cells is regulated by the guanine nucleotide exchange factor Vav2. Exp. Cell Res. 313, 3285–3297 (2007)
75. Yang, J., Zeng, Y., Zhang, C., Chen, Y.-X., Yang, Z., Li, Y., Leng, X., Kong, D., Wei, X.-Q., Sun, H.-F., et al.: The prevention of restenosis in vivo with a VEGF gene and paclitaxel co-eluting stent. Biomaterials 34, 1635–1643 (2013)

76. Mel, A. de, Jell, G., Stevens, M.M., Seifalian, A.M.: Biofunctionalization of Biomaterials for Accelerated in Situ Endothelialization: A Review. Biomacromolecules 9, 2969–2979 (2008)
77. Alberts, B. (ed.): Molekularbiologie der Zelle. VCH Verlagsgesellschaft, Weinheim, 3. Auflage (1995)
78. Çelebi, B., Mantovani, D., Pineault, N.: Effects of extracellular matrix proteins on the growth of haematopoietic progenitor cells. Biomed. Mater. 6, 55011 (2011)
79. Berneel, E., Desmet, T., Declercq, H., Dubruel, P., Cornelissen, M.: Double protein-coated poly-ε-caprolactone scaffolds: Successful 2D to 3D transfer. J. Biomed. Mater. Res. 100, 1783–1791 (2012)
80. Sun, H., Mei, L., Song, C., Cui, X., Wang, P.: The in vivo degradation, absorption and excretion of PCL-based implant. Biomaterials 27, 1735–1740 (2006)
81. Pektok, E., Nottelet, B., Tille, J.-C., Gurny, R., Kalangos, A., Moeller, M., Walpoth, B.H.: Degradation and Healing Characteristics of Small-Diameter Poly(-Caprolactone) Vascular Grafts in the Rat Systemic Arterial Circulation. Circulation 118, 2563–2570 (2008)
82. Peters, K., Unger, R.E., Stumpf, S., Schäfer, J., Tsaryk, R., Hoffmann, B., Eisenbarth, E., Breme, J., Ziegler, G., Kirkpatrick, C.J.: Cell type-specific aspects in biocompatibility testing: the intercellular contact in vitro as an indicator for endothelial cell compatibility. J Mater Sci Mater Med 19, 1637–1644 (2008)
83. Untergasser, A., Cutcutache, I., Koressaar, T., Ye, J., Faircloth, B.C., Remm, M., Rozen, S.G.: Primer3--new capabilities and interfaces. Nucleic Acids Res 40, e115 (2012)
84. Kirschbaum, N.E., Gumina, R.J., Newman, P.J.: Organization of the gene for human platelet/endothelial cell adhesion molecule-1 shows alternatively spliced isoforms and a functionally complex cytoplasmic domain. Blood 84, 4028–4037 (1994)
85. Tersteeg, C., Roest, M., Mak-Nienhuis, E.M., Ligtenberg, E., Hoefer, I.E., Groot, P.G., Pasterkamp, G.: A fibronectin-fibrinogen-tropoelastin coating reduces smooth muscle cell growth but improves endothelial cell function. J. Cell. Mol. Med. 16, 2117–2126 (2012)
86. Schmittgen, T.D., Livak, K.J.: Analyzing real-time PCR data by the comparative C(T) method. Nat Protoc 3, 1101–1108 (2008)
87. Kaiser, R., Gottschalk, G.: Elementare Tests zur Beurteilung von Messdaten. Soforthilfe für statistische Tests mit wenigen Messdaten. Bibliographisches Institut, Mannheim (1972)
88. Xia, Y., Prawirasatya, M., Heng, B.C., Boey, F., Venkatraman, S.S.: Seeding density matters: extensive intercellular contact masks the surface dependence of endothelial cell-biomaterial interactions. J Mater Sci Mater Med 22, 389–396 (2011)

89. Pittelkow, M.R., Shipley, G.D.: Serum-free culture of normal human melanocytes: growth kinetics and growth factor requirements. J Cell Physiol 140, 565–576 (1989)
90. Larsson, O., Wejde, J.: Dolichol delays G1-arrest for one cell cycle in human fibroblasts subjected to depletion of serum or mevalonate. J Cell Sci 103 (Pt 4), 1065–1072 (1992)
91. Tinnemans, M.M., Lenders, M.H., ten Velde, G P, Blijham, G.H., Ramaekers, F.C., Schutte, B.: S-phase arrest of nutrient deprived lung cancer cells. Cytometry 19, 326-333 (1995)
92. Theiler, S., Diamantouros, S.E., Jockenhoevel, S., Keul, H., Moeller, M.: Synthesis and characterization of biodegradable polyester/polyether resins via Michael-type addition. Polym. Chem. 2, 2273 (2011)
93. Bas, A., Forsberg, G., Hammarström, S., Hammarström, M.-L.: Utility of the housekeeping genes 18S rRNA, beta-actin and glyceraldehyde-3-phosphate-dehydrogenase for normalization in real-time quantitative reverse transcriptase-polymerase chain reaction analysis of gene expression in human T lymphocytes. Scandinavian journal of immunology 59, 566–573 (2004)
94. Wykrzykowska, J.J., Onuma, Y., Serruys, P.W.: Advances in stent drug delivery: the future is in bioabsorbable stents. Expert Opin. Drug Deliv. 6, 113–126 (2009)
95. Wulf, K., Teske, M., Löbler, M., Luderer, F., Schmitz, K.-P., Sternberg, K.: Surface functionalization of poly(ε-caprolactone) improves its biocompatibility as scaffold material for bioartificial vessel prostheses. J. Biomed. Mater. Res. 98, 89–100 (2011)
96. Kamath, S., Bhattacharyya, D., Padukudru, C., Timmons, R.B., Tang, L.: Surface chemistry influences implant-mediated host tissue responses. J. Biomed. Mater. Res. 86, 617–626 (2008)
97. Jiao, Y.-P., Cui, F.-Z.: Surface modification of polyester biomaterials for tissue engineering. Biomed Mater 2, R24–37 (2007)
98. Goddard, J., Hotchkiss, J.: Polymer surface modification for the attachment of bioactive compounds. Progress in Polymer Science 32, 698–725 (2007)
99. Ertel, S.I., Ratner, B.D., Horbett, T.A.: Radiofrequency plasma deposition of oxygen-containing films on polystyrene and poly(ethylene terephthalate) substrates improves endothelial cell growth. J. Biomed. Mater. Res. 24, 1637–1659 (1990)
100. Davies, M.J., Woolf, N., Rowles, P.M., Pepper, J.: Morphology of the endothelium over atherosclerotic plaques in human coronary arteries. Heart 60, 459–464 (1988)
101. van Belle, E., Tio, F.O., Couffinhal, T., Maillard, L., Passeri, J., Isner, J.M.: Stent Endothelialization: Time Course, Impact of Local Catheter Delivery, Feasibility of Recombinant Protein Administration, and Response to Cytokine Expedition. Circulation 95, 438–448 (1997)

102. Asahara, T., Bauters, C., Pastore, C., Kearney, M., Rossow, S., Bunting, S., Ferrara, N., Symes, J.F., Isner, J.M.: Local Delivery of Vascular Endothelial Growth Factor Accelerates Reendothelialization and Attenuates Intimal Hyperplasia in Balloon-Injured Rat Carotid Artery. Circulation 91, 2793–2801 (1995)
103. Walter, D.H.: Local Gene Transfer of phVEGF-2 Plasmid by Gene-Eluting Stents: An Alternative Strategy for Inhibition of Restenosis. Circulation 110, 36–45 (2004)
104. Weymann, A., Schmack, B., Okada, T., Soós, P., I, Istók, R., Radovits, T., et al.: Reendothelialization of Human Heart Valve Neoscaffolds Using Umbilical Cord-Derived Endothelial Cells. Circulation Journal 77, 207–216 (2013)
105. Guba, M., Breitenbuch, P. von, Steinbauer, M., Koehl, G., Flegel, S., Hornung, M., Bruns, C.J., Zuelke, C., Farkas, S., Anthuber, M., et al.: Rapamycin inhibits primary and metastatic tumor growth by antiangiogenesis: involvement of vascular endothelial growth factor. Nat. Med. 8, 128–135 (2002)
106. Stettler, C., Wandel, S., Allemann, S., Kastrati, A., Morice, M.C., Schomig, A., Pfisterer, M.E., Stone, G.W., Leon, M.B., Lezo, J.S. de, et al.: Outcomes associated with drug-eluting and bare-metal stents: a collaborative network meta-analysis. Lancet 370, 937–948 (2007)
107. Finn, A.V., Nakazawa, G., Joner, M., Kolodgie, F.D., Mont, E.K., Gold, H.K., Virmani, R.: Vascular Responses to Drug Eluting Stents: Importance of Delayed Healing. Arteriosclerosis, Thrombosis, and Vascular Biology 27, 1500–1510 (2007)
108. van Dyck, C.J., Hoymans, V.Y., Haine, S., Vrints, C.J.: New-Generation Drug-Eluting Stents. Focus on Xience V® Everolimus-Eluting Stent and Resolute® Zotarolimus-Eluting Stent. J. Int. Cardiol. 26, 278–286 (2013)
109. Clowes, A.W., Reidy, M.A., Clowes, M.M.: Kinetics of cellular proliferation after arterial injury. I. Smooth muscle growth in the absence of endothelium. Lab Invest 49, 327–333 (1983)
110. Jeremy, J.Y., Rowe, D., Emsley, A.M., Newby, A.C.: Nitric oxide and the proliferation of vascular smooth muscle cells. Cardiovasc Res 43, 580–594 (1999)
111. Castellot, J.: Cultured endothelial cells produce heparinlike inhibitor of smooth muscle cell growth. The Journal of Cell Biology 90, 372–379 (1981)
112. Garg, U.C., Hassid, A.: Nitric oxide-generating vasodilators and 8-bromo-cyclic guanosine monophosphate inhibit mitogenesis and proliferation of cultured rat vascular smooth muscle cells. J. Clin. Invest. 83, 1774–1777 (1989)
113. Tahir, H., Bona-Casas, C., Hoekstra, A.G., Wong, K.K.L.: Modelling the Effect of a Functional Endothelium on the Development of In-Stent Restenosis. PLoS ONE 8, e66138 (2013)

114. Singh, S., Wu, B.M., Dunn, James C Y: The enhancement of VEGF-mediated angiogenesis by polycaprolactone scaffolds with surface cross-linked heparin. Biomaterials 32, 2059–2069 (2011)
115. Bigalke, C., Luderer, F., Wulf, K., Storm, T., Löbler, M., Arbeiter, D., Rau, B.M., Nizze, H., Vollmar, B., Schmitz, K.-P., et al.: VEGF-releasing suture material for enhancement of vascularization: Development, in vitro and in vivo study. Acta Biomater (2014)
116. Knetsch, Menno L W, Koole, L.H.: VEGF-E enhances endothelialization and inhibits thrombus formation on polymeric surfaces. J Biomed Mater Res A 93, 77–85 (2010)
117. Adiguzel, E., Ahmad, P.J., Franco, C., Bendeck, M.P.: Collagens in the progression and complications of atherosclerosis. Vascular Medicine 14, 73–89 (2009)
118. Siow, K.S., Britcher, L., Kumar, S., Griesser, H.J.: Plasma Methods for the Generation of Chemically Reactive Surfaces for Biomolecule Immobilization and Cell Colonization - A Review. Plasma Process. Polym. 3, 392–418 (2006)
119. Wang, H.G., Yin, T.Y., Ge, S.P., Zhang, Q., Dong, Q.L., Lei, D.X., Sun, D.M., Wang, G.X.: Biofunctionalization of titanium surface with multilayer films modified by heparin-VEGF-fibronectin complex to improve endothelial cell proliferation and blood compatibility. J. Biomed. Mater. Res. 101, 413–420 (2013)
120. Wang, G.X., Deng, X.Y., Tang, C.J., Liu, L.S., Xiao, L., Xiang, L.H., Quan, X.J., Legrand, A.P., Guidoin, R.: The adhesive properties of endothelial cells on endovascular stent coated by substrates of poly-l-lysine and fibronectin. Artif Cells Blood Substit Immobil Biotechnol 34, 11–25 (2006)
121. Patel, H.J., Su, S.-H., Patterson, C., Nguyen, K.T.: A combined strategy to reduce restenosis for vascular tissue engineering applications. Biotechnol Prog 22, 38–44 (2006)
122. Pompe, T., Keller, K., Mothes, G., Nitschke, M., Teese, M., Zimmermann, R., Werner, C.: Surface modification of poly(hydroxybutyrate) films to control cell-matrix adhesion. Biomaterials 28, 28–37 (2007)
123. Cooper, T., Sefton, M.: Fibronectin coating of collagen modules increases in vivo HUVEC survival and vessel formation in SCID mice. Acta Biomaterialia 7, 1072–1083 (2011)
124. Kawashima, S., Yokoyama, M.: Dysfunction of endothelial nitric oxide synthase and atherosclerosis. Arterioscler Thromb Vasc Biol 24, 998–1005 (2004)
125. Zhang, H., Hollister, S.: Comparison of bone marrow stromal cell behaviors on poly(caprolactone) with or without surface modification: studies on cell adhesion, survival and proliferation. Journal of biomaterials science. Polymer edition 20, 1975-1993 (2009)

Eidesstattliche Erklärung

Hiermit erkläre ich, diese Arbeit selbstständig angefertigt, die verwendeten Ergebnisse und Daten anderer vollständig angegeben und korrekt zitiert sowie die weitere Mitwirkung Dritter offengelegt zu haben.

Rostock, den 20. November 2014

_____

Thilo Storm

Veröffentlichungen und Tagungsbeiträge

Veröffentlichungen

1. **Storm**, T; Wulf, K; Teske, M; Löbler, M; Kundt, G; Luderer, F et al. (2014): Chemical activation and changes in surface morphology of poly(ε-caprolactone) modulate VEGF responsiveness of human endothelial cells. In: *J Mater Sci Mater Med* 25 (8), 2003-2015. DOI: 10.1007/s10856-014-5226-0.
2. Bigalke, C; Luderer, F; Wulf, K; **Storm, T**; Löbler, M; Arbeiter, D et al. (2014): VEGF-releasing suture material for enhancement of vascularization: Development, in vitro and in vivo study. In*: Acta Biomater*. DOI: 10.1016/j.actbio.2014.09.002.
3. Hall, C, Flores, MV, **Storm, T**, Crosier K, Crosier P (2007): The zebrafish *lysozyme C* promoter drives myeloid-specific expression in transgenic fish. *BMC Developmental Biology* 7: 42. DOI: 10.1186/1471-213X-7-42
4. **Storm T**, Rath S, Mohamed SA, Bruse P, Kowald A, Oehmichen M, Meissner C (2002): Mitotic brain cells are just as prone to mitochondrial deletions as neurons: a large-scale single-cell PCR study of the human caudate nucleus. *Experimental Gerontology* 37(12):1389-400. DOI:10.1016/S0531-5565(02)00121-3
5. Hodos W, Ghim MM, Potocki A, Fields JN, **Storm T** (2002): Contrast sensitivity in pigeons: a comparison of behavioral and pattern ERG methods. *Documenta Ophthalmologica* 104(1):107-18

Tagungsbeiträge

1. **Storm T**, Teske M, Wulf K, Löbler M, Schmitz KP, Sternberg K. Enhanced Endothelialization of PCL Through Chemical Activation, Protein Precoating and VEGF Stimulation. Biomedizinische Technik 2013, September 2013, DOI: 10.1515/bmt-2013-4092.
2. **Storm T**, Teske M, Löbler M, Wulf K, Schmitz KP, Sternberg K. Influence of cell source and adhesion substrate on growth factor responsiveness in primary endothelial cells. Biomedizinische Technik 2012, August 2012, DOI: 10.1515/bmt-2012-4369.
3. **Storm T**, Löbler M, Wulf K, Schmitz KP, Sternberg K. Influence of cell source and adhesion substrate on growth factor responsiveness in primary endothelial cells. 4th International Symposium Interface Biology of Implants 2012, Rostock, Mai 2012
4. **Storm T**, Wulf K, Löbler M, Theiler S, Keul H, Schmitz KP, Sternberg K. Influence of surface-bound ligands on cellular adhesion at the implant-endothelial interface. Biomedizinische Technik 2011, September 2011, DOI: 10.1515/bmt-2011-815

5. **Storm T**, Hall C, Flores MV, Crosier K, Crosier P. Monitoring inflammation within the zebrafish intestine. Asia Pacific Zebrafish Network Meeting, Auckland, New Zealand, Februar 2008

Danksagung

Ich danke dem Institut für Biomedizinische Technik für die Ermöglichung dieser Promotion, die ohne die Fürsprache und Unterstützung von Katrin Sternberg und Marian Löbler nicht zustandegekommen wäre. Desweiteren danke ich Marina Hovakimyan für die Übernahme der Betreuerfunktion und den Kollegen in Warnemünde für die interessante gemeinsame Zeit, insbesondere Jana Brietzke, Christian Kastner, Ingo Minrath, Olaf Specht und Dalibor Bajer. Ein zusätzlicher und besonderer Dank geht an Michael Teske und Katharina Wulf für die Einbringung des erforderlichen chemischen Sachverstands und das stets harmonische gemeinsame wissenschaftliche Arbeiten, ebenso wie an Martina Sombetzki für ihre freundliche Begleitung und immer vorhandene Bereitschaft zur Bereitstellung von Zellmaterial „auf Zuruf“. Herzlichen Dank an Gabi Karsten, Martina Nerger und Babette Hummel für die ausnahmslos gute Zusammenarbeit im Labor.

Günther Kundt danke ich für die hilfsbereite offene Art und die Einbringung der statistischen Expertise bei der nicht eben geradlinigen Auswertung der Zellkulturexperimente. In ähnlicher Weise hat die fachkundige Hilfe von Frank Kamke und Jörg Kaminsky ein gutes Scherflein dazu beigetragen, diese Dissertation überhaupt erstellen zu können.

Ferner danke ich auch den Forschungspartnern in Greifswald, Raila Busch und Anne Strohbach, für die gute Kooperation, wenn sie auch nicht so umfangreich ausgefallen ist wie einst geplant.

Meiner Familie danke ich für all die kleinen und großen Hilfestellungen durch die Jahre. Für die Eröffnung ganz neuer Lebenshorizonte während dieser Promotionszeit danke ich meinen Kindern Louisa und Laszlo. Und natürlich meiner Frau Lara Marshall für die erneute fortwährende Motivation und ihr Durchhaltevermögen durch die dunklen Rostocker Winter.

Schließlich möchte ich noch der Fachbibliothek DDR-Geschichte der Universität, hinter deren Gittern der weitaus größte Teil dieser Dissertationsschrift entstand, einen besonderen Dank für die häufig über die Öffnungszeiten hinausgehende Nutzung ihrer Räumlichkeiten und die ausgezeichnete Arbeitsatmosphäre und Ruhe dort aussprechen.

Appendix

A.1. Manufacturing of polymer

Polymer films were prepared using the following procedure: 1 g PCL (M_w = 65,000 g/mol, Sigma-Aldrich, Taufkirchen) was dissolved in 25 ml chloroform ($CHCl_3$). This solution was transferred to glass Petri dishes (Ø = 9 cm) where the solvent was allowed to evaporate. The resulting film (thickness: approximately 150 µm) was cut from the Petri dish, then washed for two days in methanol and for two more days in distilled water. Finally it was vacuum dried for seven days at 40°C and 40 mbar. These procedures were carried out according to [95]. For salt leaching of PCL, 5 g sodium chloride (NaCl) were added after dissolving 1.75 g of polymer in 25 ml $CHCl_3$ and the polymer-salt suspension was poured into a Petri dish (Ø = 9 cm). After evaporation of $CHCl_3$ and cutting of the film from the Petri dish, a 2 day wash in methanol ensued. The washing with distilled water was extended to seven days (with daily water changes) until all salt crystals were washed out and the salt free film was then vacuum dried for seven days at 40°C and 40 mbar. For surface degradation of PCL with sodium hydroxide (NaOH), each PCL film was immersed in 2 M NaOH solution at 50°C for 8 h to increase the number of carboxyl (-COOH) and hydroxyl (-OH) groups (see **figure A.1** i).

For electrospinning, PCL was dissolved in a 3:1 mixture of chloroform and methanol to obtain a 9% (w/v) solution. The PCL fiber mat was prepared with an in-house developed electrospinning device. The PCL solution was pumped at a flow rate of 0.1 ml/min to a capillary (inner diameter = 0.4 mm) connected to a high voltage power supply. At a voltage of +12 kV a fluid jet was ejected from the nozzle opening, and the fibers were collected on a metallic mesh (mesh size = 0.5 mm, wire thickness = 0.5 mm), resulting in a PCL fiber mat that was vacuum dried at 40°C and 40 mbar for 7 days. These procedures were carried out according to [59].

A.2. Surface activation of PCL via 4,4′-methylenebis(phenyl-isocyanate) (MDI)

Each PCL sample (Ø = 6 mm) was first degraded in 2 ml sodium hydroxide solution (2 M) at 50°C for 8 h to increase the number of carboxyl (-COOH) and hydroxyl (-OH) groups (**figure A.1** i). Then all samples were washed with distilled water and vacuum dried for 12 h. The resulting -OH groups on the PCL surface were reacted with MDI, solubilized in 2 ml n-heptane (1.6 mM) for 5 h under stirring at 50°C (figure A.1 ii). After washing with n-heptane and vacuum drying for 12 h, the terminal isocyanate (-NCO) groups of PCL underwent aminolysis or hydrolysis to amino ($-NH_2$) groups by means of 2 ml ammonia solution (25 %)

(figure A.1 iii). Finally the PCL samples were once more washed with distilled water and vacuum dried.

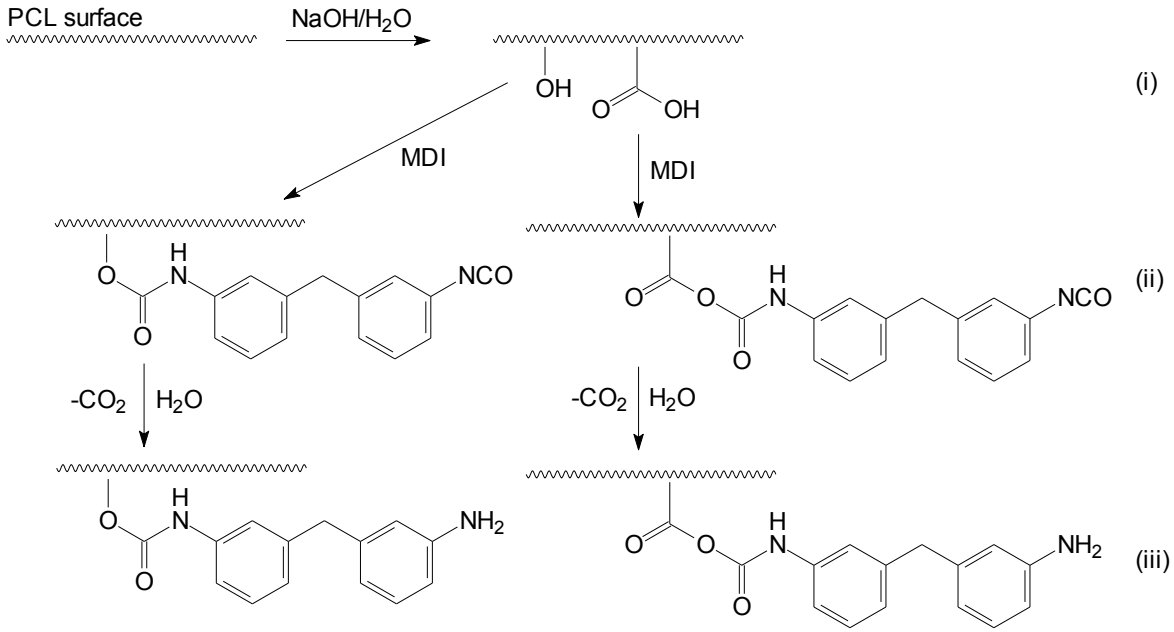

Figure A.1. Reaction scheme of chemical surface modification of PCL with MDI: (i) after alkaline hydrolysis, (ii) coupling of MDI, (iii) formation of terminal amino groups.

A.3. Surface activation of PCL via hexane-1,6-diamine (HMDA)

For generating amino groups (**figure A.2**)., non-activated PCL films were immersed in hexane-1,6-diamine (HMDA) in isopropanol (78 mg/ml), stirred in HMDA solution for one hour at 37°C and finally washed with pure water, as described by Zhang and Hollister [125].

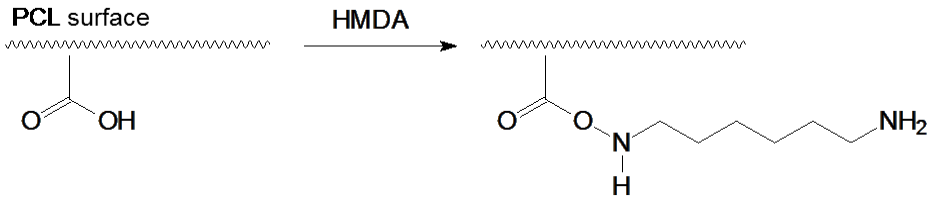

Figure A.2. Reaction scheme for generation of terminal amino groups on PCL via aminolysis with HMDA.

A.4. Surface activation of PCL via aminopropyltriethoxysilane (APTES)

As described in detail in [51], the PCL samples (Ø = 6 mm) were first modified by means of O_2 plasma activation (capacity 30 %), then incubated in 2 ml APTES (0.2 M in water) and

stirred for 24 h at room temperature. Through the addition of APTES, which acts as spacer, an amino-functionalized silyl ether containing terminal amino groups was generated (**figure A.3**). In the end the samples were rinsed with water and vacuum dried for 12 h.

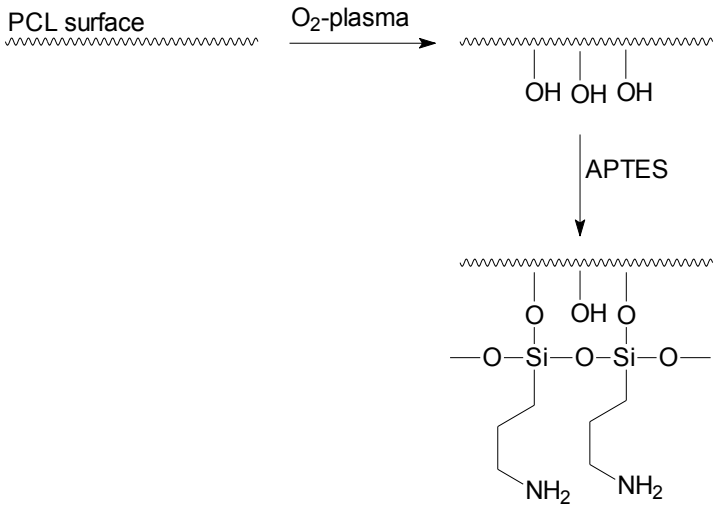

Figure A.3. Reaction scheme for generation of terminal amino groups on PCL by means of O_2 plasma activation and reaction with APTES.

A.5. Surface activation of PCL via ammonia plasma

The NH_3 plasma activation process for PCL was performed via plasma etching (PE) electrode in ammonia (NH_3) gas in a radio frequency (RF) plasma generator (frequency 13.56 MHz, Diener Electronic GmbH & Co. KG, Ebhausen) at 30 W and a low pressure of 0.3 mbar (**figure A.4**). Plasma chemical activation parameters were optimized to yield maximum wettability of the activated material.

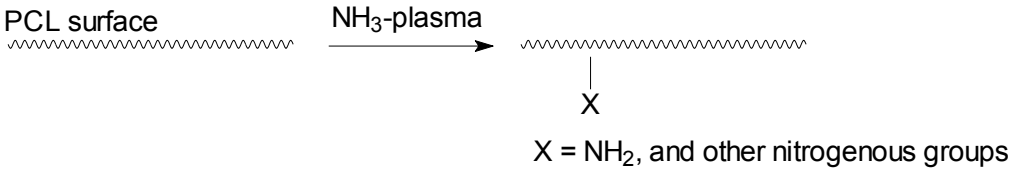

Figure A.4. Reaction scheme for generation of terminal amino groups on PCL with NH_3 plasma.

A.6. Surface activation of PCL via oxygen plasma

The O_2 plasma activation process for PCL was also performed via plasma etching (PE) electrode in an oxygen plasma generator (frequency 13.56 MHz, Diener Electronic,

Ebhausen) at 100 W and 0.3 mbar (**figure A.5**). For cell culture experiments, all activated polymer films were washed three times in water for an hour at room temperature with gentle shaking. The procedure was repeated with 0.05% Tween 20 in water and finally with pure water again.

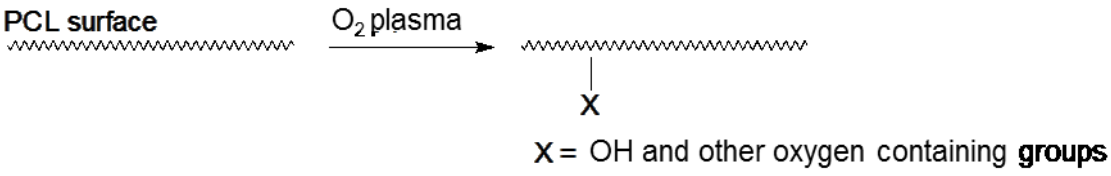

Figure A.5. Reaction scheme for generation of terminal oxygenous groups on PCL with O_2 plasma.

A.7. Covalent coupling of VEGF to sPCL-A

Immobilization of vascular endothelial growth factor (VEGF) to 4-star-shaped poly(ε-caprolactone) with terminal acrylate groups (sPCL-A) was performed either by adsorption or by employing the crosslinkers N,N-disuccinimidyl carbonate (DSC) or 1-ethyl-3-[3-dimethyl-aminopropyl]carbodiimide (EDC) and N-hydroxysuccinimide (NHS) in combination. Crosslinking with DSC results in the formation of ester bonds which can be cleaved by hydrolysis. In contrast, crosslinking with EDC/NHS leads to stable amid bonds, such that VEGF is coupled to sPCL-A in a way that is physiologically more stable.

A.8. Characterization of functionalized polymer

For confirmation of surface modification, the polymer films were examined by means of contact angle measurement (with water to determine hydrophilicity), 4-chloro-7-nitrobenzo-2-oxa-1,3-diazole (NBD-Cl) labeling (where fluorescence intensity correlates with the number of amino groups present) and environmental scanning electron microscopy (ESEM) as previously described [95]. These measurements are shown in **figure A.6**.

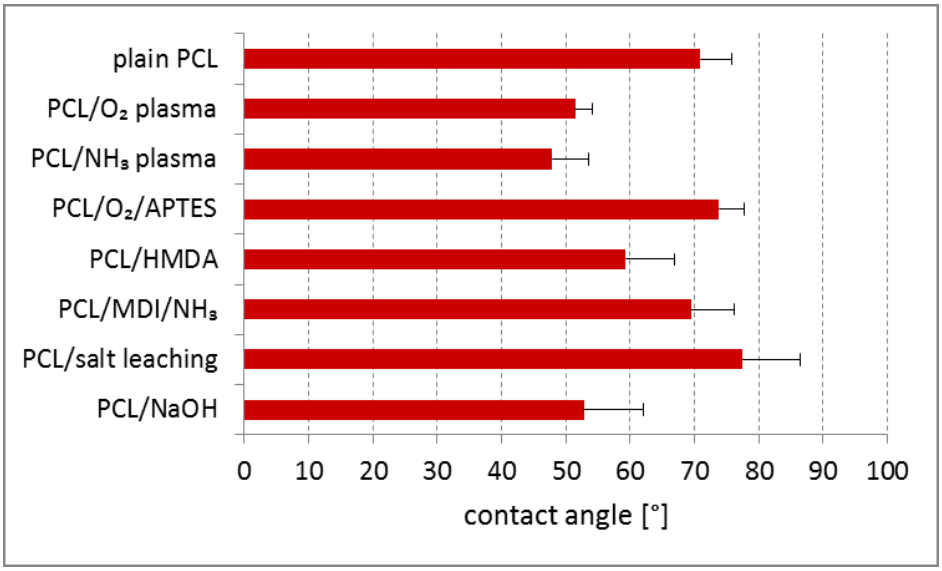

Figure A.6. Contact angle Θ of water as per sessile drop static measurement (n≥10) as a function of PCL modification.

A.9. Problem of teflon rings

In order to standardize the growth conditions for cells inside the microtiter wells, teflon rings were used to fix the circular substrate discs at the bottom of the wells.

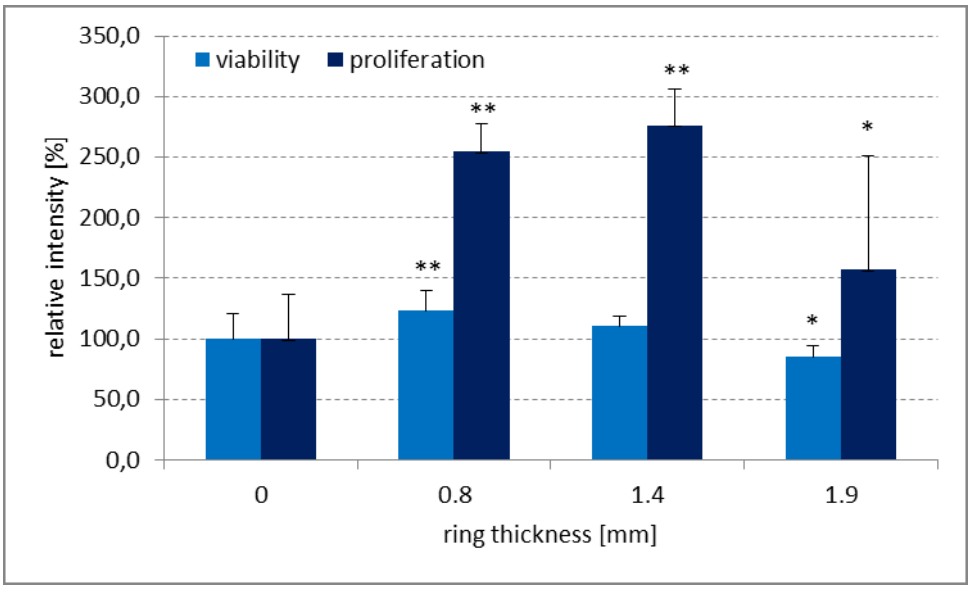

Figure A.7. The presence of teflon rings during measurement of cell proliferation and viability greatly influences biocompatibility test results. The outer diameter of the rings was always 6.1 mm, while their thickness varied from 0.8 to 1.9 mm. Shown is the relative intensity compared to cells incubated and measured without rings (100%) after 96 h of growth. Asterisks denote statistical significance of difference to that 100% control.

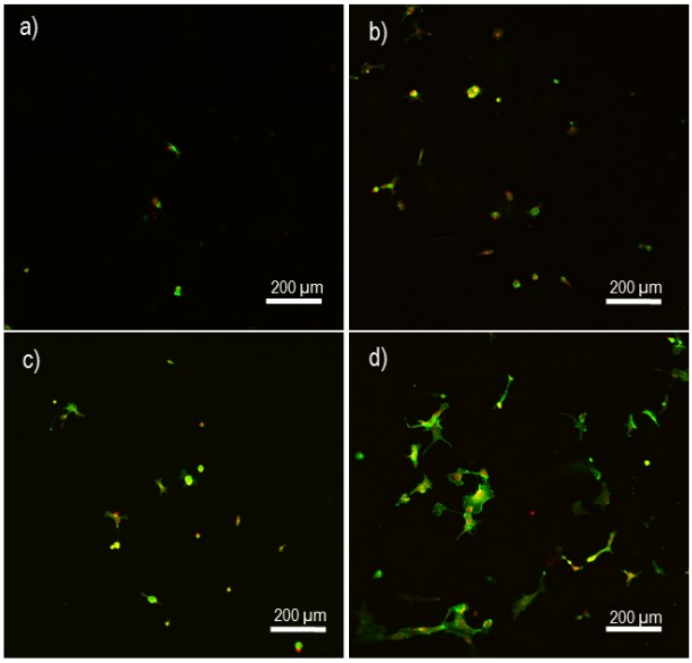

Figure A.8. ECM protein precoating of PCL positively impacts on HUVEC adhesion to the polymer. CLSM micrographs of HUVECs grown for 72 h on PCL coated with fibronectin, laminin or collagen type I (50 µg/ml each). After formalin fixation on the PCL films, cells were stained with phalloidin-FITC (green) and ethidium dimer (red). (a) uncoated PCL, (b) PCL+laminin, (c) PCL+ collagen type I, (d) PCL+ fibronectin. Scale bar: 200 µm

f	q_{crit} α=0.05	q_{crit} α=0.01	q_{crit} α=0.001	f	q_{crit} α=0.05	q_{crit} α=0.01	q_{crit} α=0.001
1	1.409	1.414	1.414	19	1.936	2.454	2.975
2	1.645	1.715	1.730	20	1.937	2.460	2.990
3	1.757	1.918	1.982	25	1.942	2.483	3.047
4	1.814	2.051	2.178	30	1.945	2.498	3.085
5	1.848	2.142	2.329	35	1.948	2.509	3.113
6	1.870	2.208	2.447	40	1.949	2.518	3.134
7	1.885	2.256	2.540	45	1.950	2.524	3.152
8	1.895	2.294	2.616	50	1.951	2.529	3.166
9	1.903	2.324	2.678	100	1.956	2.553	3.227
10	1.910	2.348	2.730	200	1.958	2.564	3.265
11	1.916	2.368	2.774	300	1.958	2.566	3.271
12	1.920	2.385	2.812	400	1.959	2.568	3.275
13	1.923	2.399	2.845	500	1.959	2.570	3.279
14	1.926	2.412	2.874	600	1.959	2.571	3.281
15	1.928	2.423	2.899	700	1.959	2.572	3.283
16	1.931	2.432	2.921	800	1.959	2.573	3.285
17	1.933	2.440	2.941	1000	1.960	2.576	3.291
18	1.935	2.447	2.959				

Table A.1. Threshold values for the outlier test after Nalimov. f= degrees of freedom (= n-2), q_{crit}= critical threshold, α= level of significance. The table values used here were for α=0.05.